Chemical Proteomic Tools for Studying Protein Kinase Active Sites

Bulathsinhalage Gayani Kanchana Perera

A dissertation
submitted in partial fulfillment of the
requirements for the degree of

Doctor of Philosophy

University of Washington

2012

Reading Committee:
Prof. Dustin J. Maly, Chair
Prof. Christophe Verlinde
Prof. Champak Chatterjee

Program Authorized to Offer Degree:
Department of Chemistry

University of Washington

Abstract

Chemical Proteomic Tools for Studying Protein Kinase Active Sites

Bulathsinhalage Gayani Kanchana Perera

Chair of the Supervisory Committee:
Assistant Professor Dustin James Maly
Department of Chemistry

Protein kinases constitute one of the largest protein families in humans. These enzymes catalyze phosphorylation of serine, threonine or tyrosine residues in their protein substrates. As protein kinases regulate most signal transduction pathways in cells and play important roles in many cellular functions, deregulation of their activity can lead to a number of diseases including cancer, diabetes and inflammation. Targeted inhibition of protein kinases has therefore become an attractive therapeutic strategy for the treatment of a number of diseases.

Small molecule inhibitors that target the active site of protein kinases can be used to study their catalytic function and regulation. We have designed and generated a set of small molecule ligands that bind to protein kinase active sites in a conformation-specific manner. These ligands have been used as proteomic tools to study the active sites of a

wide range of protein kinases. These efforts have been particularly focused on a class of ligands, type II inhibitors, which stabilize an inactive conformation of the ATP-binding site, called the DFG-out. We have shown that type II inhibitors can be extensively modified and that these reagents can be used in a range of proteomic applications. These proteomic efforts have provided insight into the roles of specific kinases during signaling events. Furthermore, these chemical tools have significantly contributed towards our understanding of the structure and regulation of protein kinases.

TABLE OF CONTENTS

Chapter 4: Determinants of type II inhibitor selectivity

LIST OF ABBREVIATIONS

3D	SH2, SH3 and catalytic domains of SRC/ABL kinases
ABL	Abelson tyrosine-protein kinase
AGT	O^6-alkylguanine DNA alkyltransferase
ATP	Adenosine-5'-triphosphate
BG	Benzyl guanine
Boc	*tert*-butyl-carbamate
BSA	Bovine Serum Albumin
CML	Chronic Myeloid Leukemia
DBD	DNA-binding domain
DCM	Dichloromethane
DFG	Asp-Phe-Gly
DIPEA	Diisopropylethylamine
DME	Dimethoxyethane
DMF	*N,N*-dimethylformamide
DMSO	Dimethyl sulfoxide
EDCI	1-ethyl-3-(3-dimethylaminopropyl) carbodiimide
EDTA	Ethylenediaminetetraacetic acid
ER	Endoplasmic reticulum
ESI	Electrospray ionization
EtOAc	Ethyl acetate
HOBt	1-Hydroxybenzotriazole

HEPES	(4-(2-hydroxyethyl)-1-piperazineethanesulfonic acid)
HPLC	high performance liquid chromatography
IC_{50}	half maximal inhibitory concentration
i-PrOH	Isopropyl alcohol
KD	Kinase domain (catalytic domain)
MeCN	Acetonitrile
MeOH	Methanol
MS	Mass spectrometry
NaHMDS	Sodium hexamethyldisilazide
NHS	N-Hydroxysuccinimide
NMR	Nuclear magnetic resonance
PEG	Polyethylene glycol
PP	Polyproline
ppm	parts per million
rt	room temperature
TFA	Trifluoroacetic acid
THF	Tetrahydrofuran
UPR	Unfolded protein response
WT	Wild type

<u>Units</u>

Ci	Curie

ºC	degrees Celsius
g	grams
L	liter
m	milli; meter
M	molar
mol	moles
n	nano
µ	micro

NMR

d	doublet
dd	doublet of doublets
J	coupling constant in Hz
m	multiplet
MHz	megahertz
s	singlet
t	triplet
q	quartet
δ	chemical shift in parts per million

LIST OF FIGURES

Figure Number Page

Chapter 1: Introduction

Chapter 2: Design, Synthesis and Characterization of "Clickable" 4-Anilinoquinazoline kinase inhibitors

Chapter 3: Bivalent Inhibitors for Protein Kinases

Chapter 4: Determinants of type II inhibitor selectivity

LIST OF SCHEMES

Scheme Number Page

LIST OF TABLES

Acknowledgements

I would like to thank my advisor, Professor Dustin Maly, for all the support, guidance and valuable advice given to me during my graduate career. I thank him for giving me the opportunity to be a part of these interesting research projects.

I would like to thank all of my committee members; Prof. Christophe Verlinde, Prof. Champak Chatterjee, Prof. Christine Luscombe, Prof. Mike Heinekey and Prof, Pradeep Rathod for all the help and useful suggestions given to me.

I would also like to acknowledge all my collaborators including Dr. Zachary Hill, Dr. Pratistha Ranjitkar, Jennifer Brigham, Dr. Kayode Ojo, Prof. Van Voorhis, Prof. Christophe Verlinde, Dr. Likun Wang and Prof. Feroz Papa for their valuable collaborations during my research in Maly lab.

I thank everyone in the Maly lab for being great lab mates and for their kind support during my ups and downs.

Special thanks go to my wonderful family, Sampath and Kumarangi for their excellent support and understandingness during my studies. I thank my brothers, Rushan and Ayeshmantha for all the encouraging discussions and also Sampath and my parents for many sacrifices they have made for me.

Dedication

To my loving family….

Sampath, Kumarangi, my parents & brothers….

You have given up your dreams, to make my dreams come true….!

Chapter 1

Introduction

1.1 Protein Kinases

Protein phosphorylation is the most widespread post-translational modification used in signal transduction. This process is carried out by enzymes called protein kinases.[1] The human genome encodes for 518 kinases, making it the largest enzyme family in humans. The protein kinases are divided into nine groups (TKL, TK, STE, CK1, AGC, CAMK, RGC, CMGC and atypical), which are further subdivided into 134 families and 230 subfamilies based on catalytic domain sequence similarity and biochemical function.[2] Protein kinases catalyze the transfer of the γ-phosphate of ATP to a serine, threonine or a tyrosine residue on a protein substrate.[1, 3] Since protein kinases play an important role in many cellular processes including cell growth, metabolism, cytoskeletal rearrangement, cell movement, differentiation and apoptosis, mis-regulation of kinases leads to a number of diseases such as cancer, diabetes and inflammation. Therefore, targeted inhibition of specific protein kinases has become an important therapeutic strategy towards treating such diseases.[4,5] The first protein kinase inhibitors were developed in the early 1980s.[6] Breakthrough advances over the past decade have so far resulted in several small molecule kinase inhibitors approved for clinical use by US Food and Drug Administration. (Table 1.1) Currently, it is estimated that approximately one third of drug discovery programs target protein kinases.[4,7]

Table 1.1 – Small molecule kinase inhibitors approved for clinical use by US FDA

Kinase inhibitor	Disease treated	Targeted Kinase(s)
Axitinib (Inlyta)	Advanced renal cell carcinoma	Receptor tyrosine kinases including vascular endothelial growth factor receptors (VEGFR)-1, VEGFR-2, and VEGFR-3
Crizotinib (Xalkori)	Locally advanced or metastatic non-small cell lung cancer (NSCLC) that is anaplastic lymphoma kinase (ALK)-positive as detected by an FDA-approved test	Receptor tyrosine kinases including ALK, Hepatocyte Growth Factor Receptor (HGFR, c-Met), and Recepteur d'Origine Nantais (RON)
Dasatinib (Sprycel)	Philadelphia chromosome-positive (Ph+) chronic myeloid leukemia (CML)	BCR-ABL, SRC family (SRC, LCK, YES, FYN), c-KIT, EPHA2, and PDGFRβ
Erlotinib (Tarceva)	Locally advanced or metastatic non-small cell lung cancer (NSCLC) with gemcitabine	Inhibits the intracellular phosphorylation of tyrosine kinase associated with the epidermal growth factor receptor (EGFR)
Gefitinib (Iressa)	Clinical antitumor action	Inhibits the intracellular phosphorylation of numerous tyrosine kinases associated with transmembrane cell surface receptors, including the tyrosine kinases associated with the epidermal growth factor receptor (EGFR-TK)
Imatinib (Gleevec)	Philadelphia chromosome positive chronic myeloid leukemia (Ph^+ CML)	Bcr-abl tyrosine kinase, the constitutive abnormal tyrosine kinase created by the Philadelphia chromosome abnormality in CML
Lapatinib (Tykerb)	Advanced or metastatic breast cancer	Epidermal Growth Factor Receptor (EGFR [ErbB1]) and Human Epidermal Receptor Type 2 (HER2 [ErbB2])
Nilotinib (Tasigna)	Philadelphia chromosome positive chronic myeloid leukemia (Ph^+ CML)	BCR-ABL kinase
Pazopanib (Votrient)	Advanced renal cell carcinoma	Vascular endothelial growth factor receptor (VEGFR)-1, VEGFR-2, VEGFR-3, platelet-derived growth factor receptor (PDGFR)-α and -β, fibroblast growth factor receptor (FGFR) -1 and -3, cytokine receptor (Kit), interleukin-2 receptor inducible T-cell kinase (Itk), leukocyte-

		specific protein tyrosine kinase (Lck), and transmembrane glycoprotein receptor tyrosine kinase (c-Fms)
Ruxolitinib (Jafaki)	Intermediate or high-risk myelofibrosis, including primary myelofibrosis, post-polycythemia vera myelofibrosis and post-essential thrombocythemia myelofibrosis	Janus Associated Kinases (JAKs) JAK1 and JAK2
Sorafenib (Nexavar)	Unresectable hepatocellular carcinoma (HCC)	VEGFR and PDGFR and Raf kinases
Sunitinib (Sutent)	Gastrointestinal stromal tumor (GIST), advanced renal cell carcinoma and progressive, well-differentiated pancreatic neuroendocrine tumors (pNET)	Platelet-derived growth factor receptors (PDGFRα and PDGFRβ), vascular endothelial growth factor receptors (VEGFR1, VEGFR2 and VEGFR3), stem cell factor receptor (KIT), Fms-like tyrosine kinase-3 (FLT3), colony stimulating factor receptor Type 1 (CSF-1R), and the glial cell-line derived neurotrophic factor receptor (RET)
Vandetanib (Caprelsa)	Symptomatic or progressive medullary thyroid cancer with unresectable locally advanced or metastatic disease	Tyrosine kinases including members of the epidermal growth factor receptor (EGFR) family, vascular endothelial cell growth factor (VEGF) receptors, rearranged during transfection (RET), protein tyrosine kinase 6 (BRK), TIE2, members of the EPH receptors kinase family, and members of the Src family of tyrosine kinases
Vemurafenib (Zeboraf)	Unresectable or metastatic melanoma with $BRAF^{V600E}$ mutation	Some mutated forms of BRAF serine threonine kinase, including $BRAF^{V600E}$

Protein kinases consist of a highly conserved catalytic domain and widely varying regulatory subunits. The catalytic domain is bi-lobal with a smaller N-lobe, mainly composed of β-strands, and a larger α-helical C-lobe. (Figure 1.1) The two lobes are connected by a hinge linker forming a catalytic cleft. Adenosine triphosphate (ATP), the phosphate source in the catalytic reaction, binds in this catalytic cleft where the adenine ring of ATP makes key hydrogen bonding interactions with the hinge region of the kinase.

A set of conserved catalytic residues and a Mg^{2+} ion help align the phosphate groups of ATP for catalysis.[3,8,9] (Figure 1.2)

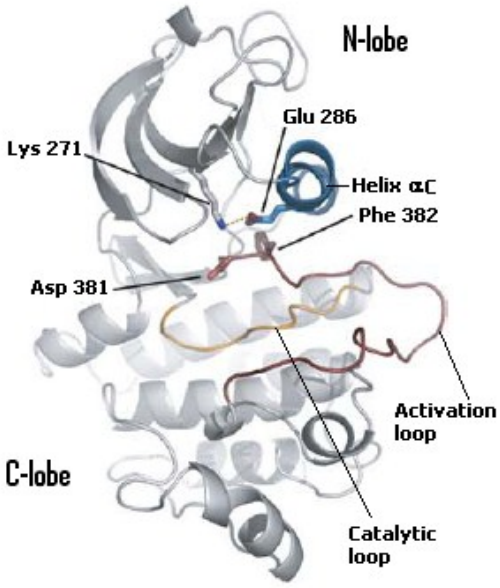

Figure 1.1 - Catalytic domain of Abl kinase [7]

The lysine (Lys 271 in figure 1.1) in β3 strand which is conserved in all kinase enzymes is functionally important for kinase catalysis. It forms ion pairs with the α and β phosphates of ATP in the active state and the lysine-ATP contact is further stabilized by an ion pair formed between this lysine and the catalytic glutamate residue (Glu 286 in figure 1.1) located at the center of the αC helix.[4] A Mg^{2+} ion identified as the activator Mg^{2+} binds to the β and γ phosphates of ATP and to the aspartate of the highly conserved DFG-motif (Asp 381 in figure 1.1) which is located in the activation loop. These interactions help to orient the γ phosphate for its transfer. [4,7,10,11] Another aspartate residue which is invariant in all kinases is located in the catalytic loop in the C-lobe and it is presumed to act as a base to remove a proton from the substrate hydroxyl group which attacks the γ phosphate of ATP. This aspartate residue is called the catalytic base.[10,11]

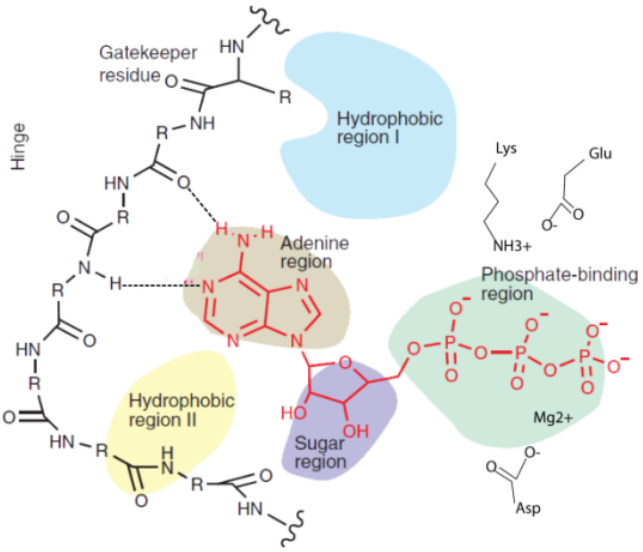

Figure 1.2 – ATP bound to the catalytic site of a kinase. The diagram also indicates the catalytically important residues in the kinase active site.[9]

1.2 Conformations of protein kinases and conformation specific ligands

Most protein kinases possess at least two distinct catalytic states; an active state where all the catalytic residues are in an optimal position for phosphate transfer and an inactive state with reduced catalytic activity.[2,12] The active conformations of most kinases appear to be very similar and conserved but the inactive conformations are more heterogeneous in nature.[3] ATP-competitive small molecule inhibitors that bind to specific active or inactive conformations of kinases have been developed and characterized. These ligands are categorized as Type I or Type II inhibitors. Type I inhibitors bind to the active conformation of kinases (Figure 1.3), while Type II inhibitors bind to a specific inactive conformation of kinases known as the 'DFG-out' conformation[3,9] (Figure 1.4). These conformation-specific 'DFG-in' and 'DFG-out' inhibitors can be used to probe the active site of kinases.

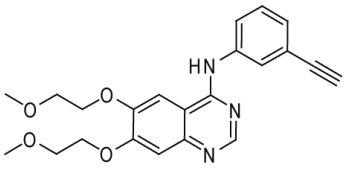

Erlotinib

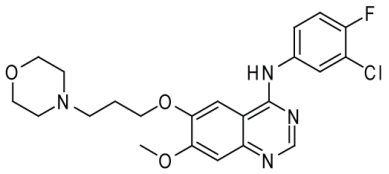

Gefitinib

Figure 1.3 – Clinically-approved small molecule inhibitors that bind to the active 'DFG-in' conformation of kinases.

Large and distinct conformational shifts in several catalytically important residues are observed between active and inactive kinases. A number of phosphorylation events along with protein-protein interactions regulate the conformation of the kinase active site and determines the activation state of the enzyme.[13]

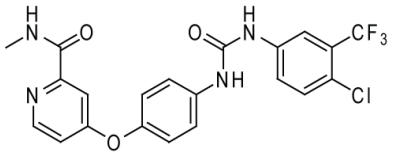

Sorafenib

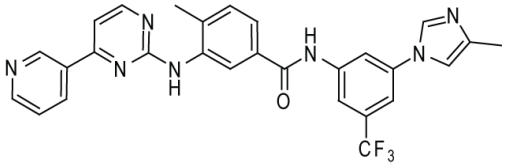

Nilotinib

Figure 1.4 – Clinically-approved small molecule inhibitors that bind to the 'DFG-out' inactive conformation of kinases.

For example, SRC family kinases contain regulatory SH2 and SH3 domains which make intramolecular interactions, locking the enzyme in an inactive conformation. The SH3 domain recognizes proline rich sequences and binds to the kinase-SH2 linker region, while the SH2 domain docks onto the back of the kinase C-lobe. Additionally, SRC kinases have a short C-terminal tail, which bears an autoinhibitory phosphorylation site that binds to the SH2 domain upon phosphorylation. These interactions stabilize the inactive conformations of SRC kinases.[14] (Figure 1.5) It has been shown that these intramolecular

interactions of the regulatory subunits can be disrupted by externally added peptide ligands. [15, 16, 17]

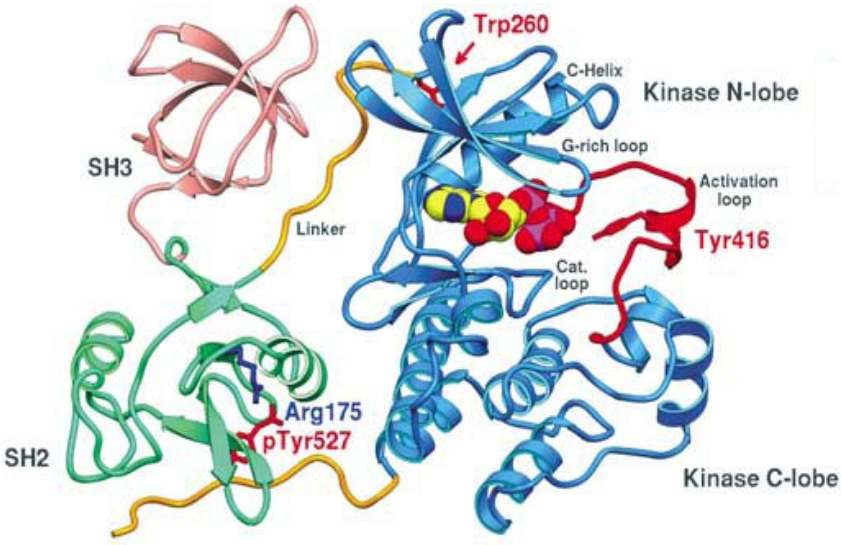

Figure 1.5 – SRC kinase containing its catalytic domain and regulatory SH2 and SH3 domains.[14] Phosphorylated Tyr527 residue is bound to the SH2 domain facilitating the inactive conformation of the enzyme. Proline rich linker region shown in yellow interacts with the SH3 domain in the inactive conformation.

Adjacent to the ATP-binding site all kinases contain an activation loop, which contains one or more residues that increase kinase catalytic activity upon phosphorylation. The activation loop also contains a highly conserved Asp-Phe-Gly (DFG) motif, the conformation of which is directly coupled to the activation state of the kinase.[3] In active kinases, the DFG-motif is said to be in a 'DFG-in' conformation where the Phe residue of the DFG-motif is buried in an adjacent hydrophobic pocket while the Asp residue faces towards the ATP-binding site. Type I inhibitors bind to this active conformation and are also known as 'DFG-in' inhibitors. Type I inhibitors typically bind in the region occupied by the adenine of ATP and form 1-3 hydrogen bonds with the backbone amides of the kinase hinge region. (Figure 1.6 a) In a distinct inactive state of

kinases known as the 'DFG-out' conformation, the Phe residue of the DFG-motif rotates away from its position in the active kinase and is directed into the ATP-binding site. This rotation of the Phe residue creates an allosteric binding site which is occupied by the type II or 'DFG-out' inhibitors. In addition to the extra hydrophobic contacts with the DFG-out pocket, type II inhibitors also form a pair of characteristic hydrogen bonds; one with a conserved glutamate in the αC helix and another with the backbone amide of the aspartate in the DFG-motif. Similar to type I inhibitors, type II inhibitors also maintain hydrophobic contacts with the adenine site and 1 - 2 hydrogen bonding interactions with the amide backbone of the hinge region.[3,9] (Figure 1.6 b)

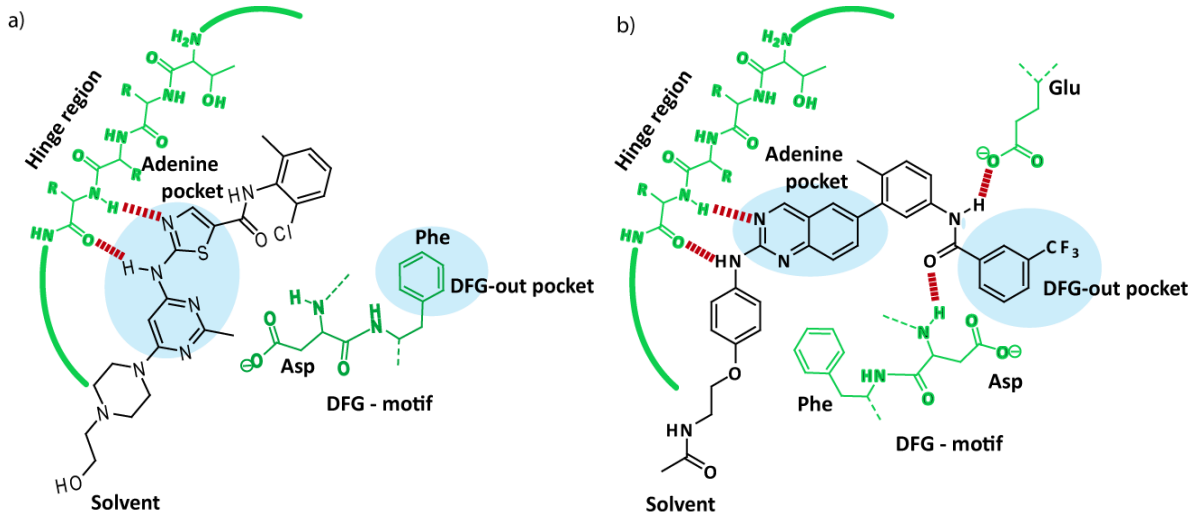

Figure 1.6 - a) A schematic representation of a type I inhibitor Dasatinib bound to its target in the active, DFG-in conformation. b) A schematic representation of a type II quinazoline inhibitor bound to its target in the inactive, DFG-out conformation

1.3 Tools for studying protein kinases

The conformation specific ligands can be extensively modified to obtain molecular tools that can be used to probe kinase active sites in order to understand their structure,

function and regulation. Therefore, our efforts were focused towards obtaining a set of ligands that could be used in a wide range of applications and aid us towards understanding the structure activity relationships of target protein kinases.

We have generated a panel of linkable protein kinase inhibitors (chapter 2) which can be successfully immobilized on chemically derivatized resins in order to generate affinity matrices useful towards enriching target kinases from complex lysate mixtures.[18] Additionally, proper modifications of these linkable inhibitors also permitted us to immobilize them on small proteins via SNAP-tag technology or Halo-tag technology and the resulting small molecule-protein conjugates have been used for the generation of bivalent inhibitors which are highly selective and could be localized to a desired cellular compartment during cellular studies (chapter 3).[19,20,21] This latter feature permits one to study the site specific function of a desired kinase target and thus can be beneficial towards understanding the function of the targeted kinase at different sub-cellular locations.

It is clear that the conformations of kinase active site are directly correlated to their activation states. Therefore, understanding the conformational dynamics of protein kinases and the factors that control them will aid in our understanding of the regulation of protein kinases. Activation loop phosphorylation, along with other phosphorylation events and protein-protein interactions, plays a significant role in controlling the conformation of protein kinase active sites. These events maintain the proper activation state of these important signaling enzymes. However, the exact mechanisms in which these phosphorylation events and regulatory domain interactions control the

conformation and activity of kinases still remain unclear. For example, the 'DFG-out' conformation appears to be energetically accessible to a number of kinases but the sequence and structural determinants that allow this transition are still poorly understood. Thus, it is still not possible to predict which kinases can be effectively targeted by Type II inhibitors, which are selective for the DFG-out inactive conformation.[12] Further knowledge of kinase conformational dynamics could be highly beneficial towards efficient inhibitor design. Therefore, there is a compelling need to explore the active site conformations of protein kinases and the factors that cause a kinase to adopt a specific conformation. This will also aid in our understanding of the catalytic regulation of protein kinases. To this end, I have generated conformation-specific, small molecule inhibitors that can be used to study the active site conformations of the SRC-family of protein kinases. In addition, these probes have been used to study the non-receptor tyrosine kinase ABL (Abelson tyrosine kinase), a kinase that is closely related to SRC. These inhibitors were used to study how different factors, including phosphorylation state, ligand binding, and ATP concentration, affect the active site conformations of the SRC- and ABL-family of kinases.

We have also generated small molecule inhibitors for protein kinases whose structural and functional relationships are still not properly understood. A panel of inhibitors was generated targeting IRE1α (Serine/threonine-protein kinase/endoribonuclease), which displays phosphorylation capacity via a kinase domain and endonuclease activity via an RNase domain. IRE1α plays a major role in the cellular unfolded protein response (UPR) pathway during ER stress conditions, but the structural

and functional relationship between the two enzymatic domains towards controlling the UPR pathway is not well understood.[22,23] Previously reported inhibitors of the IRE1α kinase domain have been shown to increase the RNase activity of the enzyme while inhibiting its kinase activity.[24] We have synthesized and tested a panel of type II inhibitors which bind to the kinase active site of IRE1α inhibiting both the kinase and RNase activity of this bi-enzymatic protein in a dose dependent manner. Due to this ability to decouple these enzymatic activities of IRE1α, these molecular tools aid us in controlling and understanding the fine relationship between the kinase and RNase domains and their roles in determining cellular fate under ER stress conditions.

1.4 References

1. Ubersax, J. A.; Ferrell, J. E., Jr., Mechanisms of specificity in protein phosphorylation. *Nature reviews* **2007,** *8* (7), 530-41.
2. Krishnamurty, R.; Maly, D. J., Chemical genomic and proteomic methods for determining kinase inhibitor selectivity. *Combinatorial chemistry & high throughput screening* **2007,** *10* (8), 652-66.
3. Krishnamurty, R.; Maly, D. J., Biochemical mechanisms of resistance to small-molecule protein kinase inhibitors. *ACS chemical biology 5* (1), 121-38.
4. Liao, J. J., Molecular recognition of protein kinase binding pockets for design of potent and selective kinase inhibitors. *Journal of medicinal chemistry* **2007,** *50* (3), 409-24.
5. Manning, G.; Whyte, D. B.; Martinez, R.; Hunter, T.; Sudarsanam, S., The protein kinase complement of the human genome. *Science* **2002,** *298* (5600), 1912-34.
6. Cohen, P., Protein kinases--the major drug targets of the twenty-first century? *Nature reviews. Drug discovery* **2002,** *1* (4), 309-15.
7. Levinson, N. M.; Kuchment, O.; Shen, K.; Young, M. A.; Koldobskiy, M.; Karplus, M.; Cole, P. A.; Kuriyan, J., A Src-like inactive conformation in the abl tyrosine kinase domain. *PLoS biology* **2006,** *4* (5), e144.
8. Adams, J. A., Kinetic and catalytic mechanisms of protein kinases. *Chemical reviews* **2001,** *101* (8), 2271-90.
9. Liu, Y.; Gray, N. S., Rational design of inhibitors that bind to inactive kinase conformations. *Nature chemical biology* **2006,** *2* (7), 358-64.

10. Johnson, L. N.; Noble, M. E.; Owen, D. J., Active and inactive protein kinases: structural basis for regulation. *Cell* **1996,** *85* (2), 149-58.

11. Roskoski, R., Jr., Src protein-tyrosine kinase structure and regulation. *Biochemical and biophysical research communications* **2004,** *324* (4), 1155-64.

12. Ranjitkar, P.; Brock, A. M.; Maly, D. J., Affinity reagents that target a specific inactive form of protein kinases. *Chemistry & biology 17* (2), 195-206.

13. Seeliger, M. A.; Ranjitkar, P.; Kasap, C.; Shan, Y.; Shaw, D. E.; Shah, N. P.; Kuriyan, J.; Maly, D. J., Equally potent inhibition of c-Src and Abl by compounds that recognize inactive kinase conformations. *Cancer research* **2009,** *69* (6), 2384-92.

14. Boggon, T. J.; Eck, M. J., Structure and regulation of Src family kinases. *Oncogene* **2004,** *23* (48), 7918-27.

15. Hantschel, O.; Nagar, B.; Guettler, S.; Kretzschmar, J.; Dorey, K.; Kuriyan, J.; Superti-Furga, G., A myristoyl/phosphotyrosine switch regulates c-Abl. *Cell* **2003,** *112* (6), 845-57.

16. Okishio, N.; Tanaka, T.; Fukuda, R.; Nagai, M., Differential ligand recognition by the Src and phosphatidylinositol 3-kinase Src homology 3 domains: circular dichroism and ultraviolet resonance Raman studies. *Biochemistry* **2003,** *42* (1), 208-16.

17. Payne, G.; Shoelson, S. E.; Gish, G. D.; Pawson, T.; Walsh, C. T., Kinetics of p56lck and p60src Src homology 2 domain binding to tyrosine-phosphorylated peptides determined by a competition assay or surface plasmon resonance. *Proceedings of the National Academy of Sciences of the United States of America* **1993,** *90* (11), 4902-6.

18. Perera, B. G.; Maly, D. J., Design, synthesis and characterization of "clickable" 4-anilinoquinazoline kinase inhibitors. *Molecular bioSystems* **2008,** *4* (6), 542-50.

19. Hill, Z. B.; Perera, B. G.; Maly, D. J., A chemical genetic method for generating bivalent inhibitors of protein kinases. *Journal of the American Chemical Society* **2009,** *131* (19), 6686-8.

20. Hill, Z. B.; Perera, B. G.; Maly, D. J., Bivalent inhibitors of the tyrosine kinases ABL and SRC: determinants of potency and selectivity. *Molecular bioSystems* **2011,** *7* (2), 447-56.

21. Hill, Z. B.; Perera, B. G.; Andrews, S. S.; Maly, D. J., Targeting diverse signaling interaction sites allows the rapid generation of bivalent kinase inhibitors. *ACS chemical biology* **2012,** *7* (3), 487-95.

22. Han, D.; Lerner, A. G.; Vande Walle, L.; Upton, J. P.; Xu, W.; Hagen, A.; Backes, B. J.; Oakes, S. A.; Papa, F. R., IRE1alpha kinase activation modes control alternate endoribonuclease outputs to determine divergent cell fates. *Cell* **2009,** *138* (3), 562-75.

23. Lin, J. H.; Li, H.; Yasumura, D.; Cohen, H. R.; Zhang, C.; Panning, B.; Shokat, K. M.; Lavail, M. M.; Walter, P., IRE1 signaling affects cell fate during the unfolded protein response. *Science* **2007,** *318* (5852), 944-9.

24. Han, D.; Upton, J. P.; Hagen, A.; Callahan, J.; Oakes, S. A.; Papa, F. R., A kinase inhibitor activates the IRE1alpha RNase to confer cytoprotection against ER stress. *Biochemical and biophysical research communications* **2008,** *365* (4), 777-83.

Chapter 2*

Design, Synthesis and Characterization of "Clickable" 4-Anilinoquinazoline Kinase Inhibitors

2.1 Summary

Immobilized kinase inhibitors have emerged as powerful reagents for the determination of kinase inhibitor selectivity and for the enrichment of protein targets from cellular lysates. Here, we report the design and synthesis of a set of "clickable" 4-anilinoquinazoline kinase inhibitors. We demonstrate that the attachment of a flexible tether that contains a bio-orthogonal azide functionality does not adversely affect the potency or selectivity of these inhibitors. Furthermore, we demonstrate the utility of these inhibitors through the generation of an affinity matrix for the enrichment of interacting proteins from cellular lysates.

2.2 Introduction

Reversible protein phosphorylation cascades are one of the major pathways by which eukaryotic cells sense and respond to their environment. Intracellular protein phosphorylation is controlled by two families of enzymes; protein kinases which transfer the γ-phosphate of ATP to serine, threonine and tyrosine residues and protein phosphatases which remove these phosphate groups.[1-5] As protein kinases control many

* Portions of this chapter are reproduced by permission of The Royal Society of Chemistry, from Perera, B. G. K.; Maly, D. J., Design, synthesis and characterization of "clickable" 4-anilinoquinazoline kinase inhibitors. *Molecular bioSystems* **2008,** *4* (6), 542-50.
http://pubs.rsc.org/en/content/articlelanding/2008/mb/b720014e

important cellular processes, mis-regulation of their activity coincides with a number of diseases such as cancer, diabetes and chronic inflammation. For this reason, there has been a great deal of interest in the development of small molecule kinase inhibitors as potential new drug therapies. Indeed, protein kinases represent one of the most highly pursued target families by pharmaceutical companies.[6]

The first inhibitors of protein kinases were discovered over 20 years ago.[6] Over the last fifteen years there has been steady progress towards the development of molecules with increased potency and greater selectivity for their desired targets.[7-9] The clinical success of the inhibitor Imatinib (Gleevec®) for the treatment of chronic myelogenic leukemia (CML) has demonstrated the potential of small molecules that specifically target kinases.[10,11] Currently, at least seven small molecule inhibitors that target protein kinases (Gleevec®, Sprycel®, Tykerb®, Sutent®, Nexavar®, Tarceva®, Iressa®) are clinically approved with many more in various stages of clinical trials. Despite major advances in our understanding of how to develop potent and selective inhibitors, the overall characteristics of most kinase inhibitors remain the same. The majority of small molecule kinase inhibitors bind in the highly conserved adenosine triphosphate (ATP)-binding site located between the N- and C-terminal lobes of the catalytic domain.[7-9] In addition, these molecules tend to make many of the same contacts as the purine ring of ATP, with selectivity being achieved through interactions with adjacent sub-pockets. The highly conserved nature of the ATP-binding pocket and the vast size of this enzyme family (518 kinases) make the development of selective inhibitors very challenging.

In order to determine the potential of an identified protein kinase inhibitor as a biological reagent or as a therapeutic agent it is useful to determine how selective it is for its desired target over other cellular targets. The ability to determine all of the cellular targets of a protein kinase inhibitor can provide valuable information into any phenotypic effects that are observed. In a clinical setting, the identification of potential off-targets of a protein kinase inhibitor may help explain any adverse effects that are observed. In addition, this information can also be used to identify new clinical uses of an already clinically approved inhibitor. For example, Imatinib has been used as therapy for gastrointestinal stromal tumors (GIST) after it was demonstrated to be a potent inhibitor of the tyrosine kinase c-KIT.[12-14] In many diseases it may be necessary to inhibit multiple kinases (multiplex inhibition) in order to observe a desired effect, therefore, multi-kinase (multiplex) inhibition is preferable.[15,16] Thus, detailing the absolute selectivity of a kinase inhibitor can give valuable insight into which combination of kinases are optimal for therapeutic intervention.

While the most commonly used method for determining kinase inhibitor selectivity is to perform activity assays with a diverse panel of purified kinases,[17,18] the large size of the human kinome makes an exhaustive screen impractical. To overcome these limitations a number of new methodologies have been developed for the determination of kinase inhibitor selectivity.[19-21] One such tool is the use of affinity linked to an insoluble support through a flexible linker. This affinity matrix is used to enrich cellular lysates for proteins that bind to the immobilized inhibitor. The use of affinity purification methods is attractive because it is an unbiased sampling of all of the proteins

in a cell. To date, this methodology has been used to identify the targets of a number of inhibitors that are used as biological reagents for studying kinase function and of the clinically approved kinase inhibitors Imatinib, Iressa and Dastanib.[23-28] Recently, a related methodology for the determination of kinase inhibitor selectivity that relies upon the use of immobilized kinase inhibitors has been described.[29] This technique utilizes non-specific immobilized kinase inhibitors as bait ligands for performing competition assays with an inhibitor of interest. An exhaustive study of the cellular targets of the ABL inhibitors imatinib, dasatinib and bosutinib was performed with this methodology. Finally, immobilized inhibitors have been used to identify the targets of protein kinase inhibitors in a modification of the yeast 2-hybrid assay called the yeast 3-hybrid assay.[30] In this methodology, a protein kinase inhibitor is linked through a flexible tether to a ligand that allows it to be displayed from a DNA-binding domain (DBD) of a transcription factor.[31,32] With this construct, cDNA libraries encoding proteins that are fused to an activation-domain (AD) can be screened in yeast. If a protein has an affinity for the inhibitor that is displayed from the DBD, the transcription factor will be reconstituted and this interaction will be detected through the expression of a reporter gene.

In order to utilize an immobilized inhibitor as an affinity reagent, it is necessary to identify a site that can be modified with a flexible linker that does not disrupt binding to its desired target. In addition, the linker must contain an orthogonal functionality that allows the inhibitor to be coupled to a solid support or to another molecule in a site-specific manner. Here, we describe the design, synthesis and biochemical characterization of a set of “clickable” 4-anilinoquinazoline kinase inhibitors. These inhibitors contain an

azide that allows selective conjugation to molecules containing alkynes *via* the Huisgen 1,3-dipolar cycloaddition. Furthermore, we demonstrate that the instillation of a flexible tether that contains an orthogonal chemical handle does not alter the overall biochemical properties of these inhibitors. Finally, we demonstrate the utility of these "clickable" kinase inhibitors through the generation of an affinity matrix.

2.3 Results and discussion

To develop a general method for creating a series of linkable kinase inhibitors we chose the 4-anilinoquinazoline scaffold. This scaffold has proven to be a versatile platform for the development of highly potent and selective kinase inhibitors.[33-45] 4-anilinoquinazolines have been best characterized as inhibitors of the ErbB family of receptor tyrosine kinases (epidermal growth factor receptor (EGFR), ErbB2 and ErbB4). Despite binding in the ATP-binding cleft, these inhibitors have been demonstrated to be highly selective inhibitors for the ErbB family over other kinases.[46] Furthermore, three ErbB family directed inhibitors based on the 4-anilinoquinazoline scaffold, Tarceva, Gefitinib and Lapatinib, have been clinically approved for the treatment of certain types of cancer. In addition to the ErbB family, potent and selective 4-anilinoquinazoline inhibitors have been developed for a number of other kinases (*e. g*., the tyrosine kinases SRC, ABL and vascular endothelial growth factor-2 VEGFR2 and the serine/threonine kinases p38 mitogen-activated protein kinase (MAPK) and Aurora A). To date, there are eleven structures of 4-anilinoquinazoline derivatives non-covalently bound to kinases (two of p38 MAPK (PDBIDs: 2bak and 1di9), five of EGFR (wild type and mutants) (PDBIDs:

2ito, 2ity, 2itz, 1xkk and 1m17), one of CDK2 (PDBID: 1di8), SRC (PDBID, 2h8h), Aurora A (PDBID: 2c6e) and Ret (PDBID: 2ivu)) in the Protein Data Bank (http://www.pdb.org). These structures demonstrate that, despite the diversity of the kinase targets, the orientation of inhibitor binding is highly conserved (Figure 2.1).[43,44,47-52] In all of these structures, the quinazoline ring directly overlaps with the purine ring of ATP, making many of the same hydrophobic contacts. In addition, there is a conserved hydrogen bonding interaction between the N-1 of the quinazoline and the hinge region of the kinase. Furthermore, in all of these structures the aniline substituent makes hydrophobic contacts with residues adjacent to the gatekeeper residue or in an allosteric selectivity pocket. It has been demonstrated that these interactions are responsible for a large amount of the selectivity and potency of these inhibitors. Finally, these structures show that substituents at C-6 and C-7 position of the quinazoline are directed out of the active site and into solvent.

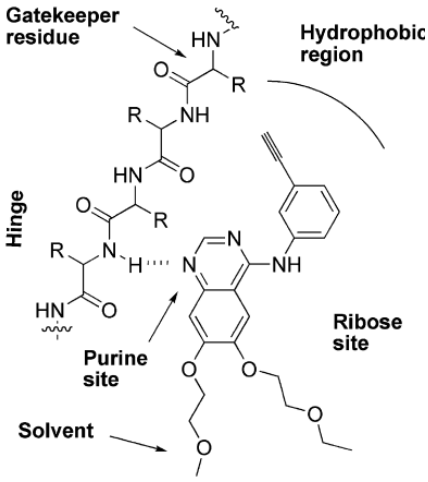

Figure 2.1 - General binding mode of 4-anilinoquinazoline kinase inhibitors.

The general structure of the "clickable" quinazoline derivatives is shown in Figure 2.2. Introduction of different anilines at the C-4 position modifies the potency and selectivity of these inhibitors. The C-7 position was chosen as the site of linker attachment because this position directly points out into solvent. Indeed, this position is often derivatized with polar functionalities to increase inhibitor solubility. For the linker, a propylpiperazine was selected because previous SAR studies for a number of kinases have shown that straight chain alkyls groups attached to a basic functionality do not disrupt inhibitor binding. Finally, a flexible polyethylene glycol (PEG) linker that contains a terminal azide was selected to link to the piperazine. The PEG linker increases inhibitor solubility and the terminal azide allows for selective derivatization with alkyne-containing molecules via the copper catalyzed Huisgen 1,3-dipolar cycloaddition.[53]

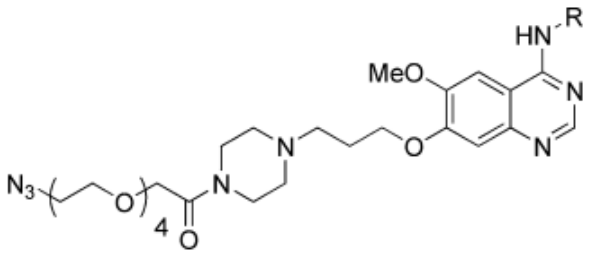

Figure 2.2 - General structure of "clickable" 4-anilinoquinazoline inhibitors.

To test the generality of this strategy, "clickable" analogs of the previously characterized 4-anilinoquinazolines shown in Figure 2.3 were generated. Inhibitor **1** and **2** are potent, ATP-competitive inhibitors of the non-receptor tyrosine kinases SRC and ABL.[42] Inhibitor **3** is a potent inhibitor of p38 MAPK.[45,48] Structural and biophysical studies have demonstrated that compound **3** preferentially binds to the inactive form of p38 MAPK. The quinazoline ring occupies the purine site, maintaining a hydrogen bond to the

hinge region, while the aminopyridine moiety occupies an adjacent sub-pocket that is formed by the displacement of a Phe from the DFG motif (DFG-out). This binding event has been shown to not only block the catalytic activity of p38, but also to block its activation by upstream MAPK kinases.[48] Inhibitor **4** is a potent inhibitor of Aurora A.[44] Structural studies have demonstrated that inhibitor **4** can also bind the DFG-out conformation of Aurora but further biochemical analysis has not been performed.

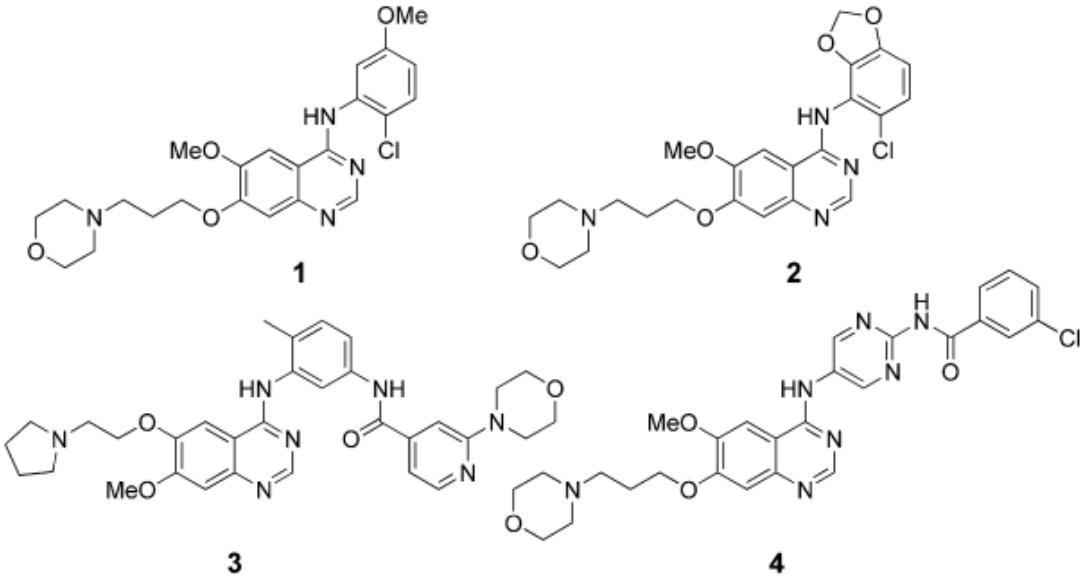

Figure 2.3 - Previously described 4-anilnoquinazoline kinase inhibitors.

In order to determine the effect of linker attachment on inhibitor potency and selectivity, quinazolines with and without a linker were generated. As shown in Scheme 2.1, the 6,7-dimethoxyquinazoline derivatives **6-9** were generated by performing an S_NAr displacement of the chloride group from the C-4 position of 4-Chloro-6,7-dimethoxyquinazoline **5** with anilines **A-D**. 2-chloro-5-methoxyaniline **A** is commercially

available and anilines **B-D** were generated from commercially available starting materials in 2-3 steps.[54-56] Subjecting quinazoline **5** to a 3-4-fold excess of anilines **A**, **C** and **D** in refluxing isopropyl alcohol yielded the desired products in high yield. When aniline **B** was subjected to the same conditions an unacceptable yield of quinazoline **7** was obtained. Deprotonation of aniline **B** with NaHMDS prior to nucleophilic displacement was found to increase the reaction rate and provided **7** in a more acceptable yield.

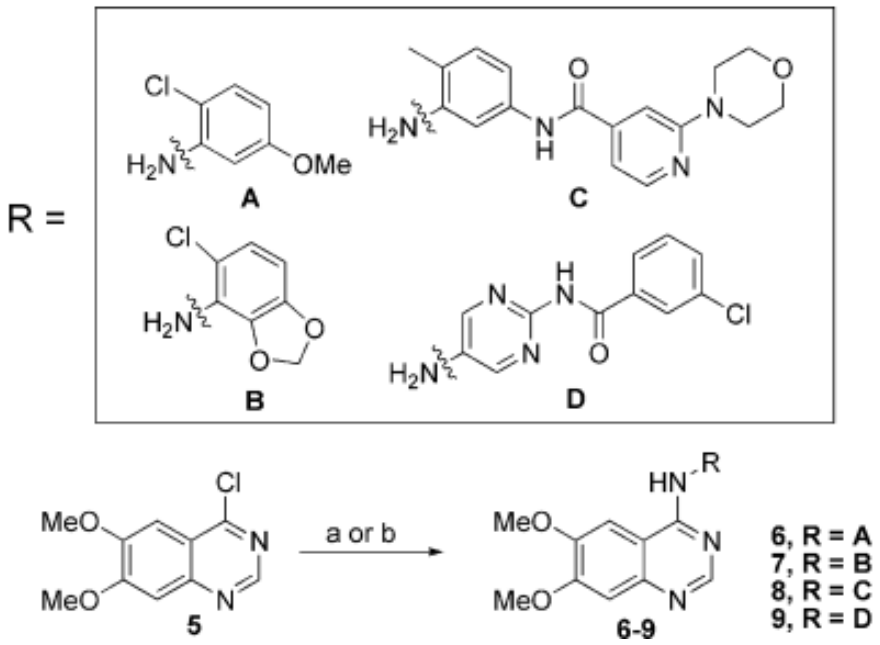

Scheme 2.1 - Synthesis of 6,7-dimethoxyquinazoline derivatives 6-9.

Reagents and conditions: a) R-NH2, i-PrOH, reflux, 76-95%; b) R-NH2, NaHMDS, 26%.

The synthesis of the "clickable" quinazoline derivatives is shown in Scheme 2.2. In order to increase the diversity of analogs that can be generated, a strategy was pursued that introduces the linker prior to instillation of the aniline substituent. The synthesis of quinazolines **17-20** began with removal of the *O*-benzyl group from 7-benzyloxy-6-

methoxy-3,4-dihydroquinazolin-4-one **10** with ammonium formate in the presence of a 3% palladium-on-carbon catalyst.[57] The subsequent phenol intermediate was acetylated with acetic anhydride in pyridine and then subjected to refluxing thionyl chloride to generate chloroquinazoline **11**. The acetyl protecting group was then removed with ammonia in methanol and the phenol was alkylated with 4-(3-bromopropyl) piperazine-1-carboxylic acid *tert*-butyl ester **22** to give quinazoline **12**. Despite numerous attempts to directly alkylate the phenol with 4-(3-propanol) piperazine-1-carboxylic acid tert-butyl ester **21** under standard Mitsunobu conditions, we were unable to obtain the desired product by this route. Chloroquinazoline **12** was subjected to the S_NAr conditions used for anilines **A-D** in Scheme 2.1 to generate 4-anilinoquinazolines **13-16**. The Boc group was removed from these intermediates with 28% TFA in DCM. The final "clickable" derivatives **17-20** were generated by coupling the deprotected 4-anilinoquinazolines to azido acid **23**.

To characterize the potency and selectivity of the compounds generated in Schemes 2.1 and 2.2, activity assays with purified kinases were performed (Table 2.1). The kinase targets that these inhibitors were optimized for, the tyrosine kinase SRC and the serine/threonine kinases p38 and Aurora A, were tested in these assays. In addition, the tyrosine kinase Csk and the serine/threonine kinase Slk were also tested as selectivity counter-screens. As expected, 6,7-dimethoxyquinazolines **6** and **7** inhibit SRC more strongly than the other kinases tested, with **7** demonstrating a five-fold greater potency than **6**.[42] Gratifyingly, the "clickable" analogs **17** and **18** do not show a decrease in

potency for SRC. Indeed, the presence of the piperazinyl-PEG linker was found to increase potency by 2-8 fold without a loss in selectivity.

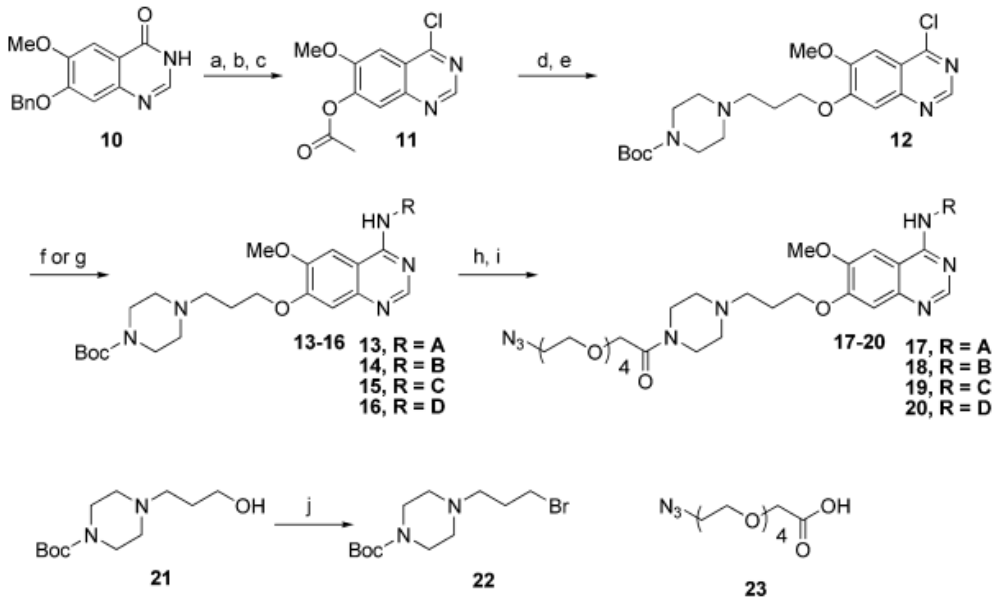

Scheme 2.2 - Synthetic route for "clickable" 4-anilinoquinazolines **17-20**.

Reagents and conditions: a) ammonium formate, 3% Pd/C, DMF, 80%; b) Ac_2O, pyridine, 120 °C, 82%; c) SOCl2, DMF, reflux; d) NH3/MeOH, reflux, 47% 2 for steps; e) 22, K_2CO_3, DMF, 80 °C, 6%; f) R-NH2, i-PrOH, reflux, 54-77%; g) R-NH2, NaHMDS, 40%; h) 28% TFA/MeOH; i) 23, HOBt, EDCI, DMF, 28-57% for 2 steps; j) CBr_4, PPh_3, THF, 46%.

6,7-dimethoxyquinazoline **8** was confirmed to be a potent and selective inhibitor of p38 MAP kinase with an IC_{50} of 24 nM.[45] Once again, the presence of the azide linker does not decrease the inhibitor's potency (IC_{50} = 10 nM) or significantly alter its selectivity. 6,7-dimethoxyquinazoline **9** was found to be a more potent inhibitor of Aurora A (IC_{50} = 0.13 µM) than the other kinases tested. The presence of the piperazinyl-PEG linker was found to increase potency for Aurora A by 2-3 fold. Notably, **9** and **20** were found to inhibit Aurora A less potently than expected (Inhibitor **4** was reported to have an

IC_{50} of <0.1 nM for Aurora A)[44] As noted earlier, these compounds have been demonstrated to bind to the DFG-out conformation of Aurora A and this decrease in observed potency may reflect a difference in activation state for the enzyme used in this assay. Regardless, the presence of the linker does not significantly alter the biochemical properties of these inhibitors as demonstrated by the similar potencies of **9** and **20**.

Table 2.1 - The in vitro activities of 6,7-dimethoxyquinazolines 6-9 and "clickable" quinazolines 17-20.

	IC_{50} (μM)				
	Src	p38	AurA	Csk	Slk
6	0.64	1.9	> 10	> 10	> 10
17	0.078	7.1	> 10	4.5	> 10
7	0.126	5.5	> 10	4.0	> 10
18	0.048	7.7	> 10	1.3	> 10
8	> 10	0.024	> 10	> 10	> 10
19	> 10	0.010	> 10	> 10	> 10
9	5.0	> 10	0.13	> 10	> 10
20	0.34	> 10	0.062	> 10	> 10

To demonstrate the utility of our "clickable" kinase inhibitors we generated an affinity matrix containing immobilized inhibitor **17**. To prepare an alkyne-derivatized solid support, a modification of a procedure that was described by Finn and coworkers was used (Scheme 2.3).[58] CarboxyLink agarose resin was incubated with 5-hexynoic acid 4-nitrophenyl ester to generate alkyne-derivatized solid support **24**. The loading of the solid support was determined by quantification of the amount of nitrophenol that was generated during the reaction. After extensive washing, agarose-alkyne beads **24** were treated with **17** in the presence DIPEA and CuI in MeOH. The reaction appeared to go to

50% completion after 48 h, as determined by the loss of soluble ligand **17** (determined by analysis of the reaction mixture with analytical HPLC). Affinity enrichment experiments with immobilized inhibitor **25**, and immobilized versions of inhibitors **18 - 20**, will be reported in due course.

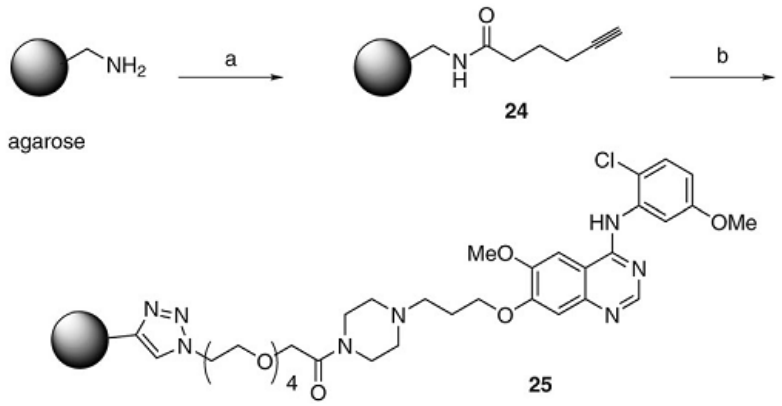

Scheme 2.3 - Preparation of immobilized inhibitor **25**.

Reagents and conditions: a) 5-hexynoic acid, NHS, EDCI, DMF; b) 19. 2,6-lutidine, 2,2'-bipyridine, CuBr, sodium ascorbate, DMF/H2O.

2.4 Conclusion

In summary, we have developed a general synthetic method for the preparation of "clickable" 4-anilinoquinazoline kinase inhibitors. The conserved binding orientation of this class of inhibitors allows for the attachment of a flexible tether at the C-7 position without altering their biochemical properties. Furthermore, the introduction of different anilines at the C-4 position allows for the generation of inhibitors that target a diverse set of kinases. In this study, we demonstrate that quinazolines that selectively target p38 MAPK, SRC and Aurora A can be modified without loss of potency or selectivity. This not only represents a diversity in kinase targets but also a diversity of kinase conformations

(active *versus* inactive). We demonstrate the utility of these inhibitors through the generation of an affinity matrix that can be used for the enrichment of interacting proteins from cellular lysates. In addition, we envision that these inhibitors can be used in a number of other applications that utilize linked kinase inhibitors.

2.5 Experimental

2.5.1 Synthetic Methods

General. Unless otherwise noted, all chemicals were purchased from commercial suppliers and used without further purification. ^{1}H-NMR was recorded on a Bruker AV300 NMR at an operation frequency of 300 MHz. Chemical shifts (δ) are given in ppm. Mass spectra were determined with a Bruker Esquire 3000 ion Trap. All HPLC analyses were performed utilizing a Varian Microsorb-MV C18 reverse-phase analytical column (4.6 mm × 150 mm).

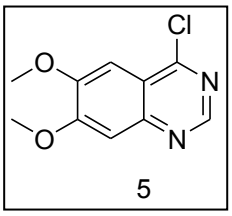

5

5. Compound **5** was prepared according to a previously reported protocol. A mixture of 6,7-dimethoxyquinazolin-4(3H)-one[59] (1.5 g, 7.3 mmol, 1.0 equiv.) and $POCl_3$ (1.8 mL, 19.7 mmol, 2.7 equiv.) was stirred at reflux for 1 h. $CHCl_3$ (6 mL) and cold H_2O (3 mL) were added to the reaction mixture and the solution was basified with 20% NaOH. The separated organic layer was washed with saturated $NaHCO_3$ (3.6 mL), H_2O (3.6 mL) and

brine (3.6 mL), then dried with Na_2SO_4 and concentrated *in vacuo* to afford 1.14 g (70%) of 4-chloro-6,7-dimethoxyquinazoline **5**. R_f = 0.5 (10% MeOH in CH_2Cl_2). ^{1}H-NMR (300 MHz, DMSO-d_6) δ 4.00 (s, 3H), 4.02 (s,3H), 7.41 (s, 1H), 7.47 (s, 1H), 8.89 (s, 1H). MS (ESI) Calcd for $C_{10}H_9ClN_2O_2$ $(M+H)^+$ 225.0, found 225.2.

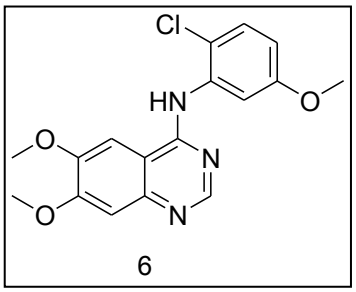

6

6. A mixture of 4-chloro-6,7-dimethoxyquinazoline **5** (0.05 g, 0.22 mmol, 1.0 equiv.) and 2-chloro-5-methoxyaniline **A** (0.14 g, 0.91 mmol, 4.0 equiv.) in *i*-PrOH was stirred at reflux for 2 days. The reaction mixture was allowed to stand and the solid that formed was filtered, washed with *i*-PrOH and dried under reduced pressure to afford 0.06 g (76%) of **6**. R_f = 0.5 (10% MeOH in CH2Cl_2). ^{1}H-NMR (300 MHz, DMSO-d_6) δ 3.78 (s, 3H), 3.99 (s, 3H), 4.01 (s, 3H), 7.04 (m, 1H), 7.18 (s, 1H), 7.28 (s, 1H), 7.57 (d, 1H, J = 9.0 Hz), 8.10 (s, 1H), 8.75 (s, 1H). MS (ESI) Calcd for $C_{17}H_{16}ClN_3O_3$ $(M+H)^+$ 346.1, found 346.3.

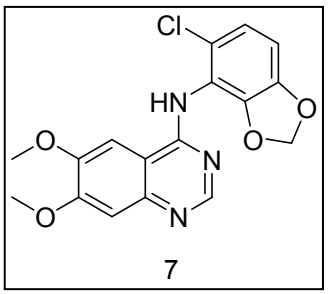

7

7. A solution of 1.5 M NaHMDS (0.32 mL, 0.48 mmol, 2.1 equiv.) was added to aniline **B**[56] (0.03 g, 0.47 mmol, 2.1 equiv.) in DMF (2.5 mL). After stirring the reaction mixture at rt

for 30 min, 4-chloro-6,7-dimethoxyquinazoline **5** (0.05 g, 0.22 mmol, 1.0 equiv.) was added and the mixture was stirred for 3 h. H_2O and EtOAc were added to the mixture and the organic phase was washed with H_2O and brine. The organic phase was concentrated and purified by reverse-phase HPLC to afford 0.034 g (26%) of **7**. R_f = 0.5 (10% MeOH in CH_2Cl_2). ^{1}H-NMR (300 MHz, MeOD) δ 4.28 (s, 3H), 4.30 (s, 1H), 6.29 (s, 2H), 7.14 (d, 1H, J = 8.4 Hz), 7.29 (d, 1H, J = 8.4 Hz), 7.46 (s, 1H), 8.15 (s, 1H), 8.85 (s, 1H). MS (ESI) Calcd for $C_{17}H_{14}ClN_3O_4$ $(M + H)^+$ 360.1, found 360.3.

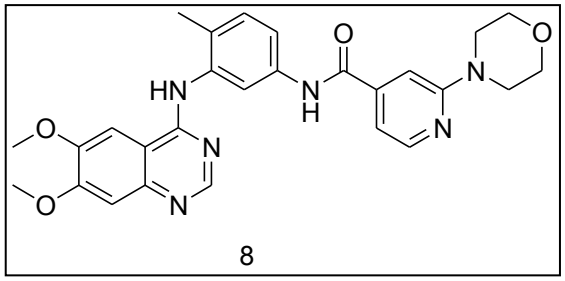

8

8. A mixture of 4-chloro-6,7-dimethoxyquinazoline (0.05 g, 0.22 mmol, 1.0 equiv.) and aniline **C**[55] (0.21 g, 0.66 mmol, 3.0 equiv.) in *i*-PrOH (5.0 mL) was stirred at reflux for 18 h. After cooling, the precipitate that formed was filtered, washed with *i*-PrOH and dried under reduced pressure to afford 0.104 g (95%) of **8**. R_f = 0.2 (10% MeOH in CH_2Cl_2). 1H-NMR (300 MHz, MeOD) δ 2.28 (s, 3H), 3.63 (t, 4H, *J* = 5.0 Hz), 3.85 (t, 4H, *J* = 5.0 Hz), 4.09 (s, 3H), 4.10 (s, 3H), 7.18 (d, 1H, *J* = 5.4 Hz), 7.23 (s, 1H), 7.39 (m, 1H), 7.44 (s, 1H), 7.57 (dd, 1H, *J* = 8.4 Hz, 2.1 Hz), 7.97 (m, 2H), 8.24 (d, 1H, *J* = 5.6 Hz), 8.60 (s, 1H). MS (ESI) Calcd for $C_{27}H_{28}N_6O_4$ $(M+H)^+$ 501.2, found 501.5

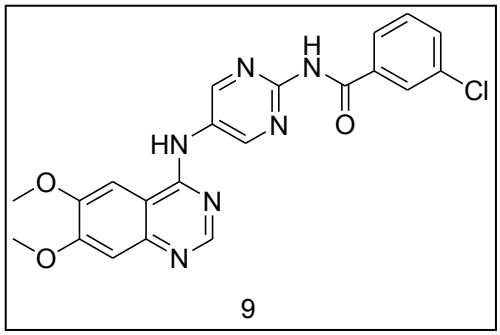

9

9. A mixture of 4-chloro-6,7-dimethoxyquinazoline (0.015 g, 0.07 mmol, 1.0 equiv.) and aniline **D**[54] (0.05 g, 0.2 mmol, 3.0 equiv.) in *i*-PrOH (1.51 mL) was stirred at reflux for 18 h. After cooling, the reaction mixture was filtered, washed with *i*-PrOH and dried under reduced pressure to afford 0.03 g (93%) of **9**. R_f = 0.4 (10% MeOH in CH_2Cl_2). ^{1}H-NMR (300 MHz, DMSO-d_6) δ 3.90 (s, 3H), 4.01 (s, 3H), 7.28 (s, 1H), 7.59 (m, 1H), 7.69 (m, 1H), 7.94 (m, 1H), 7.98 (m, 1H), 8.04 (s, 1H), 8.72 (s, 1H), 9.11 (s, 1H). MS (ESI) Calcd for $C_{21}H_{17}ClN_6O_3$ $(M+H)^+$ 437.1, found 437.2.

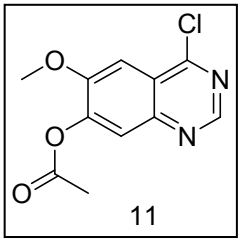

11

11. Compound **11** was prepared according to a previously reported protocol.[60] 3% Pd-on-carbon (0.32 g) was added to a suspension of **10**[57] (0.95 g, 3.36 mmol, 1.0 equiv.) in DMF (15.2 mL) under N_2. Ammonium formate (2.12 g, 33.6 mmol, 10.0 equiv.) was added portion-wise over 5 min and the reaction mixture was stirred at rt for 1 h, then heated to 80 ºC for 1 h. The hot reaction mixture was filtered and the solid was washed with DMF (10 mL). The filtrate was concentrated and the residue was suspended in water (15 mL). The pH of this solution was adjusted to 7 with 2M NaOH, followed by stirring at rt for 1 h.

The resulting solid was removed by filtration, washed with H2O and dried under reduced pressure to give 0.52 g (80%) of 7-hydroxy-6-methoxyquinazolin-4 (3H)-one. R_f = 0.3 (10% MeOH in CH_2Cl_2). ^{1}H-NMR (300 MHz, DMSO-d_6) δ 3.87 (s, 3H), 6.98 (s, 1H), 7.43 (s, 1H), 7.91 (s, 1H). MS (ESI) Calcd for $C_9H_8N_2O_3$ $(M+H)^+$ 193.1, found 193.1.

Pyridine (0.83 mL, 10.0 mmol, 2.5 equiv.) was added to a suspension of 7-hydroxy-6-methoxyquinazolin-4(3H)-one (0.8g, 4.0 mmol, 1.0 equiv.) in Ac_2O (5.9 mL). The mixture was heated to 120 ºC for 3 h and then allowed to cool to rt, poured into ice H_2O (20 mL) and stirred for 1 hour. The solid that formed was isolated by vacuum filtration and dried under reduced pressure to afford 0.8g (82%) of 3,4-dihydro-6-methoxy-4-oxoquinazolin-7-yl acetate. R_f = 0.4 (10% MeOH in CH_2Cl_2). ^{1}H-NMR (300 MHz, DMSO-d_6) δ 2.32 (s, 3H), 3.90 (s, 3H), 7.45 (s, 1H), 7.64 (s, 1H), 8.03 (s, 1H). MS (ESI) Calcd for $C_{11}H_{10}N_2O_4$ $(M+H)^+$ 235.1, found 235.1.

3,4-dihydro-6-methoxy-4-oxoquinazolin-7-yl acetate (1.17 g, 5.0 mmol) was suspended in thionyl chloride (12.2 mL) and two drops of DMF was added. The mixture was stirred at reflux for 2 h. The reaction mixture was then allowed to cool to rt and the solvent was removed *in vacuo*. After concentrating the solution, the residue was azeotroped with toluene to afford **11**. The product was used in the next reaction without further purification. MS (ESI) Calcd for $C_{11}H_{11}ClN_2O_3$ $(M+H)^+$ 253.0, found 253.1.

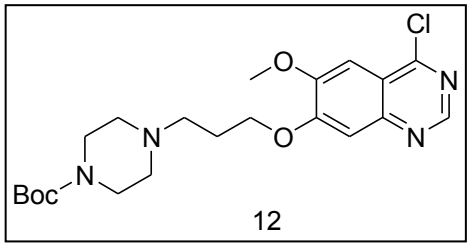

12

12. 7N NH_3 in MeOH (47.0 mL) was added to 11 (5.0 mmol) and the mixture was heated at 80 ^{o}C for 15 min. The mixture was cooled to rt and the solvent was removed *in vacuo*. The residue was dissolved in H_2O (12 mL) and the pH was adjusted to 7. The resulting solid was filtered, washed with water (5 mL) and dried under reduced pressure to afford 0.49 g (47%) of 4-chloro-6-methoxyquinazolin-7-ol. R_f = 0.5 (10% MeOH in CH_2Cl_2). ^{1}H-NMR (300 MHz, DMSO-d_6) δ 4.00 (s, 3H), 7.29 (s, 1H), 7.40 (s, 1H), 8.80 (s, 1H). MS (ESI) Calcd for $C_9H_7ClN_2O_2$ $(M+H)^+$ 211.0, found 211.1.

A mixture of 4-chloro-6-methoxyquinazolin-7-ol (0.4 g, 1.3 mmol, 1.2 equiv.), 22 (0.23 g, 1.1 mmol, 1.0 equiv.) and K_2CO_3 in DMF (1.8 mL) was heated to 80 ºC for 24 h. The crude reaction mixture was diluted with MeCN/H_2O and purified by reverse-phase HPLC to afford 0.22 g (46%) of **12**. R_f = 0.6 (10% MeOH in CH_2Cl_2). ^{1}H-NMR (300 MHz, MeOD) δ 1.51 (s, 9H), 1.65 (br m, 2H), 2.44 (t, 4H, J = 6.6 Hz), 3.49 (t, 4H, J = 7.2 Hz), 4.08 (s, 3H), 4.41 (t, 2H, J = 5.1 Hz), 7.44 (s, 1H), 7.55 (s, 1H), 8.85 (s, 1H). MS (ESI) Calcd for $C_{21}H_{29}ClN_4O_4$ $(M+H)^+$ 437.2, found 437.3.

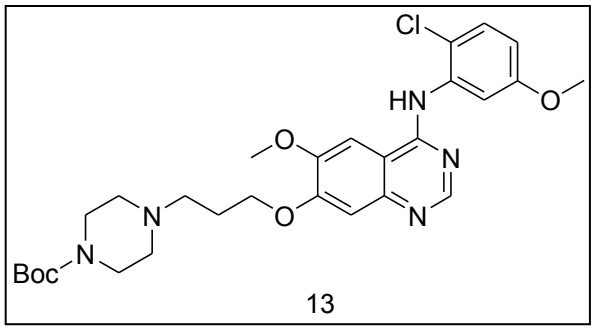

13

13. A mixture of **12** (0.04 g, 0.097 mmol, 1.0 equiv.) and aniline **A** (0.06 g, 0.39 mmol, 4.0 equiv.) in *i*-PrOH was refluxed for 17 h. The reaction mixture was concentrated in vacuo and the crude product was purified by reverse-phase HPLC to afford 0.03 g (54%) of **13**.

R_f = 0.4 (10% MeOH in CH_2Cl_2). MS (ESI) Calcd for $C_{28}H_{36}ClN_5O_5$ $(M+H)^+$ 558.1, found 558.4.

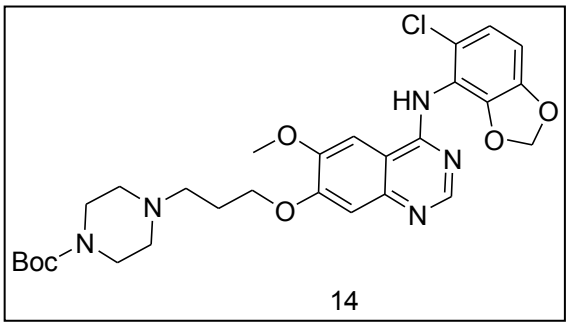

14

14. A solution of 1.5 M NaHMDS (0.07 mL, 0.11 mmol, 2.1 equiv.) was added to aniline **B**[56] (0.018 g, 0.11 mmol, 2.1 equiv.) in DMF (2.5 mL). After stirring the reaction mixture at rt for 30 min, 12 (0.029 g, 0.052 mmol, 1.0 equiv.) was added and the mixture was stirred for 3 h. H_2O and EtOAc were added to the mixture and the organic phase was washed with H_2O and brine. The organic phase was concentrated and purified by reverse-phase HPLC to afford 0.012 g (40%) of **14**. R_f = 0.4 (10% MeOH in CH_2Cl_2). MS (ESI) Calcd for $C_{28}H_{34}ClN_5O_6$ $(M+H)^+$ 572.2, found 572.4.

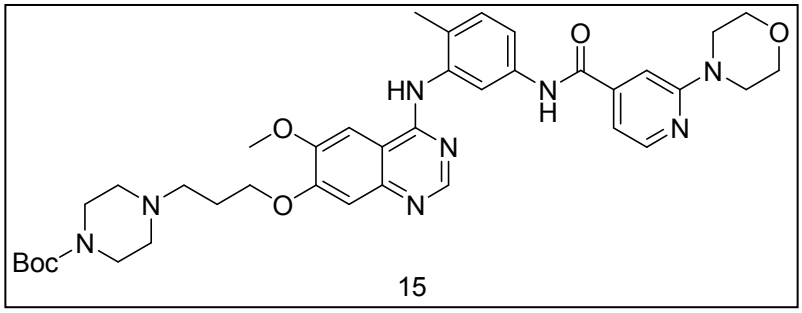

15

15. A mixture of **12** (0.05 g, 0.1 mmol, 1.0 equiv.) and aniline **C** (0.13 g, 0.37 mmol, 3.7 equiv.) in *i*-PrOH was refluxed for 12 h. The reaction mixture was concentrated in vacuo and the crude product was purified by reverse-phase HPLC to afford 0.06 g (77%) of

product **15**. R_f = 0.4 (10% MeOH in CH_2Cl_2). MS (ESI) Calcd for $C_{38}H_{48}N_8O_6$ $(M+H)^+$ 713.4, found 713.5

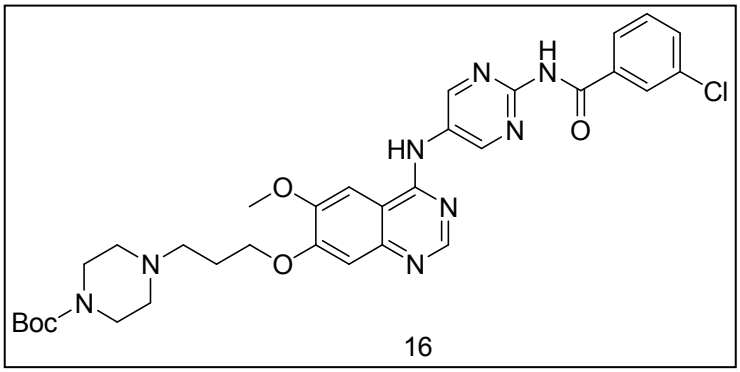

16

16. A mixture of **12** (0.054 g, 0.12 mmol, 1.0 equiv.) and aniline **D** (0.12 g, 0.5 mmol, 4.0 equiv.) in *i*-PrOH was refluxed for 12 h. The reaction mixture was concentrated in vacuo and the crude product was purified by reverse-phase HPLC to afford 0.06 g (69%) of **16**. R_f = 0.2 (10% MeOH in CH_2Cl_2). MS (ESI) Calcd for $C_{32}H_{37}ClN_8O_5$ $(M+H)^+$ 649.3, found 649.4.

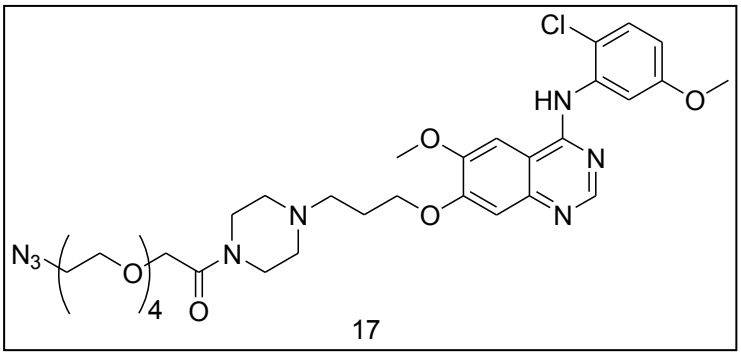

17

17. **13** (0.023 g, 0.041 mmol) was dissolved in a solution of 28% TFA in MeOH (1 mL) and the mixture was stirred for 3 h at rt. The reaction mixture was then concentrated and used in the next step without further purification. MS (ESI) Calcd for $C_{23}H_{28}ClN_5O_3$ $(M+H)^+$ 458.2, found 458.2.

EDCI (0.009 g, 0.045 mmol, 1.1 equiv.) was added to a mixture of the deprotected amine (0.019 g, 0.041 mmol, 1.0 equiv.), 23 (0.015 g, 0.054 mmol, 1.3 equiv.), HOBt (0.008 g, 0.054 mmol, 1.3 equiv.) and DIPEA (0.02 mL, 0.124 mmol, 3.0 equiv.) in DMF (0.1 mL). The reaction mixture was stirred for 12 h at rt, then diluted with MeCN/H_2O and purified by reverse-phase HPLC to afford 0.011 g (36%) of **17** after 2 steps. R_f = 0.4 (10% MeOH in CH_2Cl_2). ^{1}H-NMR (300 MHz, DMSO-d_6) δ 1.66 (m, 2H), 2.07 (t, 4H), 4.12-4.79 (m, 32H), 7.84 (dd, 1H, J = 8.7 Hz, 3.0 Hz), 7.98 (d, 1H, J = 2.7 Hz), 8.18 (s, 1H), 8.35 (d, 1H, J = 9.0 Hz), 8.84 (s,1H), 9.48 (s, 1H). MS (ESI) Calcd for $C_{33}H_{45}ClN_8O_8$ $(M+H)^+$ 717.3, found 717.5. Analytical reverse-phase HPLC analysis according to General Conditions (t_R = 13.0 min), purity >99%, 220 nM.

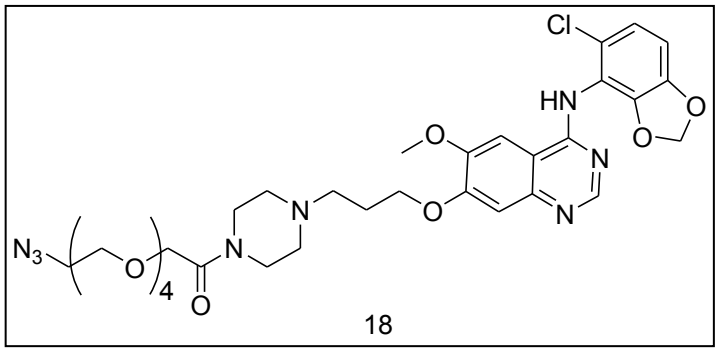

18

18. **18** was made by the same procedure as **17**. 28% yield after 2 steps. Deprotected amine. ^{1}H-NMR (300 MHz, MeOD) δ 1.40 (m, 2H), 2.21-2.46 (m, 4H), 3.46-4.44 (m, 11H), 6.09 (s, 2H), 6.94 (d, 1H, J = 8.7 Hz), 7.09 (d, 1H, J = 8.4 Hz), 7.30 (s, 1H), 8.00 (s, 1H), 8.70 (s, 1H). MS (ESI) Calcd for $C_{23}H_{26}ClN_5O_4$ $(M+H)^+$ 472.2, found 472.3. **18.** R_f = 0.4 (10% MeOH in CH_2Cl_2). MS (ESI) Calcd for $C_{33}H_{43}ClN_8O_9$ $(M+H)^+$ 731.3, found 731.3. Analytical reverse-phase HPLC analysis according to General Conditions (t_R = 13.4 min), purity >99%, 220 nM.

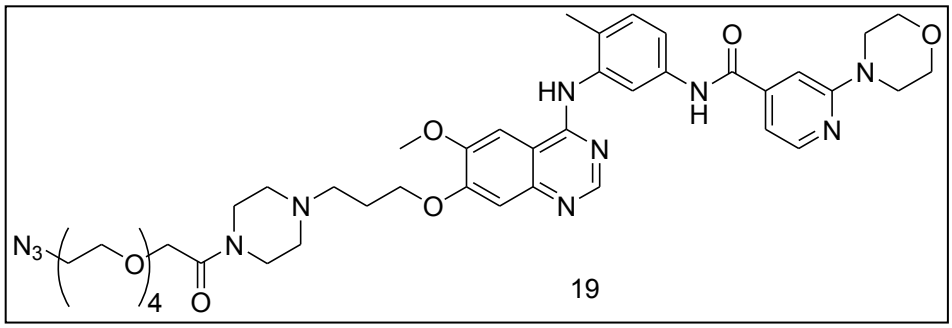

19

19. **19** was made by the same procedure as **17**. 44% yield after 2 steps. Deprotected amine. ^{1}H-NMR (300 MHz, MeOD) δ 1.36 (br m, 2H), 2.28 (s, 3H), 2.43 (m, 2H), 3.47-3.87 (m, 18H), 4.09 (s, 3H), 7.29 (m, 2H), 7.32 (s,1H), 7.62 (m, 1H), 7.72 (m, 1H), 7.94-7.99 (m, 2H), 8.15 (s, 1H), 8.62 (s, 1H). MS (ESI) Calcd for $C_{33}H_{40}ClN_8O_4$ $(M+H)^+$ 613.3, found 613.3. **19.** Rf = 0.3 (10% MeOH in CH2Cl2). MS (ESI) Calcd for $C_{43}H_{57}ClN_{11}O_9$ $(M+H)^+$ 872.4, found 872.6. Analytical reverse-phase HPLC analysis according to General Conditions (t_R = 11.5 min), purity >99%, 220 nM.

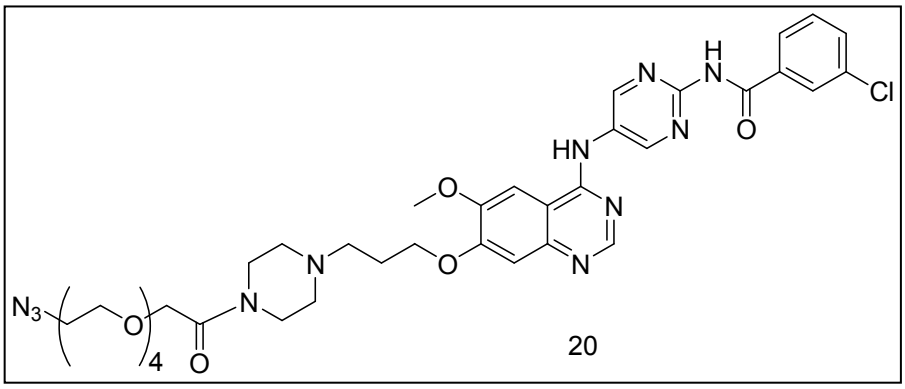

20

20. **20** was made by the same procedure as **17**. 57% yield after 2 steps. R_f = 0.3 (10% MeOH in CH2Cl2). ^{1}H-NMR (300 MHz, DMSO-d_6) δ 1.25-4.29 (m, 35H), 7.33 (s, 1H), 7.59 (m, 1H), 7.68 (m,1H), 7.96-8.03 (m, 3H), 8.66 (s, 1H), 9.12 (s, 1H). MS (ESI) Calcd for

$C_{37}H_{46}ClN_{11}O_8$ $(M+H)^+$ 808.3, found 808.5. Analytical reverse-phase HPLC analysis according to General Conditions (t_R = 13.3 min), purity >99%, 220 nM.

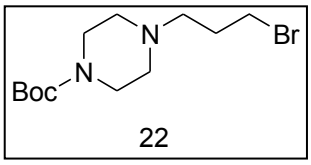

22

22. CBr_4 (4.21 g, 12.7 mmol, 1.1 equiv.) was added to a solution of **21** (2.82 g, 11.5 mmol, 1.0 equiv.) in dry THF (46.1 mL). A solution of PPh_3 (3.75 g, 13.3 mmol, 1.15 equiv.) in dry THF (12.2 mL) was added dropwise and the reaction mixture was stirred at rt for 2 days. The reaction mixture was concentrated in vacuo, extracted with diethyl ether (5 x 6 mL) and purified by flash chromatography (40% EtOAc in hexanes) to afford 1.49 g (42%) of **22**. R_f = 0.35 (40% EtOAc in hexanes). ^{1}H-NMR (300 MHz, $CDCl_3$) δ 1.48 (s, 9H), 1.20-2.09 (m, 2H), 2.40 (t, 4H, J = 4.98 Hz), 2.50 (t, 2H, J = 6.7 Hz), 3.44 (t, 4H, J = 5.1 Hz), 3.49 (t, 2H, 6.7 Hz). MS (ESI) Calcd for $C_{12}H_{23}BrN_2O_2$ $(M+H)^+$ 307.1, found 307.2.

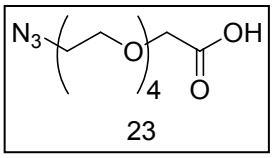

23

23. A mixture of ethyl 2-(2-(2-(2-(2-azidoethoxy)ethoxy)ethoxy)ethoxy)acetate[61] (0.9 g, 3.0 mmol, 1.0 equiv.) and K_2CO_3 (1.26 g, 9.1 mmol, 3.0 equiv.) in 80% EtOH (6.0 mL) was refluxed for 12 h. The mixture was concentrated and H_2O was added. The pH of this solution was adjusted to 2 with 5M HCl and the product was extracted into EtOAc. The organic layer was dried (Na_2SO_4) and concentrated *in vacuo* to afford 0.54 g (64%) of **23** as an oil. R_f = 0.1 (60% EtOAc in hexanes). ^{1}H-NMR (300 MHz, $CDCl_3$) δ 3.42 (t, 2H, J = 4.8

Hz), 3.69 - 3.80 (m, 14 H), 4.18 (s, 2H). MS (ESI) Calcd for $C_{10}H_{19}N_3O_6$ $(M+Na)^+$ 300.1, found 300.2.

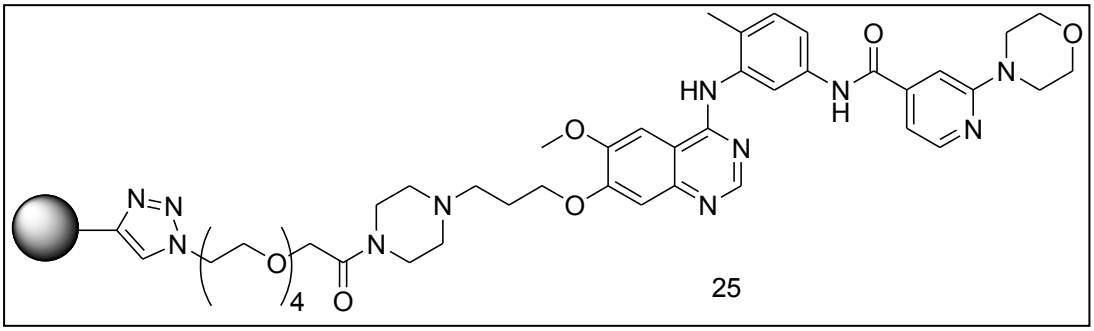

Preparation of immobilized inhibitor 25.

A solution of inhibitor **17** (0.5 µmol), DIPEA (7.5 µmol) and CuI (0.5 µmole) in 0.3 mL of MeOH was added to 50 mg of alkyne -agarose beads **24** in a disposable frit. The reaction mixture was agitated with a gentle flow of N_2 for 2 min, capped and rotated for 48 h at rt. To monitor the reaction an aliquot of the reaction mixture was removed, co-injected with a UV standard, and analyzed by analytical HPLC for the disappearance of inhibitor **17**. After 48 h, the reaction appeared to go to 50% completion. The reaction mixture was then drained and the beads were washed with 10 column volumes of DMF, H_2O, MeOH, 0.1 M EDTA, H_2O and DMF. The beads were stored at 4 °C until further use.

2.5.2 Kinase activity assays.

SRC. Inhibitors (Initial concentration: 10 µM, 3-fold dilutions: 9 dilutions) were assayed in duplicate against recombinant full-length SRC (final concentration = 13.2 nM) in an assay containing 25 mM HEPES, pH 7.4, 130 µM SRC-family peptide substrate EIYGEFKKK, 10 mM MgCl2, 0.5 µCi of γ-32P-ATP ([ATP] << Km (ATP)] and 0.1 mg/mL BSA in a final volume of 32 µL. The reactions were incubated for 1 h at rt and terminated by transferring 5 µL of

the reaction mixture to a phosphocellulose membrane. The membranes were washed with 0.5% phosphoric acid (4x) and acetone (1x) and quantitated by phosphor imaging.

p38. Inhibitors (Initial concentration: 10 μM, 3-fold dilutions: 9 dilutions) were assayed in duplicate against p38 in an assay containing 25 mM HEPES, pH 7.4, 30 μM MAPK substrate peptide, 10 mM MgCl2, 0.5 μCi of γ-32P-ATP ([ATP] << Km (ATP)] and 0.1 mg/mL BSA in a final volume of 32 μL. The reactions were incubated for 3 h at rt and terminated by transferring 5 μL of the reaction mixture to a phosphocellulose membrane. The membranes were washed with 0.5% phosphoric acid (4x) and acetone (1x) and quantitated by phosphor imaging.

Csk. Inhibitors (Initial concentration: 10 μM, 3-fold dilutions: 9 dilutions) were assayed in duplicate against recombinant Gst-Csk (final concentration = 14 nM) in an assay containing 25 mM HEPES, pH 7.4, 50 μM Csk peptide substrate KKKKEEIYFFF, 10 mM MgCl2, 0.5 μCi of γ-32P-ATP ([ATP] << Km (ATP)] and 0.1 mg/mL BSA in a final volume of 32 μL. The reactions were incubated for 3 h at rt and terminated by transferring 5 μL of the reaction mixture to a phosphocellulose membrane. The membranes were washed with 0.5% phosphoric acid (4x) and acetone (1x) and quantitated by phosphor imaging.

Slk. Inhibitors (Initial concentration: 10 μM, 3-fold dilutions: 9 dilutions) were assayed in duplicate against Slk in an assay containing 25 mM HEPES, pH 7.4, Myelin Basic Protein (0.2 mg/mL), 10 mM MgCl2, 0.5 μCi of γ-32P-ATP ([ATP] << Km (ATP)] and 0.1 mg/mL BSA in a final volume of 32 μL. The reactions were incubated for 3 h at rt and terminated by transferring 5 μL of the reaction mixture to a phosphocellulose membrane. The

membranes were washed with 0.5% phosphoric acid (4x) and acetone (1x) and quantitated by phosphor imaging.

2.6 Acknowledgements

We thank M. A. Seeliger and J. Kuriyan (University of California, Berkeley) for the plasmid containing the full length chicken c-SRC gene and for purified GST-Csk. We thank Stefan Knapp (University of Oxford, Structural Genomics Consortium) for the Slk bacterial expression vector. We thank Pratistha Ranjitkar and Charles N. Buser III for the synthesis of Csk and SRC peptide substrates, respectively. This work was supported by the University of Washington.

2.7 References

1. T. Hunter, Cell, 2000, 100, 113-127.
2. S.R. Hubbard and J. H. Till, Annu. Rev. Biochem., 2000, 69, 373-398.
3. M. Gallego and D. M. Virshup, Curr. Opin. Cell Biol., 2005, 17, 197-202.
4. N. K. Tonks, Nat. Rev. Mol. Cell. Biol., 2006, 7, 833-846.
5. G. Manning, D. B. Whyte, R. Martinez, T. Hunter and S. Sudarsanam, Science, 2002, 298, 1912-1934.
6. P. Cohen, Nat. Rev. Drug Discov., 2002, 1, 309-315.
7. Z. A. Knight and K. M. Shokat, Chem. Biol., 2005, 12, 621-637.
8. M. E. Noble, J. A. Endicott and L. N. Johnson, Science, 2004, 303, 1800-1805.
9. J. J. Liao, J. Med. Chem., 2007, 50, 409-424.
10. M. D. Moen, K. McKeage, G. L. Plosker and M. A.Siddiqui, Drugs, 2007, 67, 299-320.
11. M. A. Siddiqui and L. J. Scott, Drugs, 2007, 67, 805-820.
12. E. Buchdunger, C. L. Cioffi, N. Law, D. Stover, S. Ohno-Jones, B. J. Druker and N. B. Lydon, J Pharmacol Exp Ther, 2000, 295, 139-145.
13. M. C.Heinrich, D. J. Griffith, B. J. Druker, C. L. Wait, K. A. Ott and A. J. Zigler, Blood, 2000, 96, 925-932.
14. H. Joensuu, P. J. Roberts, M. Sarlomo-Rikala, L. C. Andersson, P. Tervahartiala, D. Tuveson, S. Silberman, R. Capdeville, S. Dimitrijevic, B. Druker and G. D. Demetri, N. Engl. J. Med. 2001, 344, 1052-1056.
15. J. Adams, P. Huang and D. Patrick, Curr. Opin. Chem. Biol., 2002, 6, 486-492

16. S. Wilhelm, C. Carter, M. Lynch, T. Lowinger, J. Dumas, R. A. Smith, B. Schwartz, R. Simantov and S. Kelley, Nat. Rev. Drug Discov., 2006, 5, 835-844

17. S. P. Davies, H. Reddy, M. Caivano and P. Cohen, Biochem. J., 2000, 351, 95-105.

18. J. Bain, H. McLauchlan, M. Elliott and P. Cohen, Biochem. J., 2003, 371, 199-204.

19. C. Kung and K.M. Shokat, ChemBioChem, 2005, 6, 523-526.

20. S. L. Gallion and D. Qian, Curr. Opin. Drug Discov. Dev., 2005, 8, 638-645

21. R. Krishnamurty and D. J. Maly, Comb. Chem. High Throughput Screening, 2007, 10, 652-666.

22. H. Daub, Biochim. Biophys. Acta, 2005, 1754, 183-190.

23. S. Bach, M. Knockaert, J. Reinhardt, O. Lozach, S. Schmitt, B. Baratte, M. Koken, S. P. Coburn, L. Tang, T. Jiang, D. C. Liang, H. Galons, J. F. Dierick, L. A. Pinna, F. Meggio, F. Totzke, C. Schachtele, A. S. Lerman, A. Carnero, Y. Wan, N. Gray and L.Meijer, J. Biol. Chem., 2005, 280, 31208-31219.

24. L. Tang, M. H. Li, P. Cao, F. Wang, W. R. Chang, S. Bach, J. Reinhardt, Y. Ferandin, H. Galons, Y. Wan, N. Gray, L. Meijer, T. Jiang and D. C Liang, J. Biol. Chem., 2005, 280, 31220-31229.

25. D. Brehmer, Z. Greff, K. Godl, S. Blencke, A. Kurtenbach, M. Weber, S. Muller, B. Klebl, M. Cotten, G. Keri, J. Wissing and H. Daub, Cancer Res., 2005, 65, 379-382.

26. K. Godl, O. J. Gruss, J. Eickhoff, J. Wissing, S. Blencke, M. Weber, H. Degen, D. Brehmer, L. Orfi, Z. Horvath, G. Keri, S. Muller, M. Cotten, A. Ullrich and H. Daub, Cancer Res., 2005, 65, 6919-6926.

27. U. Rix, O. Hantschel, G. Dürnberger, L. L. Remsing Rix, M. Planyavsky, N. V. Fernbach, I. Kaupe, K. L. Bennett, P. Valent, J. Colinge, T. Köcher and G Superti-Furga, Blood, 2007, 110, 4055-4063.

28. O. Hantschel, U. Rix, U. Schmidt, T. Bürckstümmer, M. Kneidinger, G. Schütze, J. Colinge, K. L. Bennett, W. Ellmeier, P. Valent and G. Superti-Furga, Proc. Natl. Acad. Sci. U. S. A., 2007, 104, 13283-13288.

29. M. Bantscheff, D. Eberhard, Y. Abraham, S. Bastuck, M. Boesche, S. Hobson, T. Mathieson, J. Perrin, M. Raida, C. Rau, V. Reader, G. Sweetman, A. Bauer, T. Bouwmeester, C. Hopf, U. Kruse, G. Neubauer, N. Ramsden, J. Rick, B. Kuster and G. Drewes, Nat. Biotechnol., 2007, 25, 1035-1044.

30. E. J. Licitra and J. O. Liu, Proc. Natl. Acad. Sci. U. S. A., 1996, 93, 12817-12821.

31. F. Becker, K. Murthi, C. Smith, J. Come, N. Costa-Roldan, C. Kaufmann, U. Hanke, C. Degenhart, S. Baumann, W. Wallner, A. Huber, S. Dedier, S. Dill, D. Kinsman, M. Hediger, N. Bockovich, S. Meier-Ewert, A. F. Kluge and N. Kley, Chem. Biol. 2004, 11, 211-223.

32. M. Caligiuri, F. Becker, K. Murthi, F. Kaplan, S. Dedier, C. Kaufmann, A. Machl, G. Zybarth, J. Richard, N. Bockovich, A. Kluge and N. Kley, Chem. Biol., 2005, 12, 1103-1115.

33. D. W. Fry, A. J. Kraker, A. McMichael, L. A. Ambroso, J. M. Nelson, W. R. Leopold, R. W. Conners and A. J. Bridges, Science, 1994, 265, 1093-1095.

34. W. A. Denny, Farmaco, 2001, 56, 51-56.

35. B. Lippa, G. S. Kauffman, J. Arcari, T. Kwan, J. Chen, W. Hungerford, S. Bhattacharya, X. Zhao, C. Williams, J. Xiao, L. Pustilnik, C. Su, J. D. Moyer, L. Ma, M. Campbell and S. Steyn, Bioorg. Med. Chem. Lett., 2007, 11, 3081-3086.

36. L. F. Hennequin, P. Ballard, F. T. Boyle, B. Delouvrié, R. P. Ellston, C. T. Halsall, C. S. Harris, K. Hudson, J. Kendrew, J. E. Pease, H. S. Ross, P. Smith and J. L.Vincent, Bioorg. Med. Chem. Lett., 2006, 10, 2672-2676.

37. S. Ghosh, R. K. Narla, Y. Zheng, X. P. Liu, X. Jun, C. Mao, E. A. Sudbeck and F. M. Uckun, Anticancer. Drug Des., 1999, 5, 403-410.

38. W. A. Denny, Pharmacol. Ther., 2002, 93, 253-261.

39. L. F. Hennequin, A. P. Thomas, C. Johnstone, E. S. Stokes, P. A. Plé, J. J. Lohmann, D. J. Ogilvie, M. Dukes, S. R. Wedge, J. O. Curwen, J. Kendrew and C. Lambert-van der Brempt, J. Med. Chem., 1999, 42, 5369-5389

40. S. R. Wedge, D. J. Ogilvie, M. Dukes, J. Kendrew, R. Chester, J. A. Jackson, S. J. Boffey, P. J. Valentine, J. O. Curwen, H. L. Musgrove, G. A. Graham, G. D. Hughes, A. P. Thomas, E. S. Stokes, B. Curry, G. H. Richmond, P. F. Wadsworth, A. L. Bigley and L.F. Hennequin. Cancer Res., 2002, 62, 4645-4655

41. M. F. McCarty, J. Wey, O. Stoeltzing, W. Liu, F. Fan, C. Bucana, P. F. Mansfield, A. J. Ryan and L. M. Ellis. Mol. Cancer Ther., 2004, 3, 1041-1048.

42. P. A. Plé, T. P. Green and L. F. Hennequin, J. Curwen, M. Fennell, J. Allen, C. Lambert-Van Der Brempt and G. Costello, J. Med. Chem., 2004, 47, 871-887.

43. L. F. Hennequin, J. Allen, J. Breed, J. Curwen, M. Fennell, T. P. Green, C. Lambert-van der Brempt, R. Morgentin, R. A. Norman, A. Olivier, L. Otterbein, P. A. Plé, N. Warin and G. Costello, J. Med. Chem., 2006, 49, 6465-6488.

44. N. M. Heron, M. Anderson, D. P. Blowers, J. Breed, J. M. Eden, S. Green, G. B. Hill, T. Johnson, F. H. Jung, H. H. McMiken, A. A. Mortlock, A. D. Pannifer, R. A. Pauptit, J. Pink, N. J. Roberts and S. Rowsell, Bioorg. Med. Chem. Lett., 2006, 16, 1320-1323.

45. J. G. Cumming, C. L. McKenzie, S. G. Bowden, D. Campbell, D. J. Masters, J. Breed and P. J. Jewsbury, Bioorg. Med. Chem. Lett. 2004, 14, 5389-5394.

46. M. A. Fabian, W. H. Biggs 3rd, D. K. Treiber, C. E. Atteridge, M. D. Azimioara, M. G. Benedetti, T. A. Carter, P. Ciceri, P. T. Edeen, M. Floyd, J. M. Ford, M. Galvin, J. L. Gerlach, R. M. Grotzfeld, S. Herrgard, D. E. Insko, M. A. Insko, A. G. Lai, J. M. Lelias, S. A. Mehta, Z. V. Milanov, A. M. Velasco, L. M. Wodicka, H. K. Patel, P. P. Zarrinkar and D. J. Lockhart, Nat. Biotechnol., 2005, 23, 329-336.

47. L. Shewchuk, A. Hassell, B. Wisely, W. Rocque, W. Holmes, J. Veal and L. F. Kuyper, J. Med. Chem., 2000, 43, 133-138.

48. J. E. Sullivan, G. A. Holdgate, D. Campbell, D. Timms, S. Gerhardt, J. Breed, A. L. Breeze, A. Bermingham, R. A. Pauptit, R. A. Norman, K. J. Embrey, J. Read, W. S VanScyoc and W. H. Ward, Biochemistry, 2005, 44, 16475-16490.

49. P. P. Knowles, J. Murray-Rust, S. Kjaer, R. P. Scott, S. Hanrahan, M. Santoro, C. F. Ibáñez and N. Q. McDonald, J. Biol. Chem., 2006, 281, 33577-33587.

50. C. H. Yun, T. J. Boggon, Y. Li, M. S. Woo, H. Greulich, M. Meyerson and M. J. Eck, Cancer Cell, 2007, 11, 217-227.

51. E. R. Wood, A. T. Truesdale, O. B. McDonald, D. Yuan, A. Hassell, S. H. Dickerson, B. Ellis, C. Pennisi, E. Horne, K. Lackey, K. J. Alligood, D. W Rusnak, T. M. Gilmer and L. Shewchuk, Cancer Res.. 2004. 64, 6652-6659.

52. J. Stamos, M. X. Sliwkowski and C. Eigenbrot, J. Biol. Chem., 2002, 277, 46265-46272.

53. J. E. Moses and A. D. Moorhouse, Chem. Soc. Rev. 2007, 36, 1249-1262

54. M. A. Austen and K. Nicholas John., PCT Int. Appl., 2001, WO 2001021597.

55. B. D. Sutherland and B. G. Robert, PCT Int. Appl., 2000, WO 2000007991.

56. H. L. Francois Andre and P. Patrick, PCT Int. Appl., 2001, WO 2001094341.

57. A. Pandey, D. L. Volkots, J. M. Seroogy, J. W. Rose, J. Yu, J. L. Lambing, A. Hutchaleelaha, S. J. Hollenbach, K. Abe, N. A. Giese and R.M. Scarborough, J. Med. Chem., 2002, 45, 3772-3793.

58. S. Punna, E. Kaltgrad and M. G. Finn, Bioconjug. Chem., 2005, 16, 1536-1541.

59. G. F. Kleber, A. S. Mario Jose, R. N. Roberto, M. R. Miguel and R. A. Silvana, PCT Int. Appl. , 2005, WO 2005085213.

60. L. F. Hennequin, PCT Int. Appl., 2005, WO 2005013998.

61. P.S. Shirude, V. A. Kumar and K. N. Ganesh, Eur. J. Org. Chem., 2005, 5207-5215.

Chapter 3*

Bivalent Inhibitors for Protein Kinases

3.1 Bivalent Inhibitors

Despite widespread interest in protein kinases, the functions of most kinases are still not well understood and, therefore, the contribution of specific kinases towards human diseases remain unclear.[19] Additionally, kinases tend to perform different functions depending on their localization within the cell. Furthermore, co-localization of a kinase and its substrate maintains kinases substrate fidelity.[1] Previous studies indicate that the differential subcellular localization of kinases may be important for the regulation of specific subcellular processes.[25,26] Identification of kinase targets in specific subcellular compartments is an essential starting point for our understanding of the special regulation of cell signaling.[25] However, there are not sufficient tools to study the function of a desired kinase in a specific cellular compartment. Thus, a method that allows inhibitors to selectively block the catalytic activity of a single protein kinase in a desired subcellular compartment is a promising strategy for obtaining a greater understanding of signaling complexities.[19,27,28,29,30] Since most protein kinase inhibitors bind to the highly conserved ATP-binding site of the enzyme, obtaining a selective and potent inhibitor for a kinase of interest remain challenging.[31,32,33] To achieve this task, we have pursued a bivalent inhibitor strategy of this interesting enzyme family. These inhibitors interact with the highly conserved ATP-binding site as well as another less conserved secondary binding site located outside of the ATP-binding cleft. These novel,

bivalent inhibitors show increased affinity and selectivity towards their desired targets and can be used to study the function of a single kinase of interest.[19,20]

Bivalent inhibitors of protein kinases were generated by displaying an ATP-competitive small molecule inhibitor and a ligand that binds to a secondary binding domain of the desired kinase from a modified version of the DNA repair enzyme O^6-alkylguanine DNA alkyltransferase (AGT), also known as the SNAP-tag[34,35] AGT recognizes small molecules that are linked to O^6-benzylguanine (BG) and covalently transfers them to its active site cysteine *in vitro* and *in vivo*. [34,35, 19] (Figure 3.1)

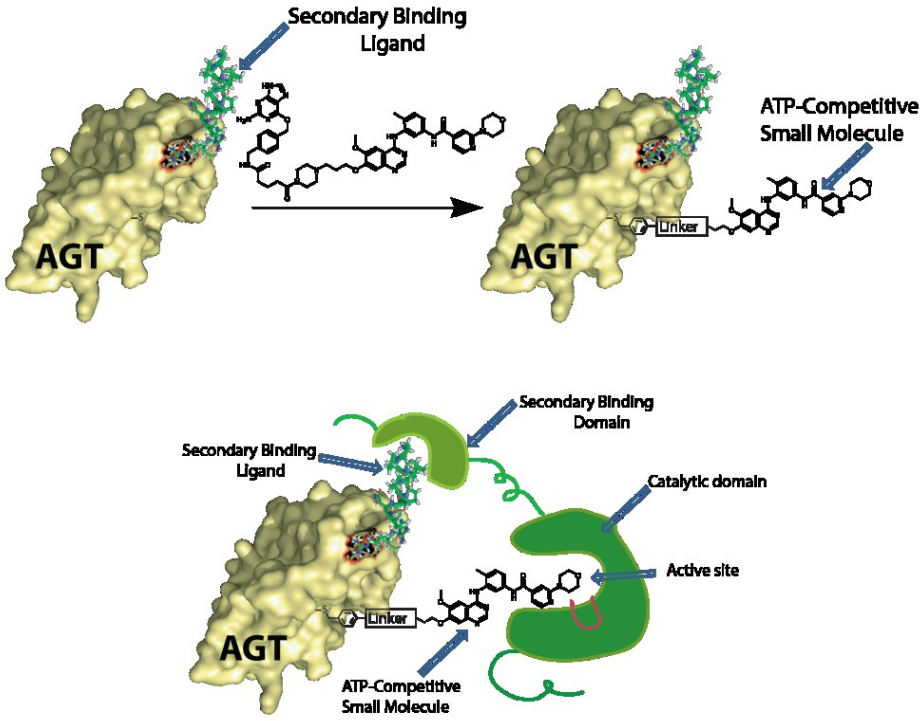

Figure 3.1 – Generation of bivalent AGT-small molecule conjugate inhibitors for SRC and ABL kinases. The bottom diagram is a schematic representation of the assembled bivalent inhibitor binding to the kinase active site *via* the small molecule inhibitor, and to a secondary (SH3) binding domain *via* the secondary binding domain ligand displayed from AGT [19]

To generate bivalent inhibitors of SRC and ABL, we have generated a panel of ATP-competitive small molecule inhibitors based on a 4-anilinoquinazoline scaffold that can be displayed from the active site of SNAP-tag. When the quinazoline scaffold binds to the ATP-binding site of a kinase, its C-6 and C-7 positions point out of the active site and into solvent. For this reason, these sites were selected for linker attachment.[18]

4-Anilinoquinazoline inhibitor **A**, a potent inhibitor of SRC and ABL, was modified to obtain BG derivatives **1** and **2,** which contain different linker lengths. Compound **B** was generated as a negative control that lacks the ATP-competitive kinase inhibitor. (Figure 3.2)[19]

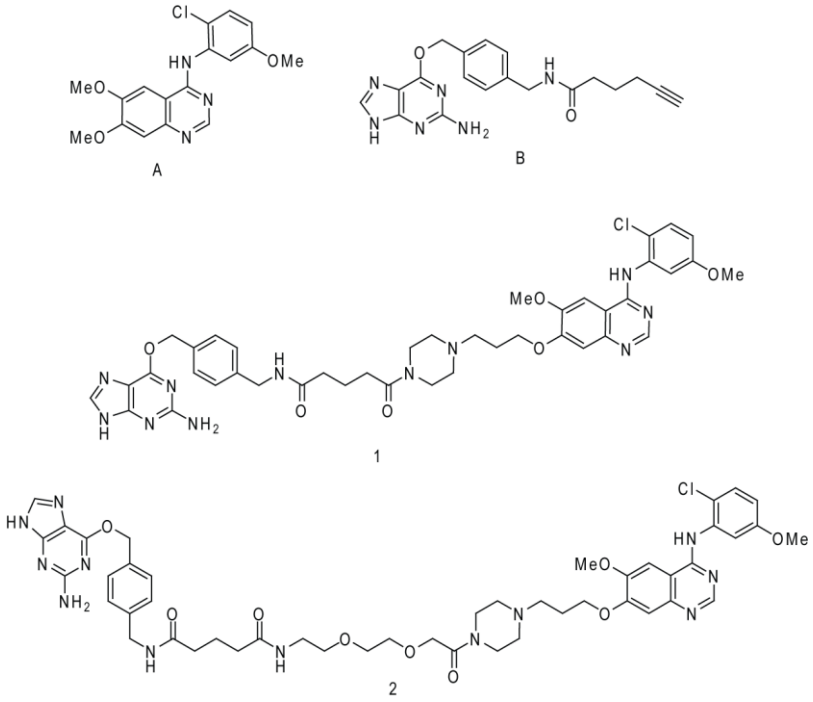

Figure 3.2 – Structure of compound **A**, the parental SRC and ABL inhibitor which was modified to obtain BG-derivatized versions compounds **1** and **2**. Compound **B**, which contains an alkyne tag, is a control compound that lacks an ATP-competitive inhibitor.

SNAP-tag fusion protein displaying polyproline motifs that target the SH3 domains of SRC and ABL kinases were generated (Figure 3.3 left) and labeled with compounds **1** or **2** to generate bivalent inhibitors. These protein-small molecule conjugates were then tested against two structurally similar tyrosine kinases and were found to have high selectivity for their intended kinase target. (Figure 3.3 right)[19]

IC_{50} (nM) Src-3D

	B	2	1
No Protein	N/T	130 ± 4	300 ± 20
AGT(wt)	> 5,000	2000 ± 300	> 5,000
AGT(PP1)	> 5,000	12 ± 1	13 ± 3
AGT(PP2)	> 5,000	15 ± 1	25 ± 6
AGT(PP3)	> 5,000	66 ± 10	72 ± 10
AGT(PP4)	> 5,000	16 ± 1	34 ± 3

IC_{50} (nM) Abl-3D

	B	2	1
No Protein	N/T	510 ± 50	410 ± 50
AGT(wt)	> 5,000	1300 ± 200	3200 ± 100
AGT(PP5)	> 5,000	< 6	18 ± 6
AGT(PP6)	> 5,000	< 6	15 ± 4
AGT(PP7)	> 5,000	< 6	18 ± 7
AGT(PP8)	> 5,000	< 6	15 ± 3

Figure 3.3 – Left: Polyproline motif-AGT fusions that target SRC and ABL kinases. Right (top): *In vitro* activities of BG derivatives and assembled AGT-small molecule conjugates against a SRC kinase construct that contains SH1, SH2 and SH3 domains (Src-3D). Right (bottom): *In vitro* activities of BG derivatives and assembled AGT-small molecule conjugates against an ABL kinase construct that contains SH1, SH2 and SH3 domains. [19]

The selectivity of the bivalent inhibitors that target SRC and ABL is achieved through the secondary binding domain ligand. Therefore, the same ATP-competitive small molecule inhibitor can be used to generate several bivalent inhibitors, because kinase selectivity is achieved through the incorporation of secondary binding domain ligands.

Since most protein kinases contain secondary binding sites outside the ATP-binding cleft, bivalent inhibitors can be generated for a wide range of protein kinases. This should allow us to study the function of a diverse number of protein kinases in a controlled and selective manner.[19]

3.2 Effect of the small molecule inhibitor tether length

To further understand the importance of the linker length between the SNAP-tag protein (AGT) and the ATP-competitive ligand towards bivalent kinase inhibitors potency and selectivity, a series of constructs containing the same ATP-competitive small molecule but variable linker lengths were synthesized and tested against SRC and ABL kinases.[19,20] The parent inhibitor **A** has been shown to be a moderate inhibitor of SRC and ABL kinases.[18] All BG-linked unconjugated inhibitors with variable linker lengths inhibited SRC with similar IC_{50}s. Furthermore, these inhibitors exhibited a similar potency against ABL. All of the inhibitors tested suffered a drop in potency upon conjugation to AGT (WT). (Figure 3.4)

AGT(WT)-**3**, which contains the longest linker length, showed the lowest IC_{50}, possibly due to the increased accessibility of the inhibitor when displayed from AGT. ABL showed the same trend, but in a less striking manner. Upon conjugating BG-linked compounds **1-3** to AGT constructs containing a polyproline motif (PP1), all assembled bivalent inhibitors gained significant potency towards SRC. It was also observed that SRC activity does not have a strong linker length dependence. All three bivalent inhibitors containing a polyproline motif (PP5) targeting ABL (AGT(PP5)-**1**, AGT(PP5)-**2** and

AGT(PP5)-**3**) showed a significant increase in potency against this kinase. In contrast to SRC, ABL inhibition was greatly affected by the tether length of the assembled bivalent conjugate. AGT(PP5)-2, which contains a medium length linker was found to be optimal for inhibition of ABL. The difference in potencies for the same three inhibitors against SRC and ABL may suggest a difference in the orientation of the SH3 and catalytic domains of the two enzymes, but this needs further structural confirmation.[20]

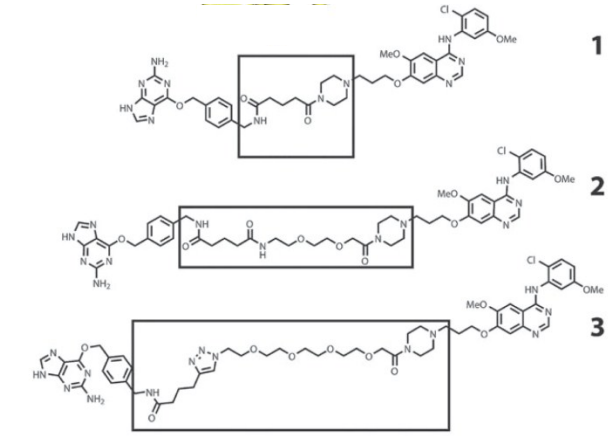

B.

SRC IC_{50} (nM)

	1	2	3
Unconjugated	300 ± 20	130 ± 20	180 ± 10
AGT(WT)	> 5000	2000 ± 300	240 ± 30
AGT(PP1)	13 ± 1	12 ± 1	< 10

ABL IC_{50} (nM)

	1	2	3
Unconjugated	410 ± 50	510 ± 50	610 ± 40
AGT(WT)	3200 ± 100	1300 ± 200	1200 ± 100
AGT(PP5)	18 ± 6	< 6	85 ± 9

Figure 3.4 – Chemical structures of BG-linked quinazoline inhibitors with variable linker lengths. Each inhibitor contains a benzyl guanine (BG) moiety linked to a chloromethoxyaniline quinazoline inhibitor through a flexible tether. *In vitro* activities of unconjugated inhibitors 1, 2, and 3 and bivalent conjugates AGT(WT)–**1**, AGT(WT)–**2**, AGT(WT)–**3**, AGT(PP1)–**1**, AGT(PP1)–**2**, and AGT(PP1)–**3** against SRC 3D. IC_{50} values of unconjugated 1, 2, and 3 and bivalent conjugates AGT(WT)–**1**, AGT(WT)–**2**, AGT(WT)–**3**, AGT(PP5)–**1**, AGT(PP5)–**2**, and AGT(PP5)–**3** against ABL 3D.[20]

3.3 Contribution of the ATP-competitive small molecule inhibitor

In order to understand the contribution of the ATP-competitive small molecule inhibitor towards the potency of the final bivalent inhibitor, a small panel of BG-linked bivalent inhibitors containing ATP-competitive molecules with variable affinities towards SRC and ABL were generated. These final bivalent inhibitors had an approximately similar tether length from AGT to the small molecule inhibitor which allows the contribution of the ATP-competitive inhibitor towards the potency of the conjugated bivalent inhibitor to be directly compared. (Figure 3.5)

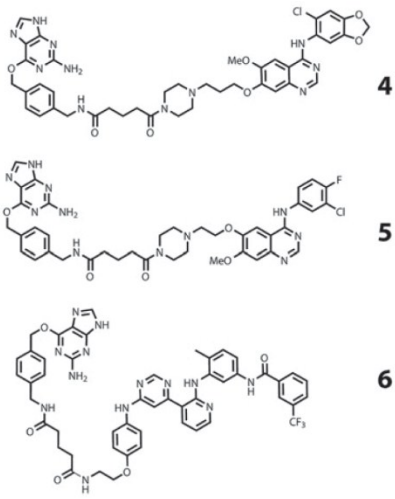

4

5

6

SRC IC_{50} (nM)

	4	5	6
Unconjugated Inh	190 ± 20	> 30000	440 ± 30
AGT(PP1)	< 10	> 2500	130 ± 10

ABL IC_{50} (nM)

	4	5	6
Unconjugated Inh	1000 ± 100	> 30000	400 ± 30
AGT(WT)	> 5000	nd	1200 ± 200
AGT(PP5)	59 ± 13	> 2500	190 ± 30

Figure 3.5 - IC_{50} values of various ATP-competitive inhibitors conjugated to AGT(PP1). (Top) Chemical structures of BG-versions of ATP-competitive kinase inhibitors **4–6**. (Bottom) *In vitro* activities of unconjugated inhibitors **4**, **5**, and **6** and bivalent conjugates AGT(PP1)–**4**, AGT(PP1)–**5**, and AGT(PP1)–**6** against SRC-3D. In vitro activities of unconjugated **4**, **5**, **6** and bivalent conjugates AGT(WT)–**4**, AGT(WT)–**6**, AGT(PP5)–**4**, AGT(PP5)–**5**, and AGT(PP5)–**6** against ABL-3D.[20]

Compound **4** contains a 5-chlorobenzo[1,3]dioxol-4-ylamine attached to the 4-anilino position of the quinazoline scaffold instead of the 2-chloro-5-methoxyaniline[18] in parent compound **1**. This change in the aniline group of the ATP-competitive inhibitor resulted in the unconjugated form being 1.5-fold more potent towards SRC (IC_{50} = 190 ± 20 nM) than the parent compound **1** (IC_{50} = 300 ± 20 nM). In contrast, the above change resulted in the unconjugated compound **4** to be 2.4-fold less potent towards ABL (IC_{50} = 1000 ± 100 nM) than the parent compound **1** (IC_{50} = 410 ± 50 nM). Compound **5** is based on gefitinib, a highly selective inhibitor of the epidermal growth factor receptor kinase (EGFR).[36] Despite the structural similarity to compound 1, compound 5 shows no significant inhibition of SRC or ABL kinases at the highest concentration tested (30 μM). This indicates that the BG-derivatized version of this EGFR inhibitor retains a selectivity profile similar to its parent compound gefitinib.[37,33] Another equipotent inhibitor of SRC and ABL was modified to obtain BG-linked compound **6**. This compound has a similar potency against SRC and ABL as the parent compound it is derived from. This pyrimidinepyridine based ATP-competitive inhibitor binds to an inactive conformation of the target kinases known as the DFG-out conformation, whereas all the previously mentioned compounds **1**, **4** and **5** bind to the active conformation of their kinase targets. Compound **6** was found to be an equipotent inhibitor of SRC (IC_{50} = 440 ± 30 nM) and ABL (IC_{50} = 400 ± 30 nM), showing a similar selectivity profile to its parent compound.[13]

Compounds **4**-**6** were all conjugated to AGT(PP1) and the assembled bivalent inhibitors (AGT(PP1)-**4**, AGT(PP1)-**5** and AGT(PP1)-**6**) were tested for the ability to inhibit SRC kinase. AGT(PP1)-**4** was found to be a more potent inhibitor of SRC than AGT(PP1)-**1**.

This is consistent with the increased affinity of compound **4** for the active site of SRC. Additionally, both bivalent inhibitors AGT(PP1)-**1** and AGT(PP1)-**4** were found to be 20 to 25-fold more potent inhibitors of SRC than their unconjugated analogs **1** and **4**. This also indicates the contribution of the SH3 domain ligand towards bivalent inhibitor potency. Compounds **4**-**6** conjugated to AGT(PP5), (AGT(PP5)-**4**, AGT(PP5)-**5** and AGT(PP5)-**6**) were tested for their ability to inhibit ABL kinase. Similar to the trend observed in the unconjugated molecules **1** and **4**, the conjugated bivalent inhibitor AGT(PP5)-**4** (IC_{50} = 59 ± 13 nM) was 3-fold less potent than inhibitor AGT(PP5)-**1** (IC_{50} = 18 ± 6 nM). A similar trend was seen with the AGT(WT)-**1** (IC_{50} = 3200 ± 100 nM) and AGT(WT)-**4** (IC_{50} = > 5000 nM) against ABL kinase. Overall, all of the final AGT(PP5)-small molecule conjugates were at least 15-fold more potent inhibitors of ABL than their free BG-derivatized analogs.

The BG-version of gefitinib, which showed no inhibition of SRC and ABL kinases, was converted into bivalent inhibitors AGT(PP1)-**5** or AGT(PP5)-**5** and tested against SRC and ABL, respectively. Despite the presence of specific SH3 binding ligands that target SRC or ABL, neither of the bivalent inhibitor was found to have any detectable inhibition at the highest concentration tested (2.5 μM). The lack of demonstrated inhibition by the bivalent inhibitors towards their kinase targets agree with the low potency seen for the unconjugated analog **5**. This clearly demonstrates that despite the structural similarity of compounds **1**, **4** and **5**, mere presentation of the inhibitor from the AGT scaffold is not sufficient for the inhibition of a target kinase. Additionally, these data indicate that differences in the affinity of the ATP-competitive ligand are directly correlated to the relative potencies of their corresponding bivalent inhibitors. Thus, the affinity and

selectivity of a bivalent inhibitor can be fine-tuned by careful selection of the ATP-competitive small molecule.

Bivalent inhibitor versions of compound **6** were also generated by conjugating to AGT(PP1) or AGT(PP5). These bivalent inhibitors, which bind to the inactive, DFG-out conformation of these kinases, were tested against SRC and ABL, respectively. Even though unconjugated compound **6** has a similar potency against SRC and ABL as BG-derivatized compound **1**, bivalent inhibitors containing this compound do not show a significant increase in potency against these kinases. This could be due to conformational changes that are necessary for kinases to be able to bind this ATP-competitive inhibitor. These conformational changes might increase the intra-molecular interactions of the kinase between the SH3 domain and its own polyproline motif, thus reducing the ability of SRC and ABL to bind to the SH3 binding ligand displayed on the AGT construct. Further biochemical and biophysical analysis is needed in order to validate the true cause of the difference in gain of potency for the bivalent inhibitors based on compound **6**.

Compound **1** has been used in further studies to explore the contribution of the SH3 domain ligands toward bivalent inhibitor selectivity and it has been shown that proper selection of a SH3 binding ligand allows the generation of highly selective bivalent inhibitors.[19-20]

3.4 Conclusion

Developing selective inhibitors towards a specific kinase of interest is extremely challenging. We have demonstrated one way to overcome this obstacle by generating

bivalent inhibitors for the desired targets. The self-labeling O^6-alkylguanine DNA alkyltransferase (AGT/SNAP-tag) is used to display an ATP-competitive small molecule and a peptidyl ligand which binds to a secondary binding domain of the target kinase. A panel of small molecule inhibitors was successfully modified to generate bivalent inhibitors that were tested against SRC and ABL kinases. Upon success in generating selective bivalent inhibitors for these kinases, the small molecules were further modified to explore the molecular binding determinants of the bivalent inhibitors against their targets. This led to the discovery that SRC and ABL have differential sensitivities towards the distance and orientation of the ATP-competitive molecule displayed from AGT. Additionally, the importance and contribution of the small molecule inhibitor towards determining the overall potency of the bivalent inhibitor was also shown with a small panel of bivalent inhibitors generated using different ATP-competitive inhibitors. Due to the modular nature of these bivalent inhibitors, this method is an attractive way to rapidly generate inhibitors with high selectivity using a relatively small panel of monovalent ligands.

3.5 Experimental

General.

Unless otherwise noted, all reagents were obtained from commercial suppliers and used without purification. ^{1}H-NMR spectra were obtained on a Bruker AV-300 or AV301 instrument at room temperature. Chemical shifts are reported in ppm, and coupling constants are reported in Hz. Mass spectrometry was performed on a Bruker Esquire Ion Trap MS instrument.

General HPLC Purification Conditions Preparatory reverse-phase C_{18} column (250 x 21 mm), CH_3CN/H_2O–0.1% CF_3CO_2H gradient: 1:99 to 100:0 over 60 min; 8 mL/min; 220 and 254 nm detection for 65 min. All HPLC analyses were performed utilizing a Varian Microsorb-MV C18 reverse-phase analytical column (2.1 mm x 150 mm). The purity of each final compound was determined to be > 95% by analytical HPLC. **Analytical conditions A**: [C_{18} column (2.1 mm x 150 mm), CH_3CN/H_2O–0.1% CF_3CO_2H = 1:99 to 100:0 for 30 min; 1 mL/min; 220 and 254 nm detection for 30 min. **Analytical conditions B**: [C_{18} (2.1 mm x 150 mm), CH_3OH/H_2O–0.1% CF_3CO_2H = 1:99 to 100:0 over 30 min; 1 mL/min; 220 and 254 nm detection for 30 min].

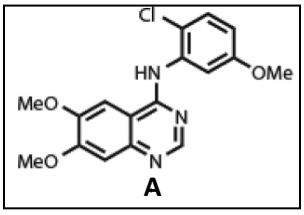

A

A. Compound **A** was prepared using a previously published procedure.[18]

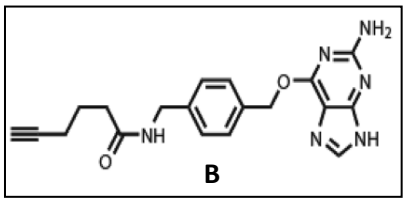

B

B. Compound **B** was prepared using a previously published procedure

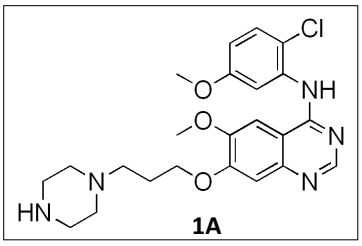

1A

1A. Compound **1A** was prepared using a previously published procedure.[18]

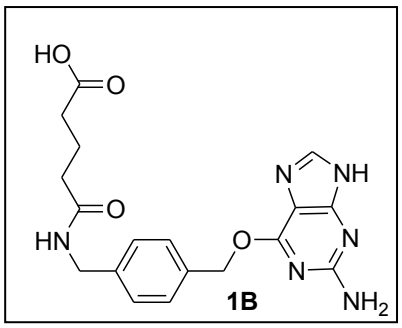

1B

1B. Compound **1A** was prepared using a previously published procedure.[38]

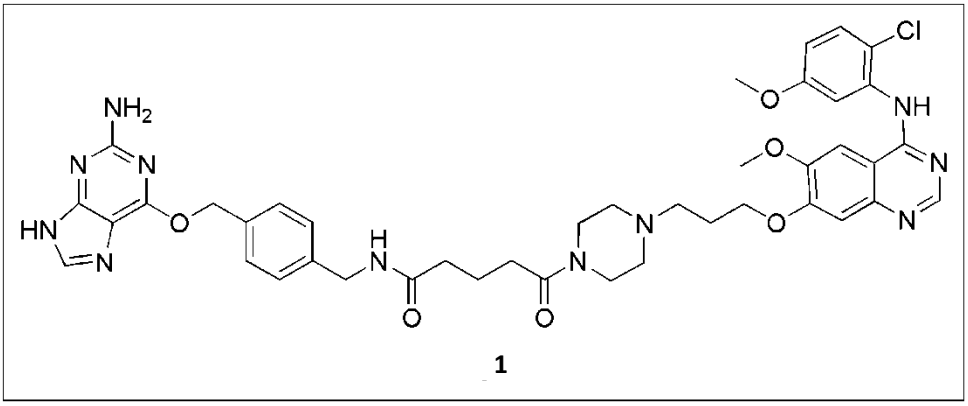

1

1. **1A** (9 mg, 16.6 μmol) was dissolved in a 30% TFA in CH_2Cl_2 solution and stirred for 3 h at rt. The solvent was evaporated and the crude product was used in the next step without further purification. To a mixture of de-protected **1A** (16.6 μmol, 1.0 equiv), **1B** (12 mg, 31 μmol, 1.9 equiv), HOBt·H_2O (3 mg, 20 μmol, 1.3 equiv) and DIPEA (3.4 μL, 20 μmol, 1.3 equiv) in DMF (50 μL), was added EDCI·HCl (4 mg, 20 μmol, 1.3 equiv). The reaction mixture was stirred for 24 h at rt, then diluted using CH_3CN/H_2O (10 mL) and purified using General HPLC Purification conditions to obtain 3 mg of **1** (22% yield) ^{1}H-NMR (MeOD-d_4) 1.34 (m, 2H), 1.92 (m, 6H), 3.17 (m, 2H), 3.1 (m, 6H), 3.45 (m, 2H), 3.85 (s, 3H), 4.04 (s, 3H), 4.32 (t, *J* = 5.4 Hz, 2H), 4.36 (m, 2H), 5.56 (s, 2H), 7.03 (m, 1H), 7.10 (s,

1H), 7.2 (m, 1H), 7.39 (d, *J* = 8 Hz, 2H), 7.49 (m, 3H), 7.86 (s, 1H), 7.99 (s, 1H), 8.56 (s, 1H).

Calcd for $C_{41}H_{46}ClN_{11}O_6$ ((M+2H$^+$)/2) : 412.7; Found 413.0.

Analytical HPLC trace of compound 1 (Acetonitrile/Water-0.1% CF_3CO_2H gradient):

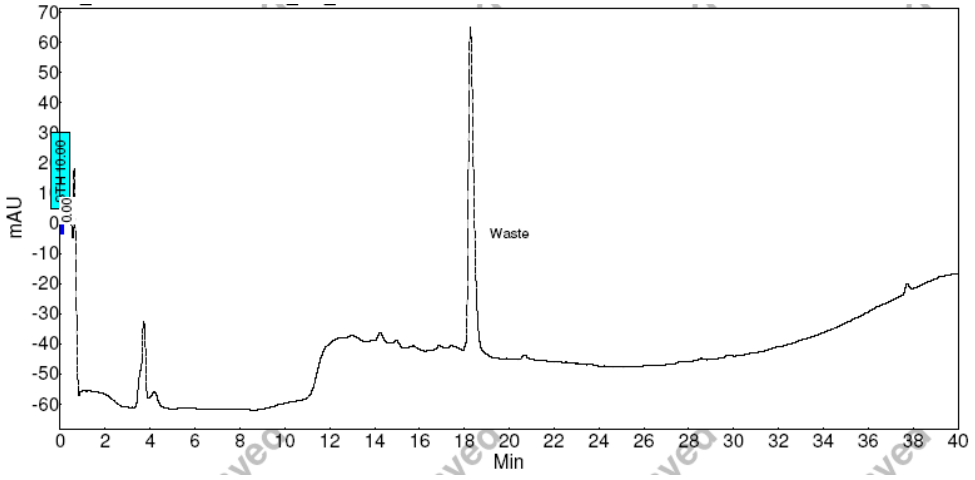

Analytical HPLC trace of compound 1 (Methanol/Water-0.1% CF_3CO_2H gradient):

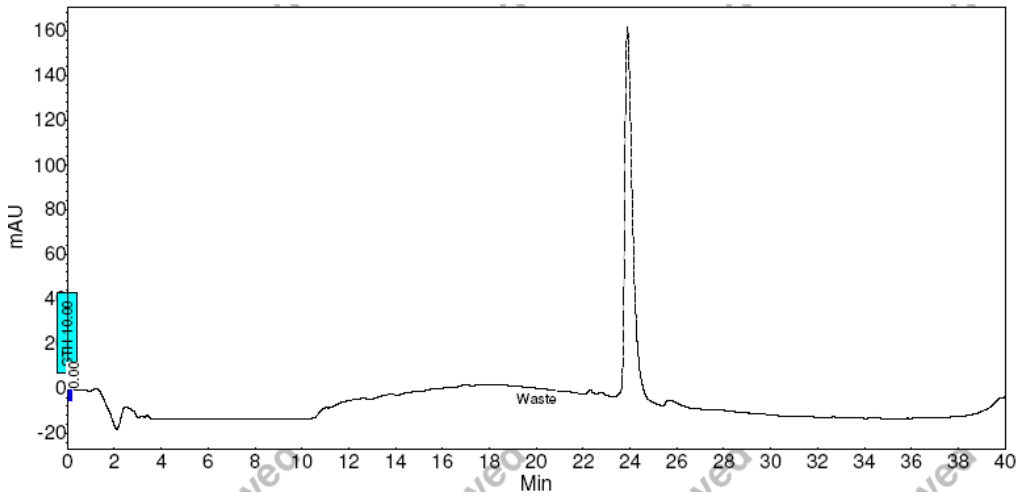

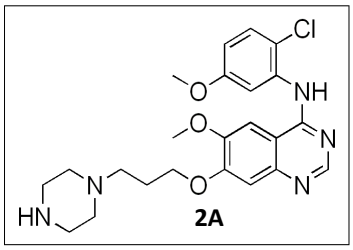

2A

2A. **2A** was prepared using a previously published procedure.[18]

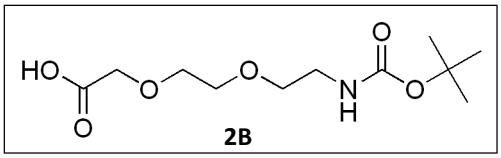

2B

2B. **2B** was prepared using a previously published procedure.[39] ^{1}H-NMR ($CDCl_3$) 1.47 (s, 9H), 3.35 (m, 2H), 3.56-3.61 (m, 2H), 3.65-3.70 (m, 2H), 3.77-3.80 (m, 2H), 4.19 (s, 2H).

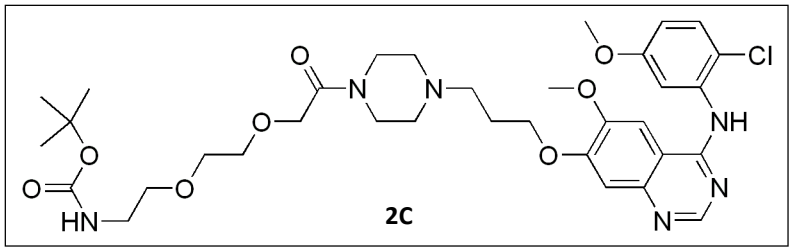

2C

2C. To a mixture of **2A** (36.7 μmol, 1.0 equiv), **2B** (12.6 mg, 47.8 μmol, 1.3 equiv), HOBt·H_2O (7.3 mg, 47.8 μmol, 1.3 equiv) and DIPEA (20 μL, 110.1 μmol, 3.0 equiv) in DMF (90 μL) was added EDCI·HCl (9.2 mg, 47.8 μmol, 1.3 equiv). The reaction was stirred at room temperature for 24 h at which time the reactions was dissolved in CH_3CN/H_2O (10 mL) and purified using General HPLC conditions to obtain 11.7 mg of **2C** (39% yield) ^{1}H-NMR (MeOH-d_4) 1.40-1.56 (m, 11H), 2.47 (m, 2H), 3.24 (t, *J* = 5.7 Hz, 4H), 3.52 (m, 6H), 3.67 (m, 6H), 3.85 (s, 3H), 4.08 (s, 3H), 4.32 (s, 2H), 4.30 (m, 2H), 7.05 (dd, *J* = 9.0, 3.0 Hz, 1H), 7.16 (d, *J* = 3.0 Hz, 1H), 7.34 (s, 1H), 7.51 (d, *J* = 9.0 Hz, 1H), 7.98 (s, 1H), 8.64 (s, 1H). Calcd for $C_{34}H_{47}ClN_6O_8$ $(M+H)^+$: 703.3; Found 703.5.

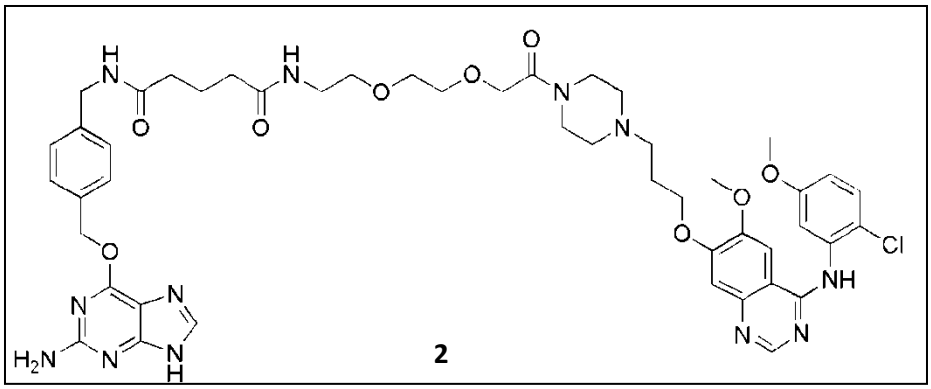

2

2. **2C** (11.7 mg, 16.6 μmol) was dissolved in a 30% TFA in CH_2Cl_2 solution and stirred for 3 h at rt. The solvent was evaporated and the crude product was used in the next step without further purification. To a mixture of de-protected **2C** (16.6 μmol, 1.0 equiv), **1B** (8.3 mg, 21.6 μmol, 1.3 equiv), HOBt·H_2O (3.3 mg, 21.6 μmol, 1.3 equiv) and DIPEA (10 μL, 50.0 μmol, 3.0 equiv) in DMF (40 μL), was added EDCI·HCl (4.1 mg, 21.6 μmol, 1.3 equiv). The reaction mixture was stirred for 24 h at rt, then diluted with CH_3CN/H_2O (10 mL) and purified using General HPLC Purification conditions to obtain 9.1 mg of **2** (56% yield) ^{1}H-NMR (MeOD-d_4) 1.52 (m, 2H), 1.94 (m, 2H), 2.47-2.68 (m, 6H), 3.22-3.71 (m, 16H), 3.86 (s, 3H), 4.08 (m, 3H), 4.30-4.39 (m, 6H), 5.51 (s, 2H), 7.04 (m, 1H), 7.18 (m, 1H), 7.27 (m, 1H), 7.31 (m, 2H), 7.49 (m, 3H), 7.91 (s, 1H), 8.05 (m, 1H), 8.59 (m, 1H). Calcd for $C_{47}H_{57}ClN_{12}O_9$ ($(M+2H)^+/2$): 485.2; Found 485.6

Analytical HPLC trace of compound 2 (Acetonitrile/Water-0.1% CF_3CO_2H gradient)**:**

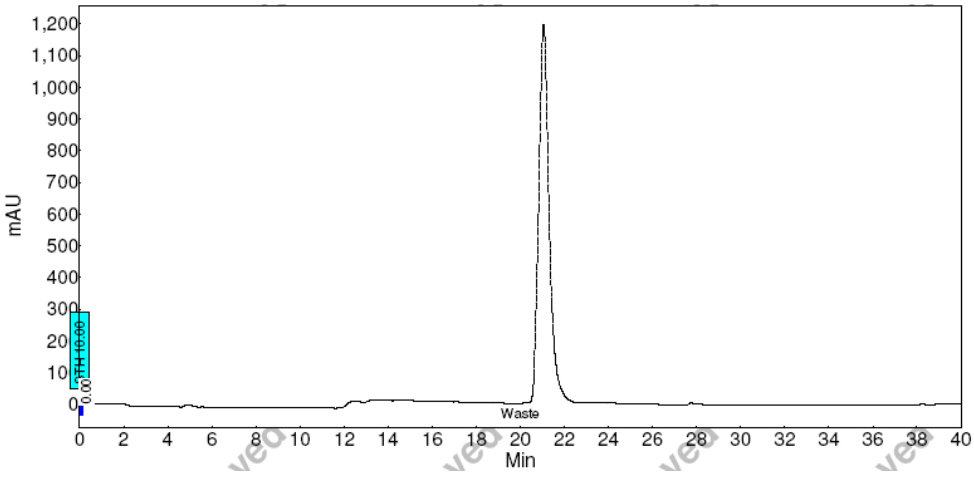

Analytical HPLC trace of compound 2 (Methanol/Water-0.1% CF_3CO_2H gradient):

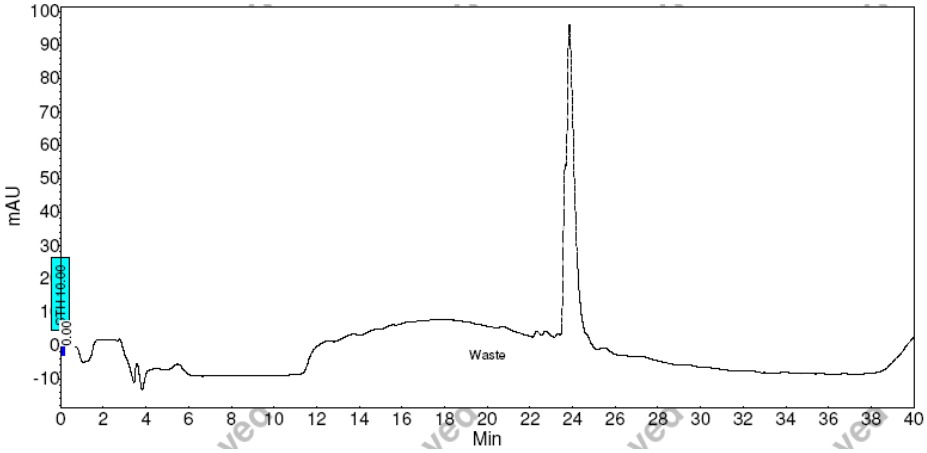

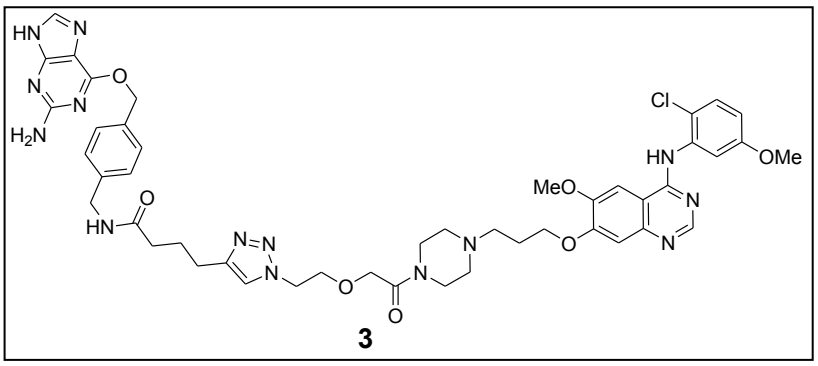

3

3. To a mixture of *O*^{6}-(4-Amino-methyl-benzyl)guanine (14.3 mg, 52.9 µmol, 1.0 equiv), 5-hexynoic acid (8.1 µL, 68.8 µmol, 1.3 equiv), HOBt·H_2O (10.7 mg, 68.8 µmol, 1.3 equiv),

and DIPEA ((30 µL, 158.7 µmol, 3.0 equiv)) in DMF (130 µL) was added EDCI·HCl (11.2 mg, 58.2 µmol, 1.1 equiv). The reaction mixture was stirred at rt for 24 h and then diluted with CH_3CN/H_2O (10 mL). The product was purified using General HPLC purification conditions to obtain 10.6 mg of pure N-((4-((2-amino-9H-purin-6-yloxy)methyl)phenyl)methyl)hex-5-ynamide (55% yield) ^{1}H-NMR (MeOD) 1.77-1.88 (m, 2H), 2.20-2.28 (m, 3H), 2.38 (t, *J* = 7.2 Hz, 2H), 4.39 (s, 2H), 5.65 (s, 2H), 7.35 (d, *J* = 8.1 Hz, 2H), 7.53 (d, *J* = 8.1 Hz, 2H), 8.30 (s, 1H). Calcd for $C_{19}H_{20}N_6O_2$ ($M+H^+$): 365.2 Found 365.2.

A mixture of N-((4-((2-amino-9H-purin-6-yloxy)methyl)phenyl)methyl)hex-5-ynamide (7.9 mg, 9.5 µmol, 3.3 equiv), 2-(2-(2-(2-(2-azidoethoxy)ethoxy)ethoxy)ethoxy)-1-(4-(3-(4-(2-chloro-5-methoxyphenylamino)-6-methoxyquinazolin-7-yloxy)propyl)piperazin-1-yl)ethanone[18] (3.5 mg, 9.5 µmol, 3.3 equiv), DIPEA (25 µL, 143.8 µmol, 49.6 equiv) and CuI (0.6 mg, 2.9 µmol, 1.0 equiv) in MeOH (0.37 mL) was stirred at rt for 2 days. The product was purified using General HPLC purification conditions to obtain 4.2 mg of **3** (37% yield). ^{1}H-NMR (MeOD) 1.15-1.34 (m, 2H), 1.79 (m, 2H), 2.13-2.74 (m, 10H), 3.00-4.26 (m, 30H), 4.46 (t, *J* = 5.1 Hz, 2H), 5.46 (s, 2H), 6.40 (m, 1H), 6.97(dd, *J* = 8.7, 3.0 Hz, 1H), 7.13-7.27 (m, 4H), 7.45 (m, 2H), 7.51 (s, 1H), 7.82 (s, 1H), 7.99 (m, 1H), 8.36 (m, 1H). Calcd for $C_{52}H_{65}ClN_{14}O_{10}$ (($M+2H^+$)/2) : 541.2 Found 541.5.

Analytical HPLC trace of compound 3 (Acetonitrile/Water-0.1% CF_3CO_2H gradient):

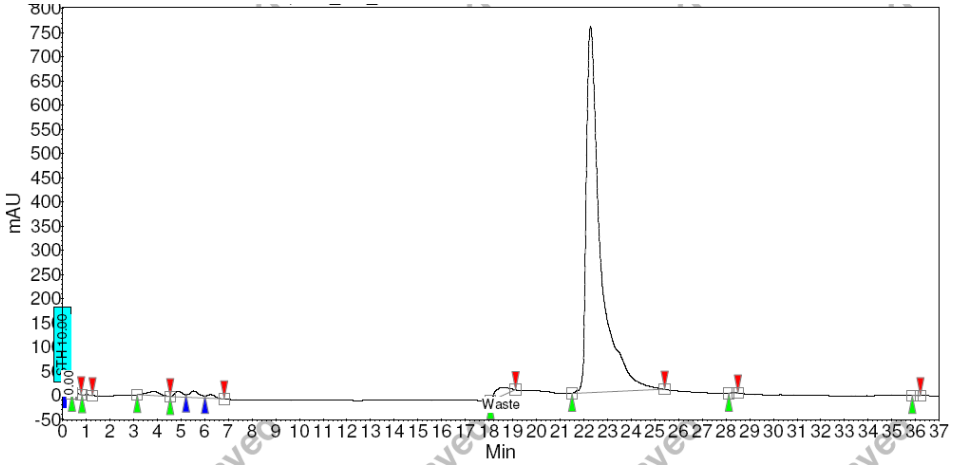

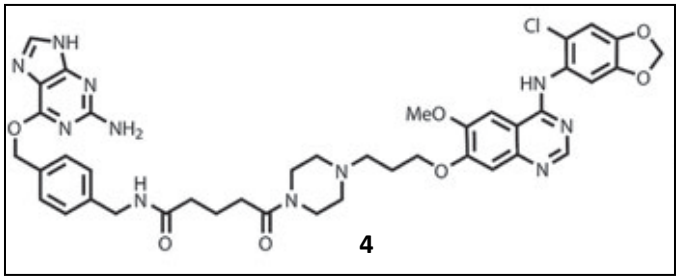

4. To a mixture of 5-((4-((2-amino-*9H*-purin-6-yloxy)methyl)benzyl)amino)-5-oxopentanoic acid[19] (2.5 mg, 6.7 µmol, 1.3 equiv), *N*-(6-chlorobenzo[*d*][1,3]dioxol-5-yl)-6-methoxy-7-(3-(piperazin-1-yl)propoxy)quinazolin-4-amine[18] (5.2 µmol, 1 equiv), HOBt·H_2O (1 mg, 6.7 µmol, 1.3 equiv), and DIPEA ((1.1 µL, 6.7 µmol, 1.3 equiv)) in DMF (50 µL), was added EDCI·HCl (1.3 mg, 6.7 µmol, 1.3 equiv). The reaction was stirred at rt for 24 h at which time the reaction was dissolved in CH_3CN/H_2O (mL) and purified using General HPLC conditions to obtain 0.6 mg of pure **4** (14% yield). Calcd for $C_{41}H_{44}ClN_{11}O_7$ ((M+2H^+)/2): 419.7 Found 420.2

Analytical HPLC trace of compound 4 (Acetonitrile/Water-0.1% CF_3CO_2H gradient):

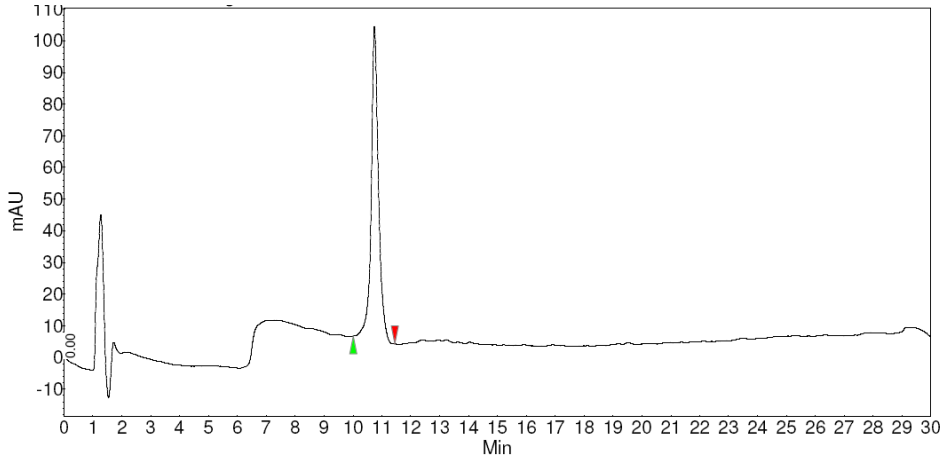

Analytical HPLC trace of compound 4 (Methanol/Water-0.1% CF_3CO_2H gradient):

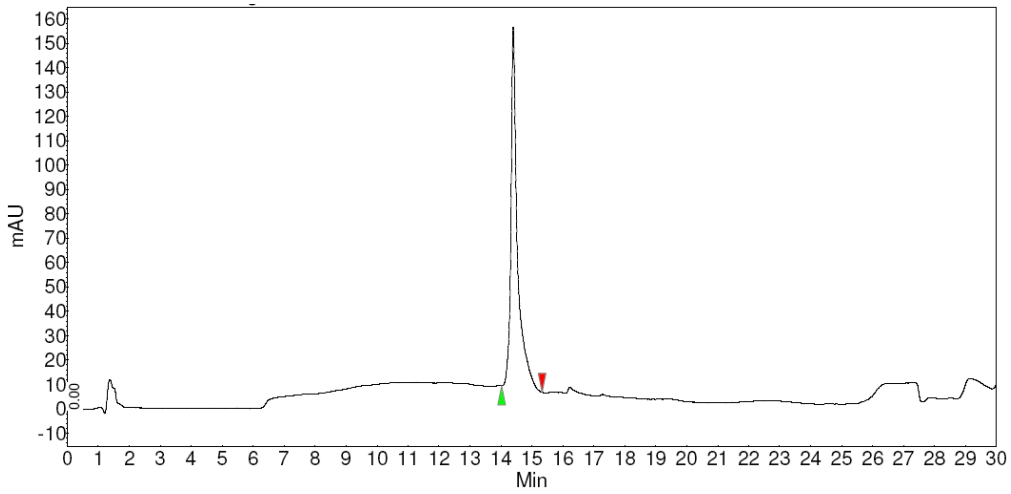

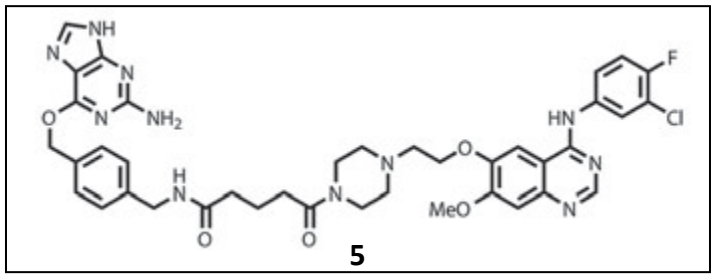

5

5. A mixture of *N*-Boc-1-(2-bromoethyl)-piperazine (40.5 mg, 138µmol, 1.2 equiv), 4-(3-chloro-4-fluoroanilino)-6-hydroxy-7-methoxyquinazoline[40] (37 mg, 115 µmol, 1 equiv),

and K_2CO_3 (127 mg, 922 µmol, 8 equiv) was stirred in DMF (280 µL) at 80 ^oC overnight. The reaction was concentrated *in vacuo* and purified using flash chromatography ($MeOH/CH_2Cl_2$) to yield 41 mg of 4-(3-chloro-4-fluoroanilino)-6-(2-(*N*-Boc-piperazin-1-yl)ethoxy)-7-methoxyquinazoline. (67 % yield) ^1H-NMR ($CDCl_3$) 1.43 (s, 9H), 2.52 (t, *J* = 4.8 Hz, 4H), 2.88 (t, *J* = 6 Hz, 2H), 3.42 (t, *J* = 4.8 Hz, 4H), 3.92 (s, 3H), 4.24 (t, *J* = 6 Hz, 2H), 7.09 (t, *J* = 8.7 Hz, 1H), 7.19 (s,1H), 7.55 (s, 1H), 7.60 (m, 1H), 7.87 (dd, *J* = 6.6, 2.7 Hz, 1H), 8.59 (s, 1H)

4-(3-chloro-4-fluoroanilino)-6-(2-(*N*-Boc-piperazin-1-yl)ethoxy)-7-methoxyquinazoline (10 mg, 19.1 µmol, 1 equiv) was stirred in 30% TFA/CH_2Cl_2 (191 µL) for 1.5 h at rt. Toluene was then added (l mL) and the reaction was concentrated *in vacuo* to afford crude 4-(3-chloro-4-fluoroanilino)-6-(2-(piperazin-1-yl)ethoxy)-7-methoxyquinazoline. The crude reaction product was carried on to the next step without further purification.

To a mixture of 5-((4-((2-amino-*9H*-purin-6-yloxy)methyl)benzyl)amino)-5-oxopentanoic acid (6 mg, 15 µmol, 1.3 equiv), 4-(3-chloro-4-fluoroanilino)-6-(2-(piperazin-1-yl)ethoxy)-7-methoxyquinazoline**.** (11 µmol, 1 equiv), HOBt·H_2O (3 mg, 20 µmol, 1.7 equiv), and DIPEA ((2.5 µL, 15 µmol, 1.3 equiv)) in DMF (60 µL), was added EDCI·HCl (3 mg, 16 µmol, 1.4 equiv). The reaction was stirred at rt for 24 h at which time the reactions was dissolved in CH_3CN/H_2O (10 mL) and purified using General HPLC conditions to obtain 0.54 mg of pure **5** (6% yield). Calcd for $C_{39}H_{41}ClFN_{11}O_5$ ((M+2H$^+$)/2): 399.7 Found 399.9.

Analytical HPLC trace of compound 5 (Acetonitrile/Water-0.1% CF_3CO_2H gradient)**:**

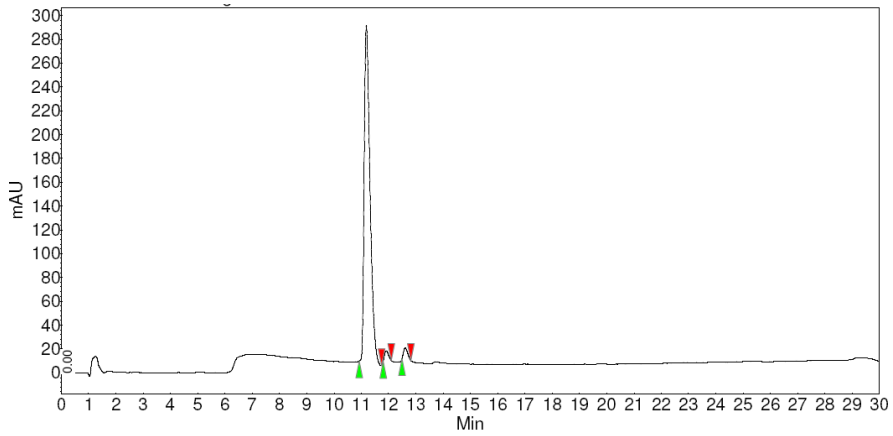

Analytical HPLC trace of compound 5 (Methanol/Water-0.1% CF_3CO_2H gradient):

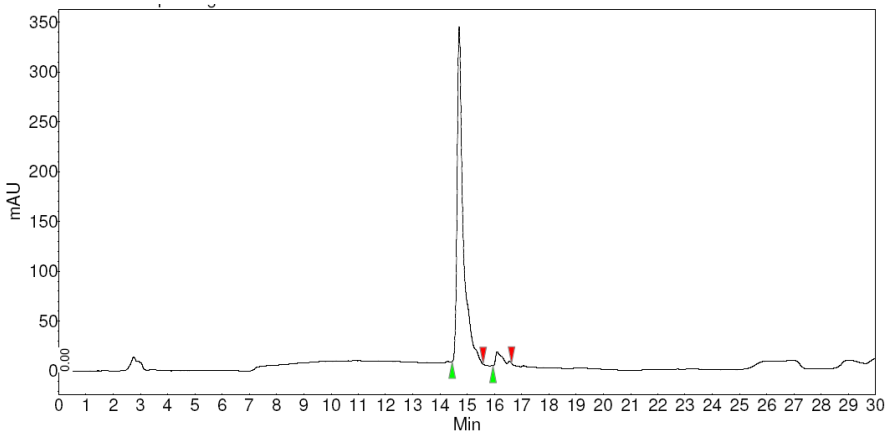

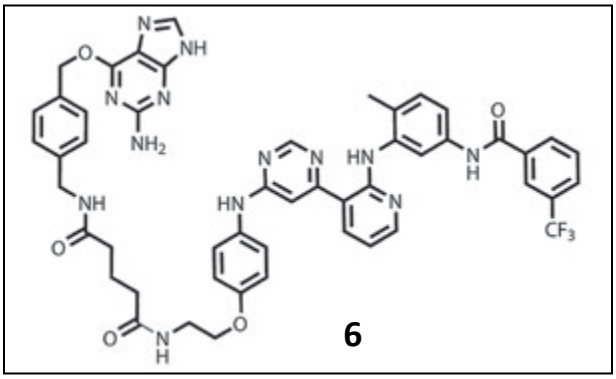

6

6. To a mixture of 5-((4-((2-amino-*9H*-purin-6-yloxy)methyl)benzyl)amino)-5-oxopentanoic acid (3.5 mg, 9.1 µmol, 1.3 equiv), N-(3-(3-(6-(4-(2-aminoethoxy)

phenylamino)pyrimidin-4-yl)pyridin-2-ylamino)-4-methylphenyl)-3-(trifluoromethyl)benzamide[12] (7 µmol, 1 equiv), HOBt·H_2O (1.4 mg, 9.1 µmol, 1.3 equiv), and DIPEA ((3.8 µL, 21 µmol, 3 equiv)) in DMF (35 µL), was added EDCI·HCl (1.7 mg, 9.1 µmol, 1.3 equiv). The reaction was stirred at rt for 24 h at which time the reaction was dissolved in CH_3CN/H_2O (10 mL) and purified using General HPLC conditions to obtain 1.2 mg of pure **6** (18% yield). Calcd for $C_{50}H_{46}F_3N_{13}O_5$ ((M+2H$^+$)/2): 483.7 Found 483.9.

Analytical HPLC trace of compound 5 (Acetonitrile/Water-0.1% CF_3CO_2H gradient):

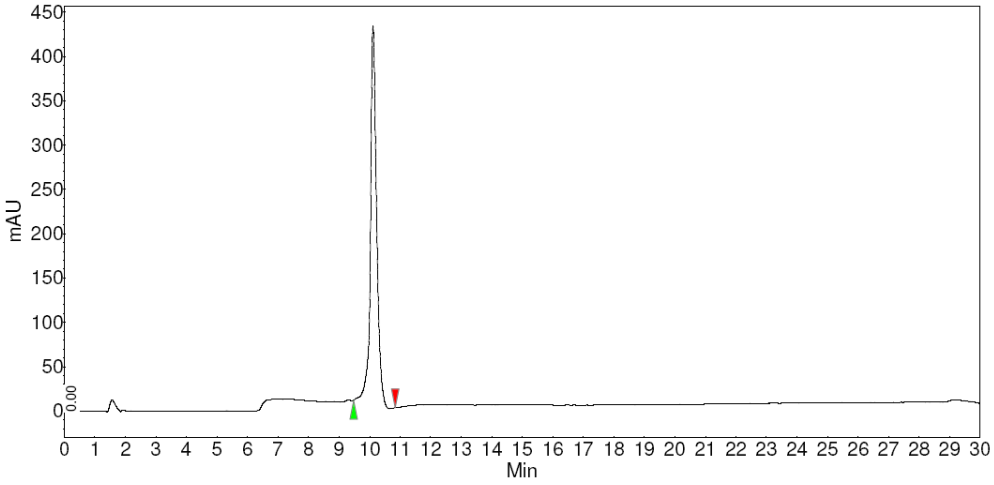

Analytical HPLC trace of compound 5 (Methanol/Water-0.1% CF_3CO_2H gradient):

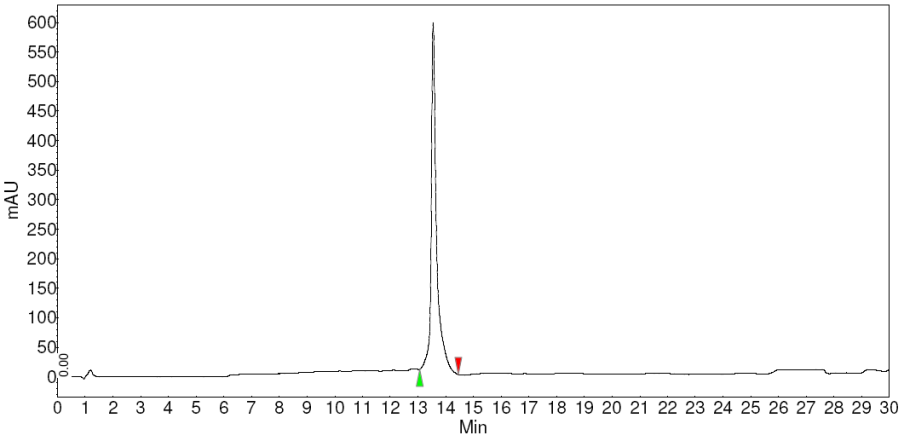

Detailed protocols of the biological experiments can be found in Zach *et. al* publications.[19-20]

3.6 References

1. Hill, Z. B.; Perera, B. G.; Maly, D. J., A chemical genetic method for generating bivalent inhibitors of protein kinases. *Journal of the American Chemical Society* **2009,** *131* (19), 6686-8.
2. Ubersax, J. A.; Ferrell, J. E., Jr., Mechanisms of specificity in protein phosphorylation. *Nature reviews* **2007,** *8* (7), 530-41.
3. Bjorge, J. D.; Jakymiw, A.; Fujita, D. J., Selected glimpses into the activation and function of Src kinase. *Oncogene* **2000,** *19* (49), 5620-35.
4. Van Etten, R. A., Cycling, stressed-out and nervous: cellular functions of c-Abl. *Trends in cell biology* **1999,** *9* (5), 179-86.
5. Johnson, S. A.; Hunter, T., Kinomics: methods for deciphering the kinome. *Nature methods* **2005,** *2* (1), 17-25.
6. Knight, Z. A.; Shokat, K. M., Chemical genetics: where genetics and pharmacology meet. *Cell* **2007,** *128* (3), 425-30.
7. Lawrence, D. S., Chemical probes of signal-transducing proteins. *Accounts of chemical research* **2003,** *36* (6), 401-9.
8. Shen, K.; Hines, A. C.; Schwarzer, D.; Pickin, K. A.; Cole, P. A., Protein kinase structure and function analysis with chemical tools. *Biochimica et biophysica acta* **2005,** *1754* (1-2), 65-78.
9. Knight, Z. A.; Shokat, K. M., Features of selective kinase inhibitors. *Chemistry & biology* **2005,** *12* (6), 621-37.

10. Fedorov, O.; Marsden, B.; Pogacic, V.; Rellos, P.; Muller, S.; Bullock, A. N.; Schwaller, J.; Sundstrom, M.; Knapp, S., A systematic interaction map of validated kinase inhibitors with Ser/Thr kinases. *Proceedings of the National Academy of Sciences of the United States of America* **2007,** *104* (51), 20523-8.

11. Karaman, M. W.; Herrgard, S.; Treiber, D. K.; Gallant, P.; Atteridge, C. E.; Campbell, B. T.; Chan, K. W.; Ciceri, P.; Davis, M. I.; Edeen, P. T.; Faraoni, R.; Floyd, M.; Hunt, J. P.; Lockhart, D. J.; Milanov, Z. V.; Morrison, M. J.; Pallares, G.; Patel, H. K.; Pritchard, S.; Wodicka, L. M.; Zarrinkar, P. P., A quantitative analysis of kinase inhibitor selectivity. *Nature biotechnology* **2008,** *26* (1), 127-32.

12. Hill, Z. B.; Perera, B. G.; Maly, D. J., Bivalent inhibitors of the tyrosine kinases ABL and SRC: determinants of potency and selectivity. *Molecular bioSystems* **2011,** *7* (2), 447-56.

13. Heinis, C.; Schmitt, S.; Kindermann, M.; Godin, G.; Johnsson, K., Evolving the substrate specificity of O6-alkylguanine-DNA alkyltransferase through loop insertion for applications in molecular imaging. *ACS chemical biology* **2006,** *1* (9), 575-84.

14. Keppler, A.; Kindermann, M.; Gendreizig, S.; Pick, H.; Vogel, H.; Johnsson, K., Labeling of fusion proteins of O6-alkylguanine-DNA alkyltransferase with small molecules in vivo and in vitro. *Methods* **2004,** *32* (4), 437-44.

15. Perera, B. G.; Maly, D. J., Design, synthesis and characterization of "clickable" 4-anilinoquinazoline kinase inhibitors. *Molecular bioSystems* **2008,** *4* (6), 542-50.

16. Barker, A. J.; Gibson, K. H.; Grundy, W.; Godfrey, A. A.; Barlow, J. J.; Healy, M. P.; Woodburn, J. R.; Ashton, S. E.; Curry, B. J.; Scarlett, L.; Henthorn, L.; Richards, L., Studies leading to the identification of ZD1839 (IRESSA): an orally active, selective epidermal growth factor receptor tyrosine kinase inhibitor targeted to the treatment of cancer. *Bioorganic & medicinal chemistry letters* **2001,** *11* (14), 1911-4.

17. Brehmer, D.; Greff, Z.; Godl, K.; Blencke, S.; Kurtenbach, A.; Weber, M.; Muller, S.; Klebl, B.; Cotten, M.; Keri, G.; Wissing, J.; Daub, H., Cellular targets of gefitinib. *Cancer research* **2005,** *65* (2), 379-82.

18. Seeliger, M. A.; Ranjitkar, P.; Kasap, C.; Shan, Y.; Shaw, D. E.; Shah, N. P.; Kuriyan, J.; Maly, D. J., Equally potent inhibition of c-Src and Abl by compounds that recognize inactive kinase conformations. *Cancer research* **2009,** *69* (6), 2384-92.

19. Lemercier, G.; Gendreizig, S.; Kindermann, M.; Johnsson, K., Inducing and sensing protein--protein interactions in living cells by selective cross-linking. *Angewandte Chemie* **2007,** *46* (23), 4281-4.

20. Zhang, Y.; So, M. K.; Loening, A. M.; Yao, H.; Gambhir, S. S.; Rao, J., HaloTag protein-mediated site-specific conjugation of bioluminescent proteins to quantum dots. *Angewandte Chemie* **2006,** *45* (30), 4936-40.

21. Tran, T.; Hoffmann, S.; Wiesehan, K.; Jonas, E.; Luge, C.; Aladag, A.; Willbold, D., Insights into human Lck SH3 domain binding specificity: different binding modes of artificial and native ligands. *Biochemistry* **2005,** *44* (45), 15042-52.

22. Ranjitkar, P.; Brock, A. M.; Maly, D. J., Affinity reagents that target a specific inactive form of protein kinases. *Chemistry & biology 17* (2), 195-206.

Chapter 4

Determinants of type II inhibitor selectivity

4.1 Introduction

Protein phosphorylation, carried out by enzymes called protein kinases is the most widespread post-translational modification used in signal transduction. The human genome encodes 518 kinases, making it the largest enzyme family in humans.[1,5] Due to the important roles that kinases play in many signal transduction pathways in cells, mis-regulation of these enzymes can cause a wide range of disease conditions including cancer, inflammation and diabetes. Currently, protein kinases have become one of the major drug targets in the pharmaceutical industry and there are 14 clinically approved small molecule inhibitors to treat protein kinase based diseases.[6,4,41]

SRC and ABL kinases are closely related members of the tyrosine kinase branch of the human kinome, each is involved in many important signaling cascades in the cell.[42,43] They share an extremely similar three dimensional structure (Figure 1), containing a catalytic domain proceeded by regulatory SH2 and SH3 domains.[14,44] The SH2 and SH3 domains of these kinases are involved in the regulation of catalytic activity. Intra-molecular engagement of these domains causes SRC and ABL to form a closed conformation, which leads to down-regulation of enzymatic activity.[44,14] The ATP-binding sites of SRC and ABL adopt several inactive conformations. One inactive conformation that has been observed in both kinases is the DFG-out conformation. This conformation is characterized by rotation and movement of the DFG-motif, which is located at the beginning of the activation loop. The Phe residue of the DFG-motif is flipped 180^{o} relative

to the active conformation, which creates a hydrophobic pocket known as the DFG-out pocket.

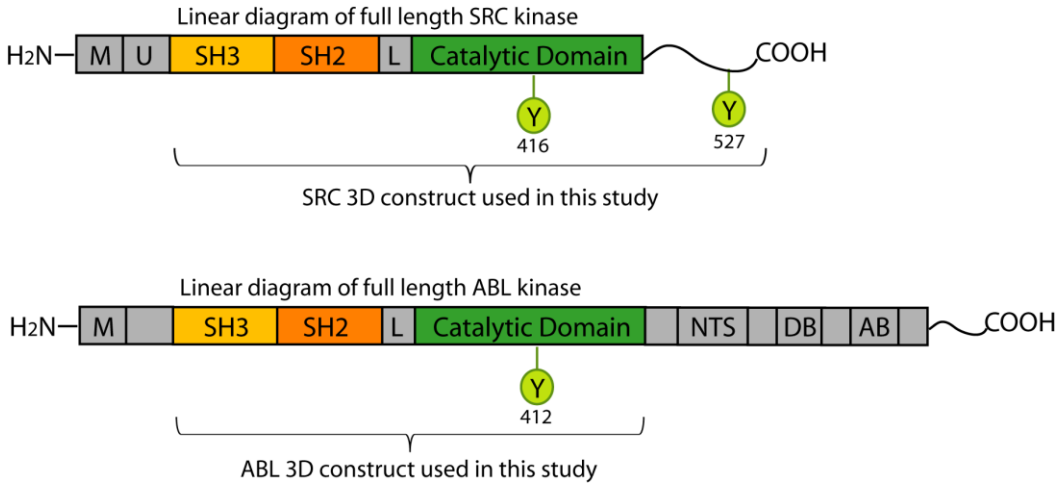

Figure 4.1 - Schematic representation of SRC and ABL 3D structures ([M] = Membrane binding region, [U] = unique region, [SH3] = SRC homology 3 domain, [SH2] = SRC homology 2 domain, [L] = linker region connecting the SH2 and catalytic domains, [Catalytic domain], [NTS] = nuclear transport signal, [DB] = DNA binding domain, [AB] = actin binding domain

4.2 Binding of type II inhibitors to SRC and ABL kinases

A class of inhibitors, called type II inhibitors, have been developed that specifically target the DFG-out conformation of protein kinases. These inhibitors contain several key structural features that interact with the DFG-out conformation of their protein kinase targets: (1) an aromatic heterocycle that makes many of the same hydrophobic and H-bond contacts as the adenine ring of ATP, (2) a hydrophobic moiety that occupies the pocket created by the movement of the Phe side chain of the DFG-motif, and (3) an amide or urea linker that forms hydrogen bonds with a glutamic acid side chain in helix-αC and the backbone of the DFG-motif. Despite the structural similarities of ABL and SRC,

the first type II inhibitor that was characterized, Imatinib (Gleevec), is capable of differentiating between the inactive conformations of these enzymes. In fact, Imatinib binds to the inactive DFG-out conformation of ABL with >2400-fold higher affinity than the closely related SRC kinase.[45,46] This was a surprising observation, given that ABL shares about 46% sequence identity with SRC. Furthermore, SRC is more structurally related to ABL than other kinases, PDGFR and c-Kit, that are sensitive to Imatinib inhibition. The selectivity of Imatinib for ABL over SRC was originally thought to be due to the inability of SRC kinase to adopt the DFG-out inactive conformation required for Imatinib binding.[47],[48] However, It has recently been shown that many type II inhibitors can inhibit both SRC and ABL.[13,49] These type II inhibitors of SRC and ABL are based on a number of different pharmacophores but contain many of the same functional groups as Imatinib.[13,50,45] For example, DSA 8 (Figure 2), which shares a significant portion of its structure with Imatinib, has been shown to bind both SRC and ABL kinases with equal affinity.[13] Therefore, it has become clear that there are not large differences in the thermodynamic propensity of these two kinases to adopt the DFG-out conformation.

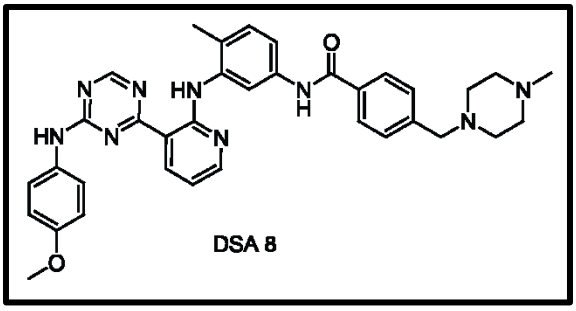

Figure 4.2 – Chemical structure of DSA 8, an equipotent inhibitor of both SRC and ABL kinases.

4.3 Significance of the P-loop and activation loop for inhibitor selectivity towards ABL

If SRC and ABL are equally stable in the DFG-out conformation, then what explains the very high selectivity of Imatinib? One theory that our group has suggested is that the differential potency that Imatinib displays for SRC and ABL is due to another structural feature in the ATP-binding site, called the phosphate-binding loop (P-loop) (glycine-rich loop).[13,12] Additionally, previous studies have also identified that the conformation of the P-loop as a potential source of selectivity for inhibitors.[51] Numerous crystal structures have shown that ABL and SRC have different P-loop conformations. Imatinib, which contains a more hydrophobic face than other type II inhibitors, requires a more hydrophobic environment when binding to its target kinase. This requirement is satisfied by the kinked P-loop conformation adopted by ABL kinase. (Figure 4.3 left, Abl-Imatinib structure)

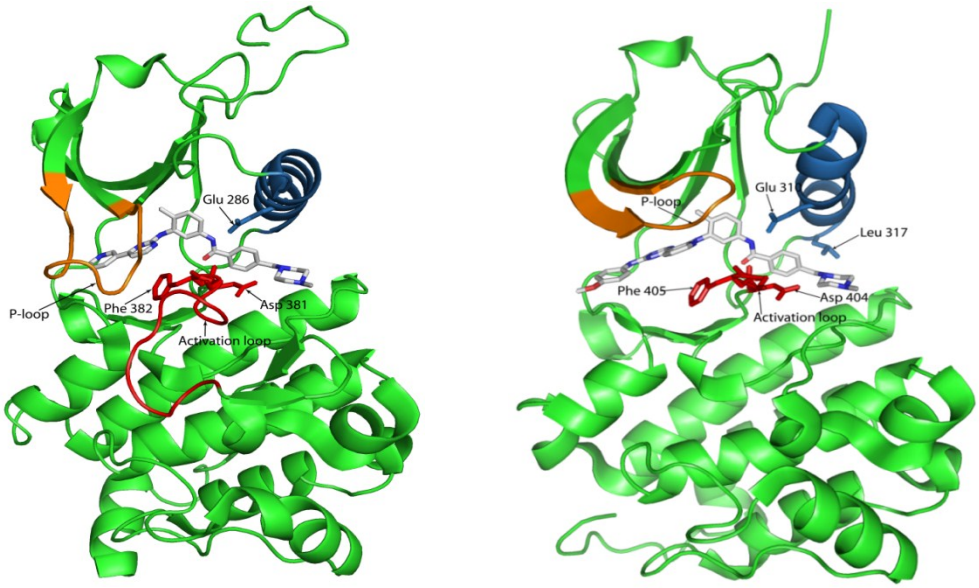

Figure 4.3 - left: Imatinib bound to ABL kinase (PDB: 1OPJ), right: DSA 8 bound to SRC kinase (PDB: 3G6G). Both type II inhibitors are bound to the inactive, DFG-out conformation of the target kinases.

The extended conformation of SRC's P-loop (observed in the SRC-Imatinib complex) fails to provide the hydrophobic pocket required for Imatinib to form a high affinity complex. The prevalence of clinically-observed P-loop mutations in BCR-ABL (BCR-ABL is the target of Imatinib in patients undergoing treatment for CML) hints at the importance of the P-loop for Imatinib binding. Furthermore, DSA 8 shows a close structural relationship to Imatinib in the amide linkage region and the portion binding in the DFG-out pocket. However, the methoxy aniline ring and the triazine ring of DSA 8, which occupy the adenine pocket, are not compatible with the kinked P-loop conformation of ABL. Furthermore, this class of inhibitors does not need to form additional interactions to potently bind to SRC or ABL (Figure 4.3 right, DSA 8-SRC structure)

Another important structural motif which affects type II inhibitor binding is the activation loop. The activation loop plays a critical role in kinase function and consists of several catalytically important residues, such as the DFG-motif and residues that increase kinase catalytic activity upon phosphorylation. For example, phosphorylation of activation loop tyrosines, Tyr416 or Tyr412, in SRC and ABL, respectively, stabilizes the active conformation of these kinases and increases their catalytic activity. Previous studies have shown that Imatinib is quite sensitive to the phosphorylation state of the activation loop of ABL.[52,45,53] Imatinib preferentially binds to the catalytically inactive DFG-out conformation of ABL and upon activation loop phosphorylation, the drug shows a significant loss in its potency.[52] Moreover other type II inhibitors including AST-487 and nilotinib have been reported to bind to activation loop un-phosphorylated ABL with

higher affinity than to the activation loop phosphorylated enzyme.[52] However, certain type II inhibitors seem to bind to their target with equal potency, irrespective of the activation loop phosphorylation state. For example, the p38α inhibitor BIRB-796 binds to activation loop phosphorylated and non-phosphorylated forms of p38α with equal affinity.[54,55]

Overall, the influence of the P-loop and activation loop towards ABL selective type II inhibitor binding is not well understood. To further explore the importance of the P-loop and the activation loop for type II inhibitor binding to SRC and ABL, we have assembled a general panel of ATP-competitive small molecule inhibitors that stabilize the DFG-out inactive conformation of protein kinases. (Figure 4.4) In addition to the core scaffold, which sits in the adenine-binding site of the ATP cleft, these inhibitors contain characteristic structural elements of a typical type II inhibitor. These include a hydrophobic moiety that occupies the DFG-out pocket in the inactive kinase conformation and an amide or urea linker that connects the DFG-pocket binding group to the core inhibitor scaffold.

The type II inhibitors used in this study are shown in Figure 4.4. GP 5, GP 17, GP 20 and GP 29 are quinazoline based inhibitors. Their quinazoline rings bind in the ATP-binding pockets of protein kinase. These inhibitors also contain a conserved methylphenyl group linked to a 3-trifluoromethylphenyl ring through an amide bond linkage. This amide is predicted to make a pair of characteristic hydrogen bonds with the catalytic Glu residue in the helix-αC and the backbone amide of the Asp residue of the DFG-motif.[56] The hydrophobic pocket exposed due to the DFG-flip in the inactive kinase conformation is

occupied by the 3-trifluoromethylphenyl group of the quinazoline inhibitors. GP 21 (AP24534) is a dual ABL/SRC kinase inhibitor in clinical trials for the treatment of Imatinib-resistant chronic myeloid leukemia (CML). This inhibitor effectively targets the Imatinib-resistant gatekeeper mutant ABL^{T315I}, which is one of the most frequently observed mutations observed in patients undergoing Imatinib treatment. The core imidazo[1,2*b*]pyridazine scaffold occupies the adenine-binding site in the ATP-cleft, while the inhibitor extends towards the DFG-out pocket of the inactive kinase. The 3-trifluoromethylphenyl group of GP 21 occupies the hydrophobic pocket created by the movement of the DFG-motif.[57,49,58]

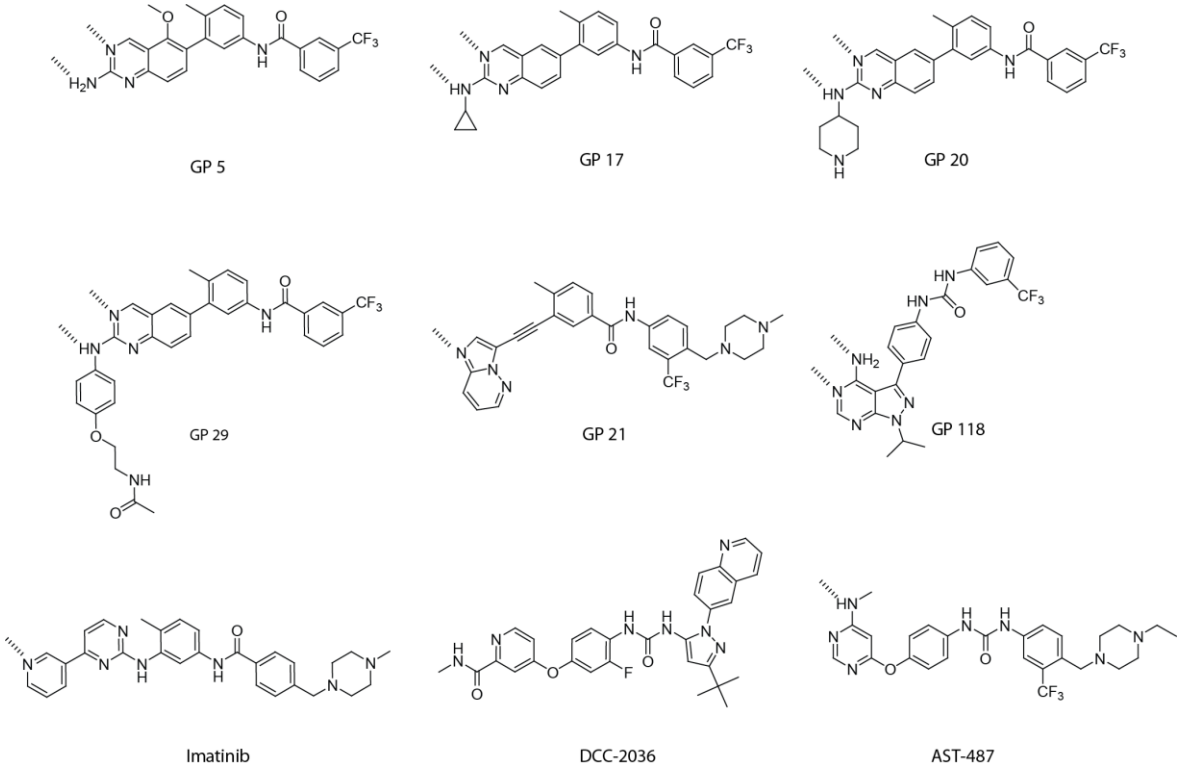

Figure 4.4 – A panel of type II inhibitors based on different core scaffolds. Hinge hydrogen bonding positions are shown with dashed lines.

Pyrazolopyrimidine-based inhibitor GP 118 has also been shown to bind to the DFG-out conformation of its target kinase.[50] The pyrazolopyrimidine ring of GP 118 mimics the adenine ring of ATP and the urea linkage extends into the DFG-out pocket, allowing the 3-trifluoromethylphenyl group to occupy this hydrophobic region. The exocyclic nitrogen of the methoxyaniline ring and one of the nitrogens from the triazine ring form hydrogen bonds with the hinge region in DSA 7. This inhibitor also contains a 3-trifluoromethylphenyl group, which occupies the DFG-out pocket of the inactive conformation of SRC and ABL kinases.[13] DCC-2036 is another well-characterized inhibitor that binds to the DFG-out conformation of ABL kinase. AST-487 is a type II inhibitor developed for the treatment of AML, caused by aberrantly activated receptor tyrosine kinase FLT3.[59,60] This inhibitor makes hydrogen bonds to the kinases hinge region via its aminopyrimidine group, while the DFG-out pocket of the kinase inactive conformation is occupied by its 3-trifluoromethylphenyl group. In addition to its primary target FLT3, AST-487 also inhibits many other kinases with a similar potency to its primary target.

Overall, all these inhibitors consist of similar functional groups that bind to the DFG-out pocket. However, these inhibitors significantly differ in the core group that sits in the adenine-binding site of the ATP-cleft. Therefore, these inhibitors make an ideal set of analogs to test the importance of regions outside the DFG-out pocket for obtaining inhibitor selectivity. This should provide valuable information into how the type II inhibitor Imatinib is able to achieve such high selectivity for ABL over SRC and highlight differences between these kinases.

4.4 Results and Discussion

All of the compounds shown in Figure 4.4 were tested for their ability to inhibit the catalytic activities of SRC and ABL. The activities of these kinases were tested at low ATP concentrations to allow direct comparison of the inhibitory constants. The results of these assays are summarized in Table 4.1.

Table 4.1 – Inhibitory constants of type II inhibitors against SRC, SRC^{L317I} and ABL catalytic domains were obtained by kinase activity assays.

Inhibitor	K_i (nM)		
	SRC KD	SRC Lue317Ile KD	ABL KD
GP 5	10 ± 0.3	N/T	2.9 ± 0.1
GP 17	0.7 ± 0	N/T	0.1 ± 0
GP 20	9.3 ± 0.3	20 ± 2	1.1 ± 0
GP 21	1.0 ± 0.1	0.6 ± 0	0.1 ± 0
GP 29	0.1 ± 0	N/T	0.2 ± 0
GP 118	7.9 ± 0.8	6.0 ± 0.5	2.1 ± 0.1
Imatinib	> 10000	> 10000	11 ± 2.9
DSA 7	1.5 ± 0.1	N/T	1.5 ± 0.2
AST-487	84 ± 1.2	135 ± 5	0.4 ± 0
DCC-2036	4.8 ± 0.2	N/T	0.4 ± 0
PR 1	8.5 ± 0.5	72 ± 18	0.3 ± 0
PR 4	503 ± 24	1375 ± 123	2.7 ± 0.1
PR 5	18 ± 0.4	N/T	0.4 ± 0
PR 7	22 ± 1.1	N/T	0.5 ± 0.1

Inhibitors GP 5, GP 17, GP 21, GP 29, GP 118, DSA 7 and DCC-2036 effectively inhibit both SRC and ABL kinases with ≤ 10 nM inhibitory constants. On the other hand, AST-487 inhibits ABL kinase 200-fold more potently over the closely related SRC kinase, possibly due to having a similar binding mode to that of Imatinib when inhibiting ABL. (Table 4.1) Both Imatinib and AST-487 contain pyrimidine rings which occupy the adenine-binding site and it is possible that AST-487 also requires a similar arrangement of

the P-loop when binding to its target, as seen in ABL-Imatinib complex. The inability of SRC to adopt this kinked P-loop conformation could be the same reason for the selectivity of AST-487 towards ABL over SRC.

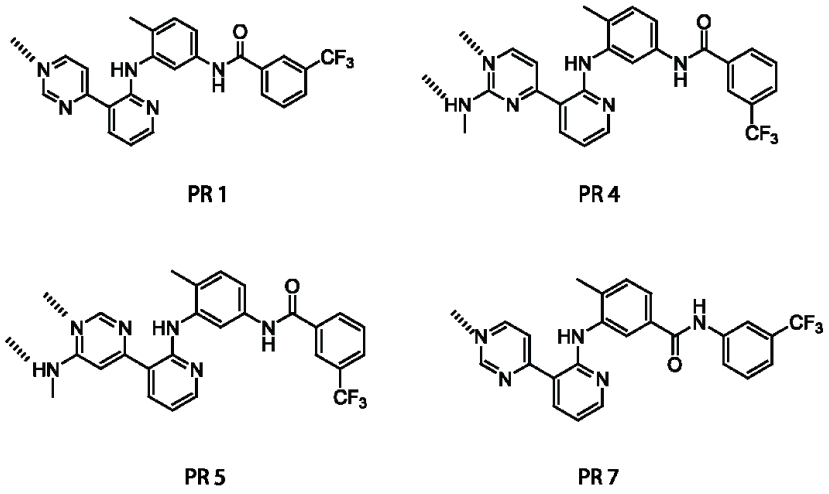

Figure 4.5 – Structures of the ABL selective type II inhibitors. Hinge hydrogen bonding interactions are shown with dashed lines.

By comparing the structural differences between the equipotent SRC and ABL inhibitors and the inhibitors selective for ABL, we investigated a series of inhibitors; PR 1, PR 4, PR 5 and PR 7[61,62], that has been previously described as potent inhibitors of the receptor tyrosine kinase Tie2. (Figure 4.5) Similar to Imatinib, these inhibitors contain differentially connected pyrimidine and pyridine groups that occupy the adenine-binding site. Furthermore, these compounds more potently inhibit the catalytic activity of ABL over SRC (Table 4.1). PR 1 and PR 7, which only differ in the direction of the amide linker that connects the 3-trifluoromethylphenyl group, are 28-fold and 44-fold more potent against ABL than SRC, respectively. Compounds PR 4 and PR 5, which only differ in the regio-selective substitution of the pyrimidine ring, are 186-fold and 45-fold more potent

against ABL than SRC, respectively. Since these new type II inhibitors share the same structural motifs occupying the region extending from the adenine site towards DFG-out pocket, and only differ in the portion occupying the adenine site, these results highlight the importance of the moiety that occupies the ATP-binding site next to the hinge region.

We also screened some of the type II inhibitors in our panel against a SRC mutant (SRC Leu317Ile) that was predicted using molecular dynamics to more stably adopt the DFG-out conformation.[63] Despite the prediction that converting Leu317 into an Ile would thermodynamically stabilize the DFG-out conformation of SRC, all of the inhibitors only showed a modest increase in potency against SRC Leu317Ile (Table 4.1). In fact, this mutation increases the K_i values of GP 20, PR 1, PR 4 and AST-487 (1.6 - 8.5 fold increase in K_i) for SRC Leu317Ile over wild type SRC. GP 21 and GP 118 show modestly lower K_i values (1.3 - 1.7 fold decrease in K_i). These observations further support the suggestion that SRC is equally able to adopt the DFG-out inactive conformation as ABL.[13]

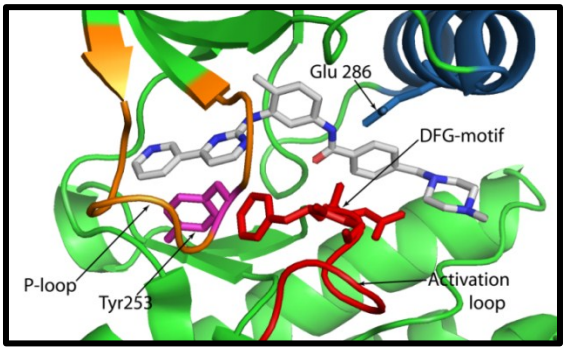

Figure 4.6 – The kinked orientation of the ABL P-loop in an Imatinib bound conformation is shown. Tyr253, a residue which causes resistance to Imatinib binding upon mutation, is highlighted in pink.

Since we hypothesized that a major part of Imatinib's selectivity for ABL is due to the conformation of the P-loop, we tested whether this structural feature is important for

the binding of PR 1-7. Previous work has shown that the orientation of the P-loop in ABL is important for Imatinib binding and that mutations that occur in ABL's P-loop lead to drug resistance in CML patients. The P-loop mutations Tyr253His and Glu255Val account for approximately 30% of the clinically-observed resistance mutations observed in patients undergoing Imatinib treatment.[13,64] In order to study the importance of the P-loop in binding type II inhibitors, we screened our panel of inhibitors against an ABL construct with the Tyr253His P-loop mutation. (Figure 4.6) The ABL selective inhibitors (Imatinib, AST-487 and PR 1-7) demonstrated a significant loss (15- to 93-fold) in inhibitor potency against ABL Tyr253His. However, the equipotent inhibitors of SRC and ABL, GP 17, GP 118, and DSA 7, show only a modest loss (1- to 7-fold) against this P-loop mutant. (Table 4.2) In summary, our data suggest that the P-loop plays an important role in obtaining ABL selective inhibitors.

Table 4.2 – Inhibitory constants of type II inhibitors against ABL Tyr253His, P-loop mutant was calculated.

Inhibitor	Ki (nM)	Fold difference in K_i
	ABL Tyr253His KD	(ABL Tyr253His KD/ABL KD)
GP 17	0.3 ± 0	3
GP 21	0.2 ± 0	2
GP 29	0.2 ± 0	1
GP 118	15 ± 1.0	7
Imatinib	299 ± 29	27
DSA 7	2.2 ± 0.2	1.5
AST-487	6.0 ± 0.4	15
PR 1	15 ± 0.2	50
PR 4	250 ± 28	93
PR 5	8.5 ± 0.8	21
PR 7	16 ± 1.5	32

In order to further investigate the effect of activation loop phosphorylation towards inhibitor binding, we screened our type II inhibitors against ABL, SRC and HCK

kinase constructs that contain phosphorylated activation loops. Activation of ABL kinase was achieved by incubating it for 5 hours with HCK kinase and 1 mM ATP. This resulted in the phosphorylation of Tyr412 in the activation loop of ABL.

Table 4.3 – Effect of activation loop phosphorylation on the inhibitory constants of the type II inhibitors was investigated. K_i values for selected inhibitors are summarized against activated ABL, non-activated and activated SRC and HCK kinases are summarized in the above table.

Inhibitor	K_i (nM)	Fold difference in K_i	K_i (nM)	K_i (nM)	Fold difference in K_i	K_i (nM)	K_i (nM)	Fold difference in K_i
	pY412 ABL KD	(pY412 ABL KD / npY412 ABL KD)	SRC 3D	pY416 SRC 3D	(pY416 SRC 3D / npY416 SRC 3D)	HCK 3D	pY416 HCK 3D	(pY416 HCK 3D / npY416 HCK 3D)
GP 17	4.6 ± 0.4	46	2.6 ± 0.1	6.4 ± 0.2	2.5	9.9 ± 1	20 ± 0.3	2
GP 21	0.5 ± 0	5	5.0 ± 0.1	8.8 ± 0.7	1.8	1.5 ± 0	4.7 ± 0.3	3.1
GP 29	0.1 ± 0	0.5	0.4 ± 0	0.2 ± 0	0.5	1.8 ± 0.2	N/T	N/T
GP 118	10 ± 0.8	4.8	12 ± 0.7	39 ± 2	3.2	62 ± 3	N/T	N/T
Imatinib	1210 ± 50	110	N/T	N/T	N/T	N/T	N/T	N/T
DSA 7	0.7 ± 0.1	0.5	2.7 ± 0.1	2.6 ± 0	1	4.1 ± 0.3	7.5 ± 0.2	1.8
AST-487	94 ± 5	235	261 ± 46	753 ± 32	2.9	483 ± 32	375 ± 29	0.8
DCC-2036	7.2 ± 0.3	18	5.5 ± 0.1	62 ± 4	11.3	N/T	N/T	N/T
PR 1	88 ± 6	293	49 ± 2	214 ± 17	4.4	130 ± 15	59 ± 4	0.5
PR 4	2736 ± 245	1013	264 ± 37	2772 ± 465	10.5	863 ± 34	> 10000	> 11.6
PR 5	73 ± 2	182	13 ± 1	183 ± 18	14	99 ± 7	116 ± 6	1.2
PR 7	78 ± 4	156	16 ± 2	469 ± 28	29.3	105 ± 5	327 ± 28	3.1

This construct, ABL pY412, was then used in activity assays to determine how this phosphorylation event affects type II inhibitor binding. The equipotent type II inhibitors GP 21, GP 29, GP 118 and DSA 7 were found to only be minimally affected by activation loop phosphorylation, with only a modest increase in their K_i values (< 5-fold) against ABL pY412 (Table 4.3). DCC-2036 and GP 17 showed a more pronounced increase in their K_i values (18- and 46- fold, respectively). (Table 4.3) However, all of the ABL-selective type II

inhibitors indicated a much greater increase in their inhibitor binding constants for ABL pY412. The observed increase in K_i values for ABL selective inhibitors varied from 151-fold for Imatinib to 1013-fold for PR 4. When our panel of inhibitors was screened against an activated SRC kinase construct (py416 SRC), the fold increase in the K_i values for the equipotent type II inhibitors only increased up to 3.2-fold. DCC-2036, which is 20-fold selective for ABL over SRC, demonstrated an 11-fold increase in K_i for pY416. ABL selective inhibitors also exhibited an increase in their K_i values for SRC pY416 2.9- to 29-fold), but were not affected to the same degree as ABL. (Table 4.3) The type II inhibitors were also screened against non-activated and activated HCK kinase. A similar trend was observed for HCK as for SRC. (Table 4.3) Overall, this indicates that the equipotent inhibitors of SRC and ABL are not as sensitive to activation loop phosphorylation compared to ABL selective inhibitors, which are highly sensitive to activation loop phosphorylation.

4.5 Conclusion

Based on our experimental results, the P-loop and the activation loop of ABL kinase appear to act together to provide the necessary binding environment required by Imatinib, AST-487 and the ABL selective inhibitors (PR 1-7). The inability of SRC kinase to adopt a similar P-loop and activation loop conformation is a major reason that ABL-selective type II inhibitors have a higher affinity for ABL.

4.6 Experimental

4.6.1 Synthetic Methods

Unless otherwise noted, all reagents were obtained from commercial suppliers and used without purification. ^{1}H-NMR spectra were obtained on a Bruker AV-300 or AV301 instrument at room temperature. Chemical shifts are reported in ppm, and coupling constants are reported in Hz. ^{1}H resonances are referenced to residual solvent. Mass spectrometry was performed on a Bruker Esquire Ion Trap MS instrument. The purity of each final compound was confirmed by analytical HPLC with two different solvent systems. **Analytical conditions A:** [C_{18} (150 x 2.1 mm), CH_3CN/H_2O–0.1% CF_3CO_2H = 1:99 to 100:0 over 33 min; 1 mL/min; 220 and 254 nm detection for 33 min]. **Analytical conditions B:** [C_{18} (150 x 2.1 mm), CH_3OH/H_2O–0.1% CF_3CO_2H = 1:99 to 100:0 over 33 min; 1 mL/min; 220 and 254 nm detection for 33 min].

[1] 6-Bromo-2-iodoquinazoline

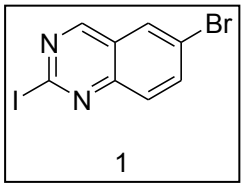

1

Compound **1** was synthesized according to a previously published protocol.[56]

[2] tert-butyl 2-(4-aminophenoxy)ethylcarbamate

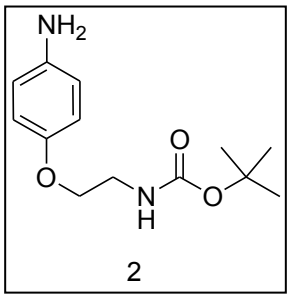

2

Compound **2** was synthesized according to a previously published protocol. [12]

[3] tert-butyl 2-(4-(6-bromoquinazolin-2-ylamino)phenoxy)ethylcarbamate

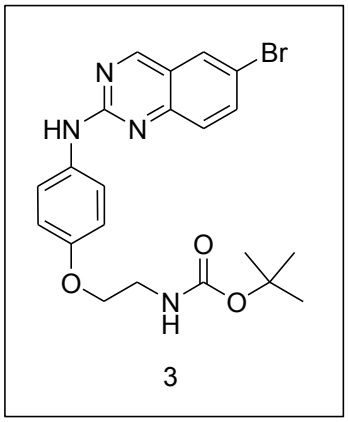

3

In a resealable Pyrex tube, compound 1 (588.5 mg, 1.76 mmol) and compound 2 (532 mg, 2.11 mmol) were taken up in of *i*-PrOH (13.5 mL). Trifluoroacetic acid (262 μL, 3.52 mmol) was added and the tube was sealed. The suspension was stirred overnight at 70 °C. Triethylamine (1.5mL) was added to neutralize the mixture and the mixture was concentrated. The residue was purified by column chromatography (50% ethyl acetate in hexanes) to afford 378 mg of compound **3** (47% yield). ^{1}H NMR (300 MHz, $CDCl_3$-d_1) δ 9.17 (s, 1H), 8.01 – 7.94 (m, 2H), 7.75 (d, *J* = 9.0 Hz, 1H), 7.57 (d, *J* = 9.0 Hz, 2H), 6.98 –

6.92 (m, 2H), 5.00 (br s, 1H), 4.06 (t, *J* = 5.1 Hz, 2H), 3.59 – 3.53 (m, 2H), 1.48 (s, 9H). MS *m/z* ($C_{21}H_{23}BrN_4O_3$) calc'd =458.1, observed: M+1 = 459.2

[4] 3-(trifluoromethyl)-N-(4-methyl-3-(4,4,5,5-tetramethyl-1,3,2-dioxaborolan-2-yl)phenyl)benzamide

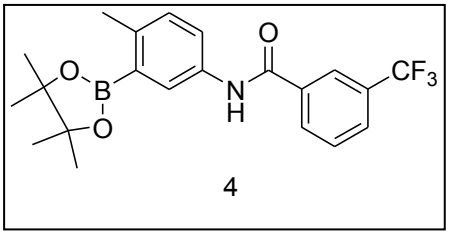

4

5-amino-2-methylphenylboronic acid pinacol ester (0.21 g, 0.86 mmol), 3-(trifluoromethyl)benzoic acid (0.21 g, 1.11 mmol), HOBt (0.17 g, 1.11 mmol), EDCI (0.21 g, 1.11 mmol) and DIPEA (450 μL, 2.58 mmol) were dissolved in DMF (2.5 mL) and stirred overnight at room temperature. The crude mixture was diluted in ethyl acetate and washed with NH_4Cl and Na_2CO_3. The organic layer was dried over Na_2SO_4 and concentrated *in vacuo* to afford 0.33 g of compound **4** (96% yield). ^{1}H NMR (300 MHz, Chloroform-d) δ 8.14 (s, 1H), 8.07 (d, *J* = 6.0 Hz, 1H), 7.98 (d, *J* = 9.0 Hz, 1H), 7.84-7.81 (m, 2H), 7.68 – 7.62 (m, 2H), 7.23 (d, *J* = 9.0 Hz, 1H), 2.55 (s, 3H), 1.37 (s, 12H). MS *m/z* ($C_{21}H_{23}BF_3NO_3$) calc'd = 405.2, observed: M+1 = 406.4

[5]

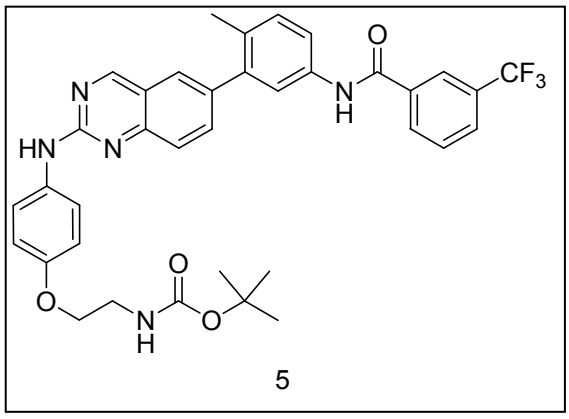

5

A mixture of compound 3 (120 mg, 0.26 mmol), compound 4 (127 mg, 0.31 mmol), Tetrakis(triphenylphosphine)palladium (9.3 mg, 7.8 μmol) and sodium carbonate (61 mg, 0.57 mmol) was dissolved in a 3:1 mixture of DME/water (1 mL). The mixture was heated overnight at 85 °C. The crude mixture was cooled to room temperature, diluted with ethyl acetate and washed with water and brine. The organic layer was dried over Na_2SO_4, concentrated *in vacuo* and the resultant crude product was purified by column chromatography (5% methanol in dichloromethane) to afford 132 mg of compound **5** (77 % yield). ^{1}H NMR (300 MHz, Methanol-d4) δ 9.03 (s, 1H), 8.23 – 8.14 (m, 2H), 7.83 (d, *J* = 9.0 Hz, 1H), 7.71 – 7.62 (m, 7H), 7.23 (d, *J* = 9.0 Hz, 1H), 6.88 (d, *J* = 9.0 Hz, 2H), 6.69 (d, *J* = 3.0 Hz, 1H), 3.98 - 3.85 (m, 2H), 3.42 – 3.37 (m, 2H), 2.23 – 2.15 (m, 3H), 1.42 (s, 9H). MS *m/z* ($C_{36}H_{34}F_3N_5O_4$) calc'd = 657.3, observed: M+1 = 658.4

[6] N-(3-(2-(4-(2-aminoethoxy)phenylamino)quinazolin-6-yl)-4-methylphenyl)-3-(trifluoromethyl)benzamide

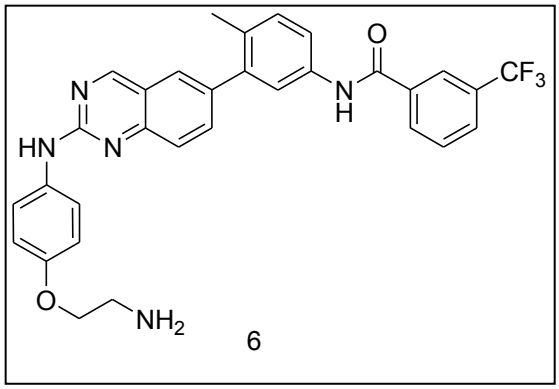

6

Compound **5** (40 mg, 0.062 mmol) was dissolved in CH_2Cl_2 (1 mL) and TFA (440 μL) and stirred for 3 h at room temperature. The reaction was concentrated and purified by reverse phase chromatography (HPLC) to obtain 20 mg (58 % yield) of the desired product **6**. ^{1}H NMR (300 MHz, Methanol-d4) δ 9.27 (s, 1H), 8.28 – 8.21 (m, 2H), 7.93 – 7.85 (m, 2H), 7.80 – 7.73 (m, 4H), 7.67 – 7.48 (m, 2H), 7.43 – 7.28 (m, 2H), 7.21 (d, *J* = 8.9 Hz, 1H), 7.08 (d, *J* = 9.1 Hz, 1H), 5.50 (s, 1H), 4.33 – 4.26 (m, 2H), 3.44 – 3.37 (m, 2H), 2.32 – 2.28 (m, 3H). MS *m/z* ($C_{31}H_{26}F_3N_5O_2$) calc'd = 557.2, observed: M+1 = 558.4

[GP 29]

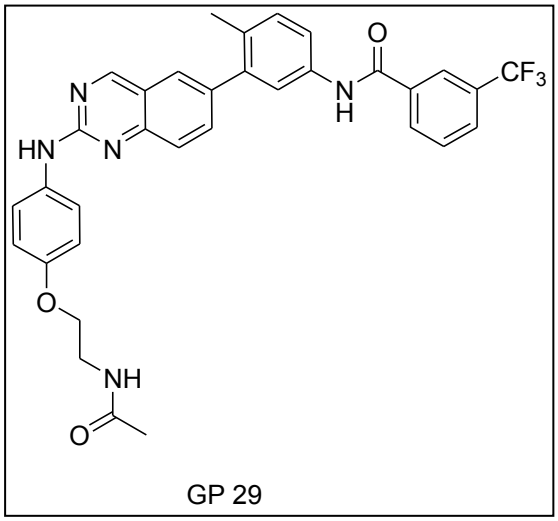

GP 29

Compound 6 (11.6 mg, 0.02 mmol) was stirred in a mixture of Ac_2O (416 uL) and triethylamine (11.6 μL) for 2.5 h at room temperature. The reaction mixture was concentrated *in vacuo*, diluted with a mixture of acetonitrile/water and purified by reverse phase chromatography (HPLC) to obtain 10.2 mg of the desired product **GP 29** (82% yield). ^{1}H NMR (300 MHz, Chloroform-d) δ 9.43 (s, 1H), 8.27 (s, 1H), 8.21 (d, *J* = 9.0 Hz, 1H), 8.03 – 7.90 (m, 2H), 7.81 – 7.71 (m, 2H), 7.64 – 7.48 (m, 4H), 7.37 – 7.29 (m, 3H),

7.16 – 7.08 (m, 2H), 5.80 (s, 1H), 4.13 (t, *J* = 6.0 Hz, 2H), 3.60 (t, *J* = 3.0 Hz, 2H), 2.34 – 2.28 (m, 3H), 2.00 - 1.99 (m, 3H). MS *m/z* ($C_{33}H_{28}F_3N_5O_3$) calc'd = 599.2, observed: M+1 = 600.5

Analytical Condition A - CH_3CN/H_2O–0.1% CF_3CO_2H

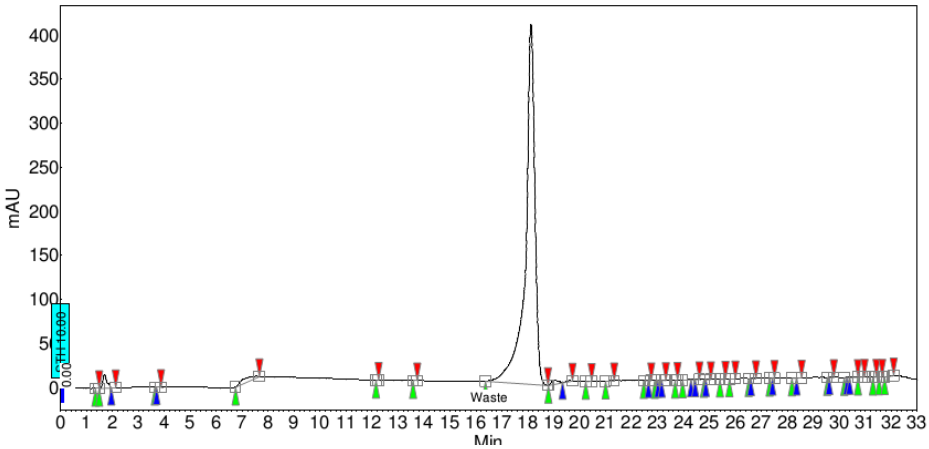

Analytical Condition B - CH_3OH/H_2O–0.1% CF_3CO_2H

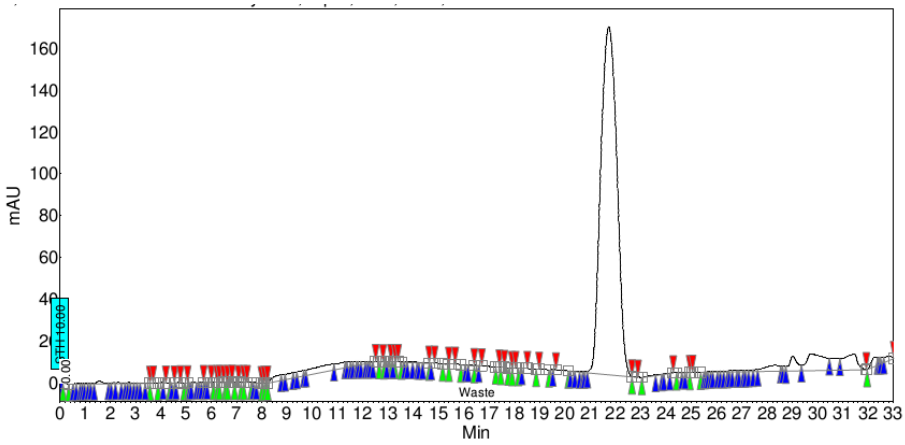

[7] tert-butyl 4-(6-bromoquinazolin-2-ylamino)piperidine-1-carboxylate

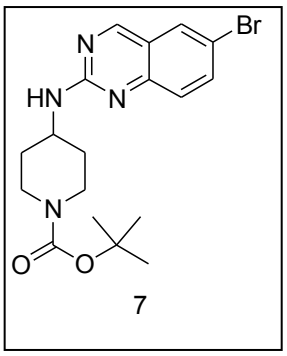

7

In a resealable Pyrex tube, 6-Bromo-2-iodoquinazoline (50.0 mg, 0.15 mmol) and tert-butyl 4-aminopiperidine-1-carboxylate (153 mg, 0.75 mmol) were taken up in of *i*-PrOH (1.1 mL). DIPEA (40 μL, 0.22 mmol) was added and the tube was sealed. The suspension was stirred for 2 h at 80 °C. The mixture was concentrated *in vacuo* and purified by column chromatography (50% ethyl acetate in hexanes) to afford 37.1 mg of compound **7** (61% yield). ^{1}H NMR (300 MHz, Chloroform-d) δ 8.90 (s, 1H), 7.81 (d, *J* = 2.2 Hz, 1H), 7.73 (dd, *J* = 9.0, 2.3 Hz, 1H), 7.46 (d, *J* = 8.9 Hz, 1H), 5.29 (d, *J* = 7.7 Hz, 1H), 4.17 - 4.07 (m, 3H), 3.01 (t, *J* = 12.5 Hz, 2H), 2.10 (t, *J* = 12.0 Hz, 2H), 1.50- 1.43 (m, 11H). MS *m/z* ($C_{18}H_{23}BrN_4O_2$) calc'd = 406.1, observed: M+1 = 407.3

[8] tert-butyl 4-(6-(5-amino-2-methylphenyl)quinazolin-2-ylamino)piperidine-1-carboxylate

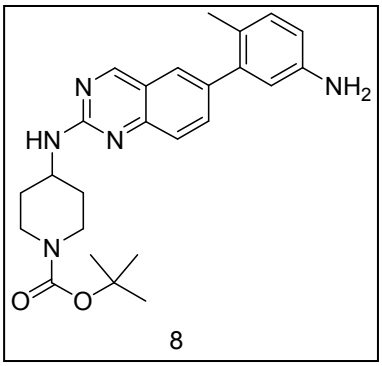

8

A mixture of compound 7 (37.1 mg, 0.09 mmol), 5-Amino-2-methylphenylboronic acid pinacol ester (24.1 mg, 0.10 mmol), Tetrakis(triphenylphosphine)palladium (3.2 mg, 2.7 μmol) and sodium carbonate (21.2 mg, 0.20 mmol) was dissolved in a 3:1 mixture of DME/water (0.36 mL). The mixture was heated overnight at 85 °C. The crude mixture was cooled to room temperature, diluted with ethyl acetate and washed with water and brine. The organic layer was dried over Na_2SO_4, concentrated *in vacuo* to obtain product **8** (79% yield). ^{1}H NMR (300 MHz, Chloroform-d) δ 9.06 (s, 1H), 7.70 – 7.63 (m, 3H), 7.05 (d, *J* = 8.8 Hz, 1H), 6.72 – 6.69 (m, 2H), 4.16 – 4.08 (m, 3H), 3.07 – 2.98 (m, 2H), 2.16 (s, 3H), 2.07 – 2.04 (m, 2H), 1.51 – 1.45 (m, 11H). MS *m/z* ($C_{25}H_{31}N_5O_2$) calc'd = 433.3, observed: M+1 = 434.4

[9] tert-butyl-4-(6-(5-(3-(trifluoromethyl)benzamido)-2-methylphenyl)quinazolin-2-ylamino)piperidine-1-carboxylate

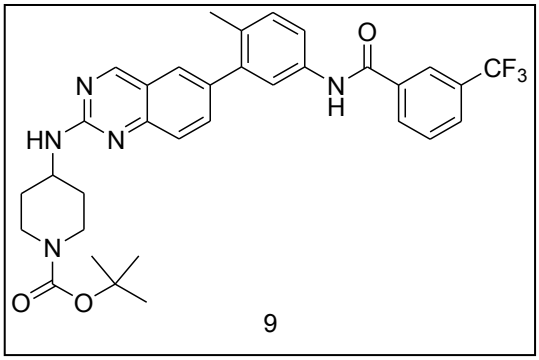

9

Compound 8 (53.1 mg, 0.12 mmol), 3-(trifluoromethyl)benzoic acid (30.9 mg, 0.16 mmol), HOBt (25.2 mg, 0.16 mmol), EDCI (31.1 mg, 0.16 mmol) and DIPEA (60 μL, 0.37 mmol) were dissolved in DMF (360 uL) and stirred overnight at room temperature. The crude mixture was diluted in ethyl acetate and washed with NH_4Cl and Na_2CO_3. The organic

layer was dried over Na_2SO_4 and concentrated *in vacuo* to yield compound **9**, which was used in the next step without further purification. MS *m/z* ($C_{33}H_{34}F_3N_5O_3$) calc'd = 605.3, observed: M+1 = 606.3

[GP20] 3-(trifluoromethyl)-N-(4-methyl-3-(2-(piperidin-4-ylamino)quinazolin-6-yl)phenyl)benzamide

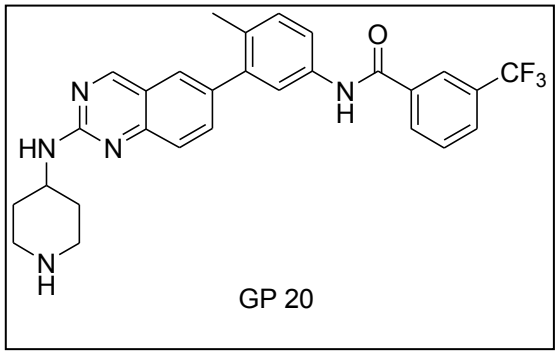

GP 20

Compound 9 (0.12 mmol) was dissolved in CH_2Cl_2 (2.1 mL) and TFA (0.9 mL) and stirred for 3 h at room temperature. The reaction mixture was concentrated *in vacuo*, diluted in acetonitrile/water mixture and purified by reverse phase chromatography (HPLC) to obtain 25.0 mg of the desired product **GP 20** (40% yield after 2 steps). ^{1}H NMR (300 MHz, Methanol-d4) δ 9.32 (s, 1H), 8.28 (s, 1H), 8.22 (d, *J* = 9.0 Hz, 1H), 7.90 – 7.93 (m, 2H), 7.77 – 7.75 (m, 2H), 7.73 – 7.70 (m, 1H), 7.61 (dt, *J* = 9.0, 3.0 Hz, 1H), 7.54 – 7.48 (m, 1H), 7.37 (d, *J* = 8.5 Hz, 1H), 4.45 - 4.36 (m, 1H), 3.59 – 3.52 (m, 2H), 3.29 – 3.17 (m, 2H), 2.41 – 2.34 (m, 2H), 2.31 – 2.28 (m, 3H), 2.00 – 1.86 (m, 2H). MS *m/z* ($C_{28}H_{26}F_3N_5O$) calc'd = 505.2, observed: M+1 = 506.3

Analytical Condition A - CH_3CN/H_2O–0.1% CF_3CO_2H

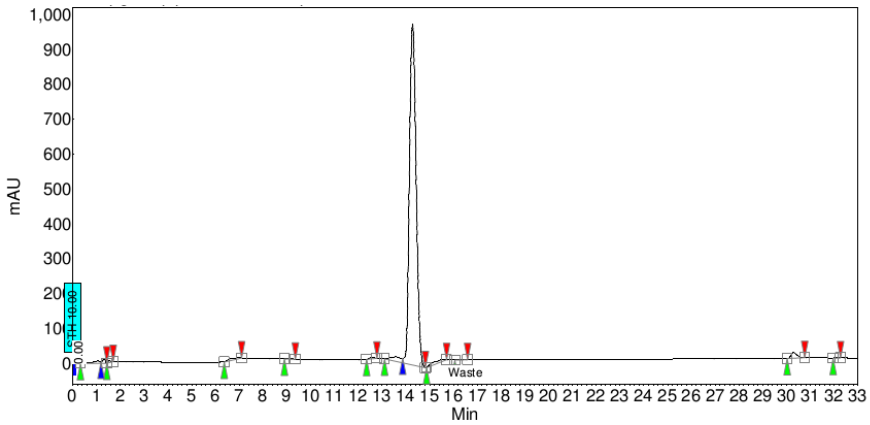

Analytical Condition B - CH_3OH/H_2O–0.1% CF_3CO_2H

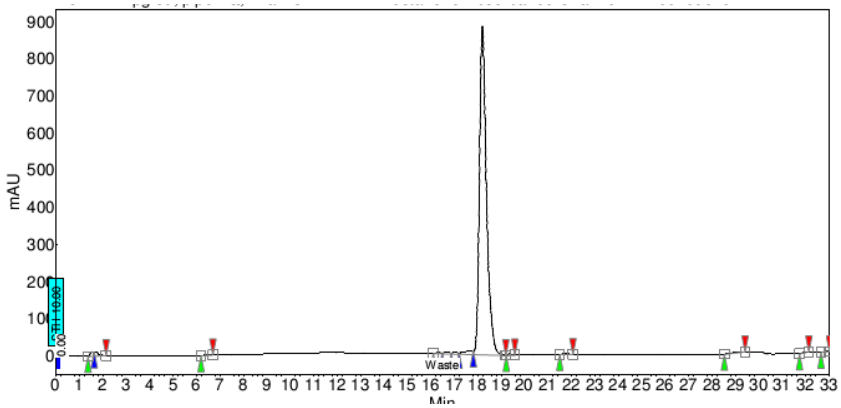

[10] 6-Bromo-N-cyclopropylquinazolin-2-amine

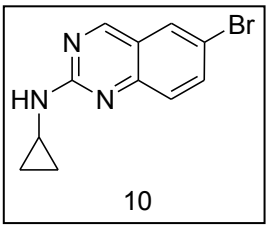

10

In a resealable Pyrex tube, 6-Bromo-2-iodoquinazoline (50.0 mg, 0.15 mmol) and cyclopropylamine (55 μL, 0.75 mmol) were taken up in of *i*-PrOH (1.1 mL). DIPEA (40 μL, 0.22 mmol) was added and the tube was sealed. The suspension was stirred for 2 h at 80

°C. The mixture was cooled to room temperature and concentrated *in vacuo* to afford 33.0 mg of compound **10** (85% yield). The crude compound was used in the next step without further purification. ^{1}H NMR (300 MHz, Chloroform-d) δ 8.89 (s, 1H), 7.78 (d, *J* = 2.2 Hz, 1H), 7.69 (dd, *J* = 9.0, 2.3 Hz, 1H), 7.49 (d, *J* = 9.0 Hz, 1H), 5.77 (s, 1H), 2.92 - 2.84 (m, 1H), 0.89 - 0.82 (m, 2H), 0.60 – 0.55 (m, 2H). MS *m/z* ($C_{11}H_{10}BrN_3$) calc'd =263.0, observed: M+1 = 264.1

[GP 17] N-(3-(2-(cyclopropylamino)quinazolin-6-yl)-4-methylphenyl)-3-(trifluoromethyl)benzamide

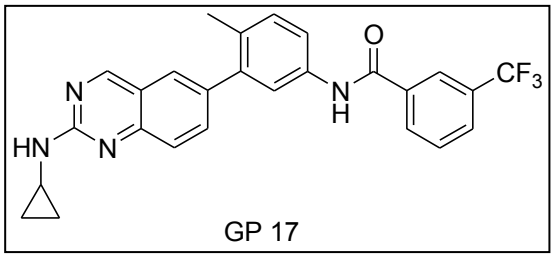

GP 17

A mixture of compound 10 (39.0 mg, 0.15 mmol), compound 4 (71.8 mg, 0.18 mmol), Tetrakis(triphenylphosphine)palladium (5.2 mg, 4.4 μmol) and sodium carbonate (34.2 mg, 0.32 mmol) was dissolved in a 3:1 mixture of DME/water (0.59 mL). The mixture was heated overnight at 85 °C. The crude mixture was cooled to room temperature, diluted in acetonitrile/water mixture and purified using reverse phase chromatography (HPLC) to obtain 20.0 mg of **GP 17** (29% yield). ^{1}H NMR (300 MHz, Methanol-d4) δ 9.47 (s, 1H), 8.28 (s, 1H), 8.22 (d, , *J* = 9.0 Hz, 1H), 8.13 – 7.99 (m, 1H), 7.91 (d, , *J* = 9.0 Hz, 1H), 7.82 – 7.70 (m, 2H), 7.63 – 7.48 (m, 3H), 7.40 – 7.32 (m, 2H), 5.88 (s, 1H), 2.82 – 2.74 (m, 1H), 2.32 –

2.28 (m, 3H), 1.17 – 1.05 (m, 2H), 0.93 – 0.80 (m, 2H) MS *m/z* ($C_{26}H_{21}F_3N_4O$) calc'd = 462.2, observed: M+1 = 463.4

Analytical Condition A - CH_3CN/H_2O–0.1% CF_3CO_2H

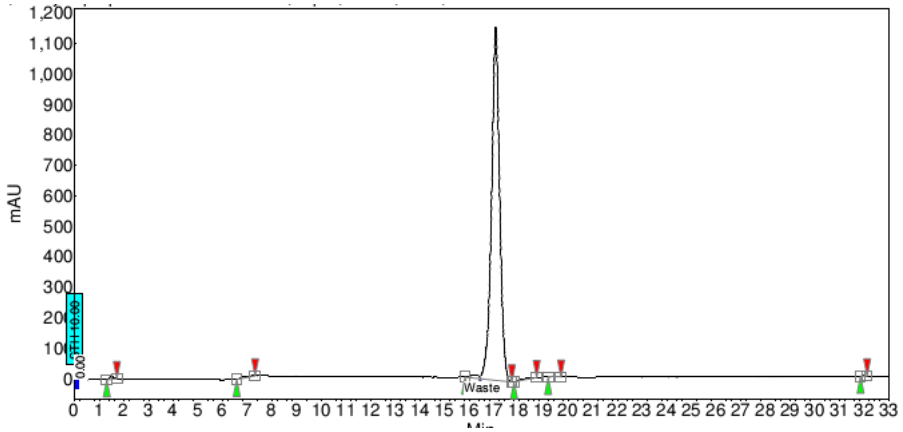

Analytical Condition B - CH_3OH/H_2O–0.1% CF_3CO_2H

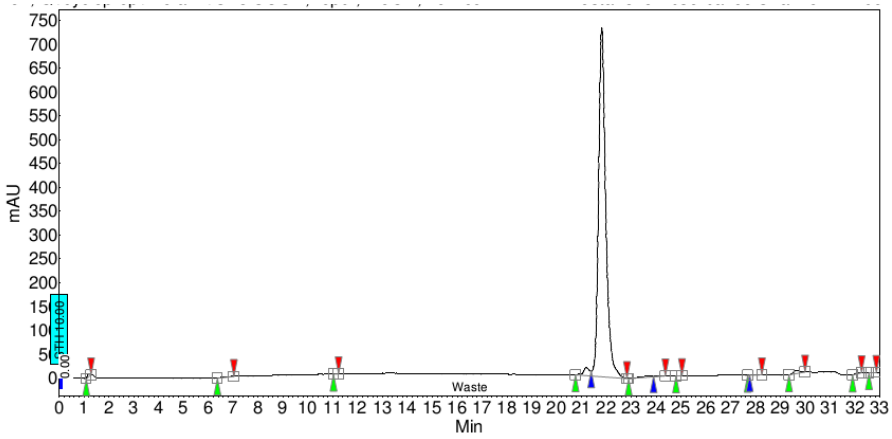

[GP 21] N-(3-(trifluoromethyl)-4-((4-methylpiperazin-1-yl)methyl)phenyl)-3-(2-(imidazo[1,2-b]pyridazin-3-yl)ethynyl)-4-methylbenzamide

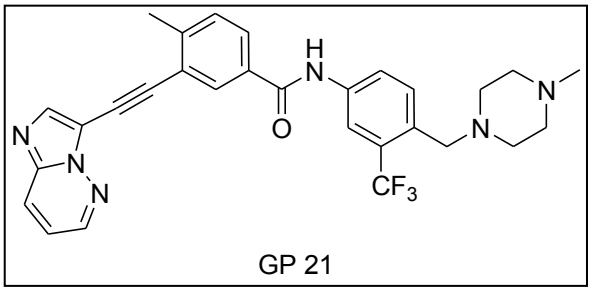

GP 21

GP 21 was synthesized according to a previously published protocol.[57,49]

[GP 118] 1-(4-(4-amino-1-isopropyl-1H-pyrazolo[3,4-d]pyrimidin-3-yl)phenyl)-3-(3-(trifluoromethyl)phenyl)urea

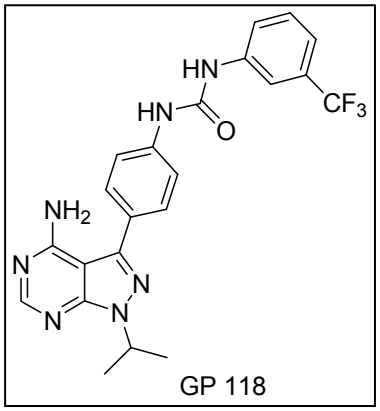

GP 118

GP 118 was synthesized according to a previously published protocol.[65]

[11] 4-(2-chloropyridin-3-yl)pyrimidine

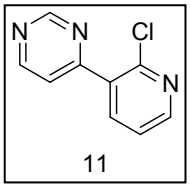

11

Compound 11 was synthesized according to a previously published protocol.[62]

[12] N-(3-amino-4-methylphenyl)-3-(trifluoromethyl)benzamide

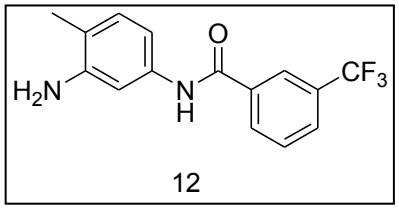

12

Compound 12 was synthesized according to a previously published protocol.[13]

[PR 1] N-(3-(3-(pyrimidin-4-yl)pyridin-2-ylamino)-4-methylphenyl)-3-(trifluoromethyl)benzamide

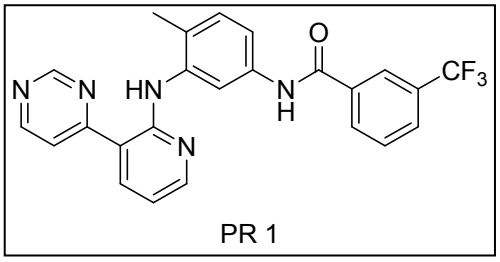

PR 1

Compound 11 (14 mg, 0.073 mmols) and compound 12 (50 mg, 0.17 mmols) were dissolved in DMSO (30 μL) and a drop of Et_3N-TFA salt was added to the reaction mixture. The reaction was stirred for 4 days at 95°C. The crude material was purified using reverse phase liquid chromatography to obtain 6.3 mg of the desired product **PR 1** (20% yield). ^1H NMR (300 MHz, $CDCl_3$-d_1) δ 9.37 (s, 1H), 9.06 (s, 1H), 9.02 (d, *J* = 3 Hz, 1H), 8.51 (d, *J* = 6 Hz, 1H), 8.28 (s, 1H), 8.20-8.16 (m, 2H), 7.95 (d, *J* = 6 Hz, 1H), 7.80-7.75 (m, 3H), 7.64-7.59 (m, 1H), 7.37 (d, *J* = 6 Hz, 1H), 7.09-7.04 (m, 1H), 2.37 (s, 3H). MS *m/z* ($C_{24}H_{18}F_3N_5O$) calc'd = 449.2, observed: ($M+H^+$) = 450.5

Analytical Condition A - CH_3CN/H_2O–0.1% CF_3CO_2H

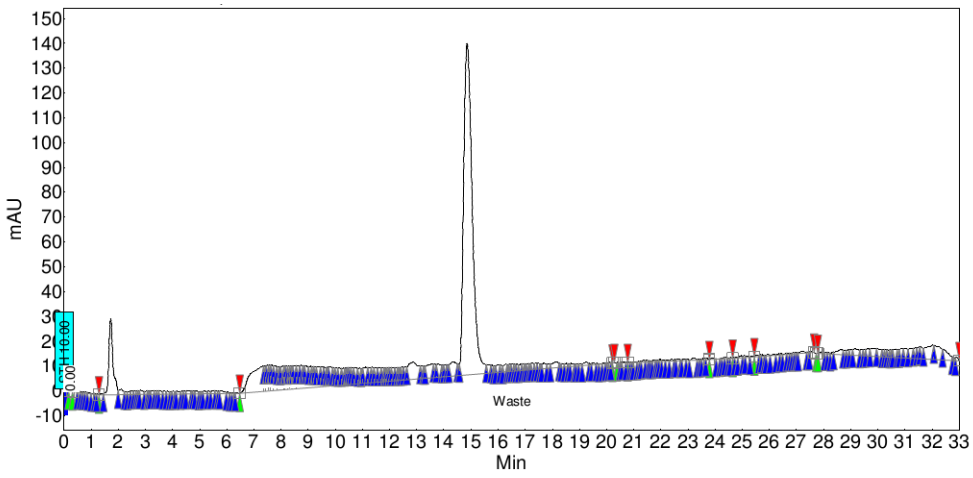

Analytical Condition B - CH_3OH/H_2O–0.1% CF_3CO_2H

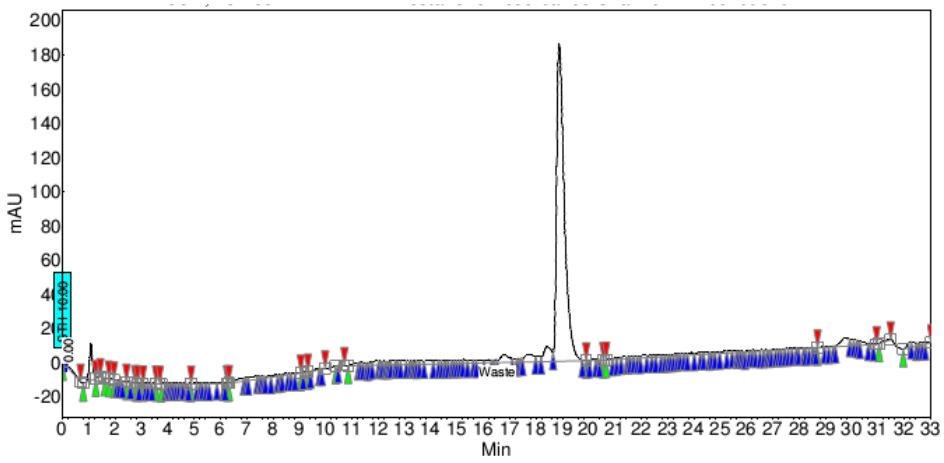

[13] (E)-1-(2-chloropyridin-3-yl)-3-(dimethylamino)prop-2-en-1-one

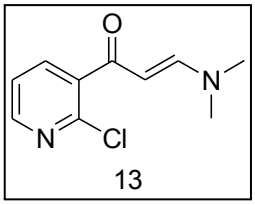

13

Compound 13 was synthesized according to a previously published protocol.[62]

[14] 4-(2-chloropyridin-3-yl)-N-methylpyrimidin-2-amine

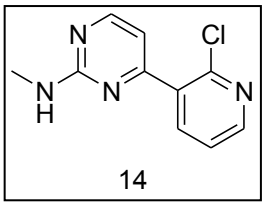

14

N-methylguanidine (126 mg, 1.15 mmols) and sodium methoxide (50 mg, 0.93 mmols) were suspended in methanol (0.2 mL) at room temperature for 30 minutes. Then compound 13 dissolved in methanol (1 mL) was added to the reaction drop wise. The reaction was refluxed at 50°C for 23 hours. The crude material was purified by column chromatography (50% ethyl acetate in hexanes) to obtain 51 mg of the desired product **14** (64% yield). ^{1}H NMR (300 MHz, DMSO-d_6) δ 8.32 (dd, *J* = 3 Hz, *J* = 6 Hz, 1H), 8.23 (d, *J* = 6 Hz, 1H), 7.84 (broad s, 1H), 7.39-7.35 (m, 1H), 7.10-7.09 (m, 1H), 6.68 (d, *J* = 6 Hz, 1H), 2.63 (d, *J* = 6 Hz, 3H).

[PR 4]

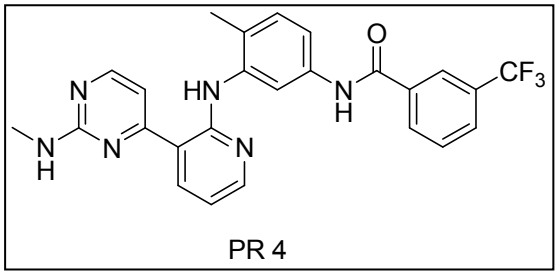

PR 4

4-(2-chloropyridin-3-yl)-N-methylpyrimidin-2-amine (20 mg, 0.09 mmols and compound 12 (63 mg, 0.21 mmols) were dissolved in DMSO (75 μL) and a drop of Et_3N-TFA salt was added to the reaction mixture. The reaction was stirred for 4 days at 95°C. The crude material was purified using reverse phase liquid chromatography to obtain 16 mg of the

desired product **PR 4** (37% yield). ^{1}H NMR (300 MHz, CD_3OD-d_4) δ 8.82 (d, *J* = 6 Hz, 1H), 8.50 (d, *J* = 6 Hz, 1H), 8.27 (s, 1H), 8.23 (d, *J* = 6 Hz, 1H), 7.98-7.91 (m, 3H), 7.78-7.73 (m, 1H), 7.65 (d, *J* = 9 Hz, 1H), 7.53 (d, *J* = 6 Hz, 1H), 7.39 (d, *J* = 6 Hz, 1H), 7.15 (t, *J* = 9 Hz, 1H), 2.98 (s, 3H), 2.34 (s, 3H). MS *m/z* ($C_{25}H_{21}F_3N_6O$) calc'd = 478.2, observed: ($M+H^+$) = 479.4

Analytical Condition A - CH_3CN/H_2O–0.1% CF_3CO_2H

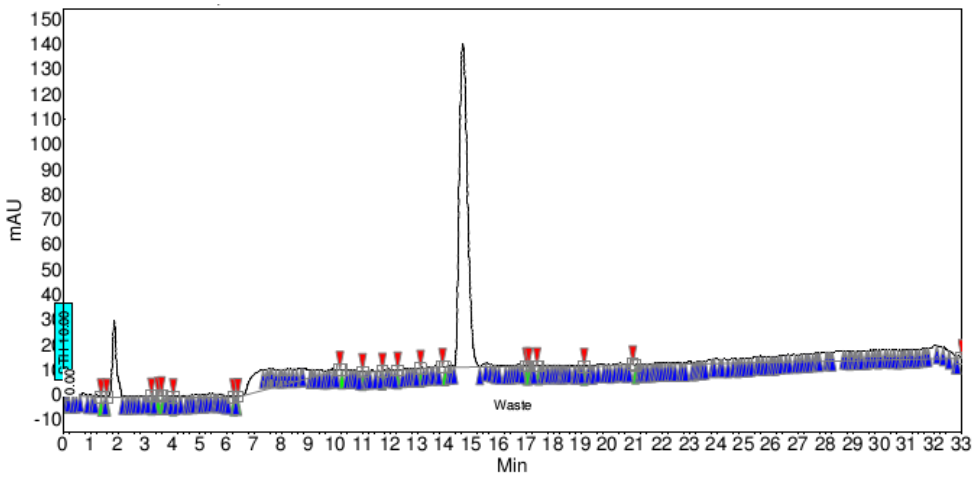

Analytical Condition B - CH_3OH/H_2O–0.1% CF_3CO_2H

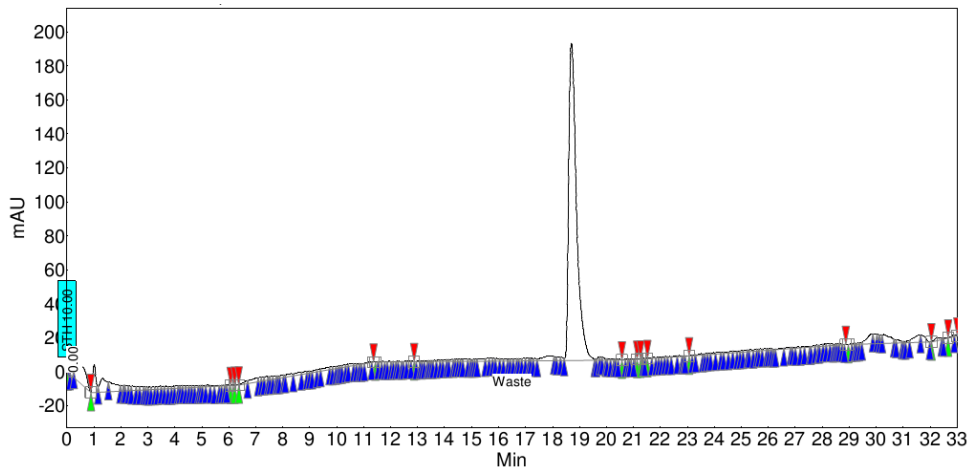

[15] 6-chloro-N-methylpyrimidin-4-amine

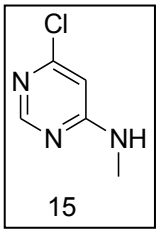

15

4,6-dichloropyrimide (600 mg, 4 mmols), methyl amine.HCl salt (570 mg, 8.4 mmols) and triethylamine (480 mg, 4.8 mmols) were suspended in 2-propanol (4 mL) and refluxed at 80°C for 5 hours. The reaction was taken up in ethyl acetate and the organic layer was washed with saturated K_2CO_3. The organic layer was collected, dried over Na_2SO_4 and concentrated *in vacuo*. The crude material was purified by column chromatography (30-50% ethyl acetate in hexanes) to obtain 390 mg of the desired product **15** (68% yield). ^{1}H NMR (300 MHz, $CDCl_3$-d_1) δ 8.37 (s, 1H), 6.37 (S, 1H), 2.98 (d, *J* = 6 Hz, 3H). MS *m/z* ($C_5H_6ClN_3$) calc'd = 143.0, observed: ($M+H^+$) = 144.0

[16] 6-(2-fluoropyridin-3-yl)-N-methylpyrimidin-4-amine

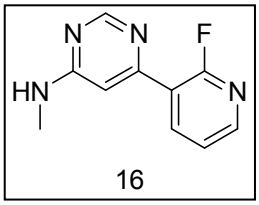

16

Compound 15 (170 mg, 1.2 mmols), 2-fluorophenylboronic acid (84 mg, 0.62 mmols), tetrakis(triphenylphosphine)palladium (36 mg, 0.031 mmols) and K_2CO_3 (170 mg, 1.2 mmols) were dissolved in 1:1 acetonitrile: H_2O (1.2 mL) in a round bottom flask. The flask was saturated with N_2 for 10 minutes and the reaction was refluxed for 2 hours at 80°C.

The reaction was then diluted with ethyl acetate and the organic layer washed with H_2O (3X). The ethyl acetate layer was collected, dried over Na_2SO_4 and concentrated in vacuo. The crude material was purified by column chromatography (60-80% ethyl acetate in hexanes) to obtain 52 mg of the desired product **16** (41% yield). ^{1}H NMR (300 MHz, CD_3OD-d_4) δ 8.53 -8.46 (m, 2H), 8.30 (s, 1H), 7.51-7.46 (m, 1H), 6.97 (s, 1H), 2.98 (s, 3H). MS *m/z* ($C_{10}H_9FN_4$) calc'd = 204.1, observed: ($M+H^+$) = 205.1

[PR 5]

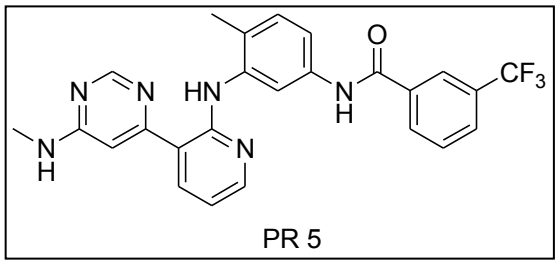

PR 5

Compound 16 (20 mg, 0.099 mmols) and compound 12 (70 mg, 0.24mmols) were dissolved in DMSO (80 μL) and a drop of Et_3N-TFA salt was added to the reaction mixture. The reaction was stirred for 3 days at 95°C. The crude material was purified using reverse phase liquid chromatography to obtain 7 mg of the desired product **PR 5** (14% yield). ^{1}H NMR (300 MHz, CD_3OD-d_4) δ 8.84 (broad s, 1H), 8.40 (broad s, 1H), 8.27 (s, 1H), 8.22 (d, *J* = 6 Hz, 1H), 8.03 (m, 1H), 7.94-7.91 (m, 2H), 7.78 -7.73 (m, 1H), 7.65-7.51 (m, 3H), 7.46-7.43 (m, 1H), 7.12-7.06 (m, 2H), 3.05 (s, 3H), 2.34 (s, 3H). MS *m/z* ($C_{25}H_{21}F_3N_6O$) calc'd = 478.2, observed: ($M+H^+$) = 479.3

Analytical Condition A - CH_3CN/H_2O–0.1% CF_3CO_2H

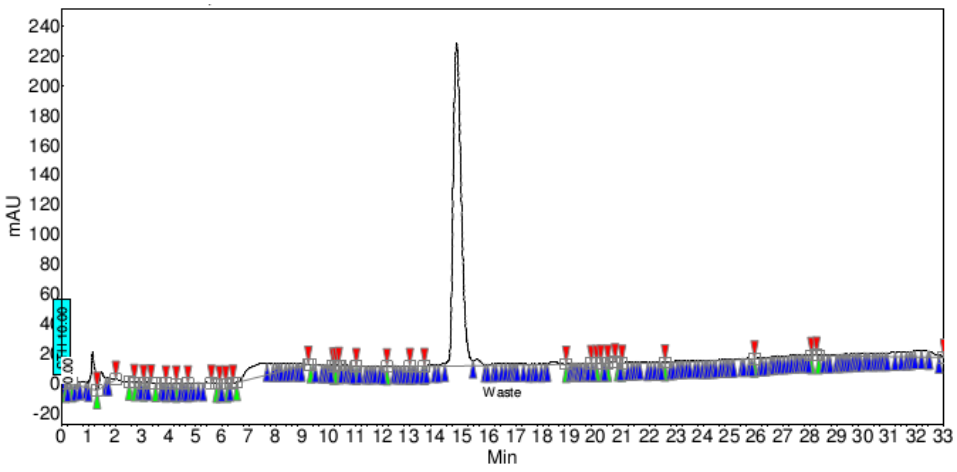

Analytical Condition B - CH_3OH/H_2O–0.1% CF_3CO_2H

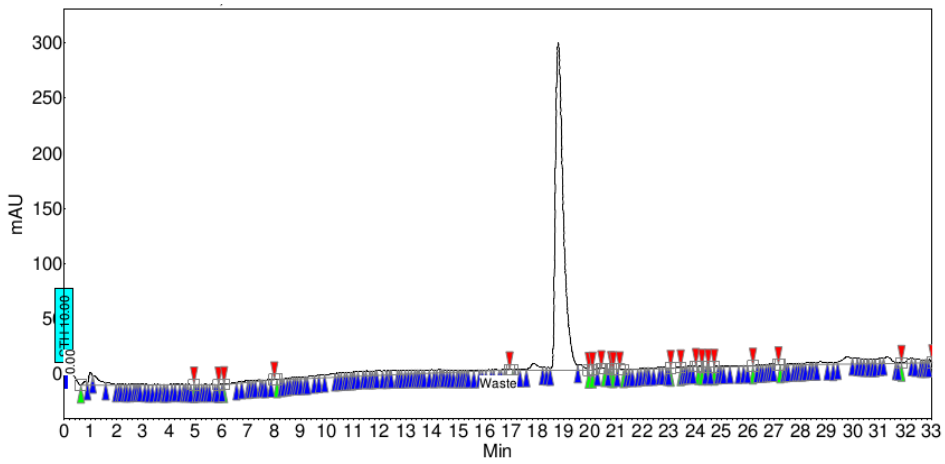

[AST-487] 1-(4-(6-(methylamino)pyrimidin-4-yloxy)phenyl)-3-(4-((4-ethylpiperazin-1-yl)methyl)-3-(trifluoromethyl)phenyl)urea

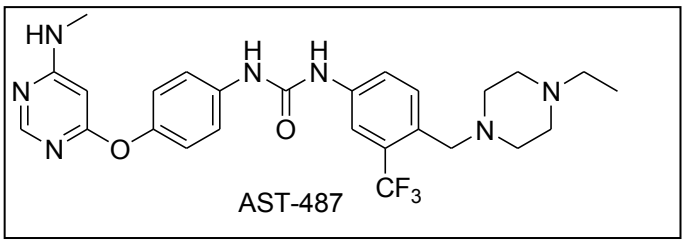

AST-487 was synthesized according to a previously published protocol.[59]

[PR 7] 3-(3-(pyrimidin-4-yl)pyridin-2-ylamino)-N-(3-(trifluoromethyl)phenyl)-4-methylbenzamide

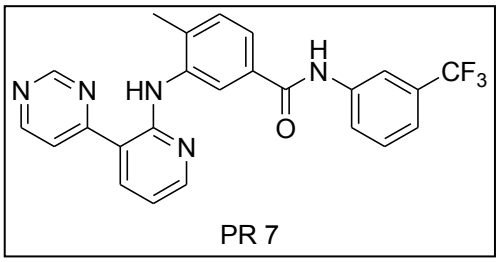

PR 7

PR 7 was synthesized according to a previously published protocol.[61,62]

4.6.2 Protein Kinase activity assays

ABL KD: Inhibitors (initial concentration = 10 µM, 3-fold serial dilutions down to 0.2 nM or 20 pM) were assayed in triplicate against the catalytic domain of His6-ABL wild type, (final concentration = 40 pM) in assay buffer containing 33.5 mM HEPES, pH = 7.5, 6.7 mM $MgCl_2$, 1.7 mM EGTA, 67 mM NaCl, 1.7 mM Na_3VO_4, 3 µM ATP, γ-^{32}P ATP (0.2 µCi/well) and an optimized ABL peptide substrate (Ac-EAIYAAPFAKKK, final concentration = 100 µM). Inhibitor dilutions were incubated with the enzyme for 1 hour prior to the addition of γ-^{32}P ATP. The final volume of each assay well was 30 µL. The enzymatic reaction was run at room temperature for 4 hours and then terminated by spotting 4.5 µL of the reaction mixture onto a phosphocellulose membrane. Membranes were washed with 0.5% phosphoric acid (4x, 10 minutes each wash), dried and the radioactivity was determined by phosphorimaging with a GE Typhoon FLA9000 scanner. The scanned membranes were quantified with ImageQuant and converted to percent inhibition. Data

was analyzed using Prism Graphpad software and IC_{50} values were determined using non-linear regression analysis.

Activated ABL KD (pY412): Same protocol as for ABL KD was used with activated ABL KD with a reaction time of 2 hours.

ABL Y253H KD: Same protocol as for ABL KD was used.

SRC KD: Inhibitors (initial concentration = 10 μM, 3-fold serial dilutions down to 0.2 nM or 20 pM) were assayed in triplicate against the catalytic domain of SRC wild type, (final concentration = 80 pM) in assay buffer containing 33.5 mM HEPES, pH = 7.5, 6.7 mM $MgCl_2$, 1.7 mM EGTA, 67 mM NaCl, 1.7 mM Na_3VO_4, 3 μM ATP, γ-^{32}P ATP (0.2 μCi/well) and an optimized SRC family peptide substrate (Ac-EIYGEFKKK-OH, final concentration = 100 μM). Inhibitor dilutions were incubated with the enzyme for 1 hour prior to the addition of γ-^{32}P ATP. The final volume of each assay well was 30 μL. The enzymatic reaction was run at room temperature for 4 hours and then terminated by spotting 4.5 μL of the reaction mixture onto a phosphocellulose membrane. Membranes were washed with 0.5% phosphoric acid (4x, 10 minutes each wash), dried and the radioactivity was determined by phosphorimaging with a GE Typhoon FLA9000 scanner. The scanned membranes were quantified with ImageQuant and converted to percent inhibition. Data was analyzed using Prism Graphpad software and IC_{50} values were determined using non-linear regression analysis.

Activated SRC 3D (pY416): Same protocol as for SRC KD was used with the following converted exceptions; Activated SRC 3D concentration in the assay was 0.1 nM and the reaction was run for 3 hours.

SRC L317I KD: Same protocol as for SRC KD was used with the following exception; concentration of SRC L317I KD was 0.12 nM in the assay.

HCK 3D: Inhibitors (initial concentration = 10 µM, 3-fold serial dilutions down to 0.2 nM or 20 pM) were assayed in triplicate against the HCK 3D construct, (final concentration = 0.5 nM) in assay buffer containing 33.5 mM HEPES, pH = 7.5, 6.7 mM $MgCl_2$, 1.7 mM EGTA, 67 mM NaCl, 1.7 mM Na_3VO_4, 3 µM ATP, γ-^{32}P ATP (0.2 µCi/well) and an optimized SRC family peptide substrate (Ac-EIYGEFKKK-OH, final concentration = 100 µM). Inhibitor dilutions were incubated with the enzyme for 1 hour prior to the addition of γ-^{32}P ATP. The final volume of each assay well was 30 µL. The enzymatic reaction was run at room temperature for 2 hours and then terminated by spotting 4.5 µL of the reaction mixture onto a phosphocellulose membrane. Membranes were washed with 0.5% phosphoric acid (4x, 10 minutes each wash), dried and the radioactivity was determined by phosphorimaging with a GE Typhoon FLA9000 scanner. The scanned membranes were quantified with ImageQuant and converted to percent inhibition. Data was analyzed using Prism Graphpad software and IC_{50} values were determined using non-linear regression analysis.

Activated HCK 3D (pY416): Same protocol as for HCK KD was used with the following converted exceptions; Activated HCK 3D concentration in the assay was 0.5 nM and the reaction was run for 1 hour.

4.6.3 Activation loop phosphorylation of kinases

Activation of SRC 3D: SRC 3D (250 nM) was incubated with 1 mM ATP in a kinase assay buffer (50 mM HEPES, 10 mM $MgCl_2$, 2.5 mM EGTA, 100 mM NaCl, 1 mg/mL BSA) for 90 minutes at 37°C. Non-phospho-SRC Y416 (mouse) and phospho-SRC Y416 (rabbit) antibodies were used to confirm the complete phosphorylation of the activation loop Tyr416. (Figure 4.7)

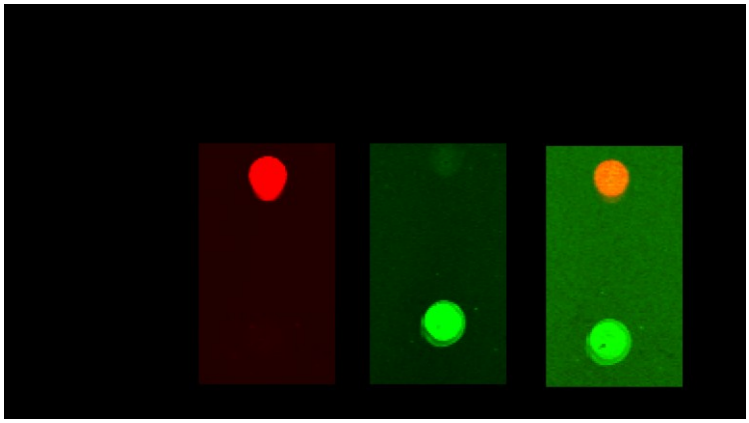

Figure 4.7 - Activation loop phosphorylation of SRC 3D. Reaction progression was detected with an immuno blot using np-SRC Y416 (anti-mouse) antibody and p-SRC Y416 (anti-rabbit) antibody

Activation of HCK 3D: Same protocol as for SRC 3D activation was used.

Activation of ABL KD: ABL KD (15 μM) was incubated with HCK 3D (750 nm) and 0.5 mM ATP in a kinase assay buffer (50 mM HEPES, 10 mM $MgCl_2$, 2.5 mM EGTA, 100 mM NaCl, 1 mM Na_3VO_4) for 5 hours at 37 °C.

4.6.4 K_m values of the kinase constructs

Kinase of interest (2 nM) was incubated with varying concentrations of cold ATP (starting at 2.5 mM; 8 x 2.5-fold dilutions down to 4 μM) in a kinase assay buffer containing 33.5

mM HEPES, pH = 7.5, 6.7 mM $MgCl_2$, 1.7 mM EGTA, 67 mM NaCl, 1.7 mM Na_3VO_4 and 0.08 mg/mL BSA. γ-^{32}P ATP was mixed into each reaction maintaining a constant concentration ratio of 1 mM of cold ATP: 1.2 μCi of γ-^{32}P ATP. At the end of 1 hour, the reaction was terminated by spotting 4.5 μL of the reaction mixture onto a phosphocellulose membrane. Membranes were washed with 0.5% phosphoric acid (4x, 10 minutes each wash), dried and the radioactivity was determined by phosphorimaging with a GE Typhoon FLA9000 scanner. The scanned membranes were quantified and data was analyzed using Prism Graphpad software. K_m values for all the enzyme constructs used in this study were determined using non-linear regression analysis and Michaelis-Menten kinetics.

Table 4.4 - K_m values for the kinase constructs used in this study. These Km values were used to calculate the K_i values of the inhibitors according to the Cheng-Prusoff equation.

Kinase	Km (μM)
SRC KD	65.9
SRC L317I	88.8
SRC 3D	74.9
Activated SRC 3D	90.7
ABL KD	109.1
Activated ABL KD	58.8
ABL Y253H	79.4
HCK 3D	117.7
Activated HCK 3D	108.7

4.7 References

1. Ubersax, J. A.; Ferrell, J. E., Jr., Mechanisms of specificity in protein phosphorylation. *Nature reviews* **2007,** *8* (7), 530-41.
2. Krishnamurty, R.; Maly, D. J., Chemical genomic and proteomic methods for determining kinase inhibitor selectivity. *Combinatorial chemistry & high throughput screening* **2007,** *10* (8), 652-66.
3. Krishnamurty, R.; Maly, D. J., Biochemical mechanisms of resistance to small-molecule protein kinase inhibitors. *ACS chemical biology 5* (1), 121-38.
4. Liao, J. J., Molecular recognition of protein kinase binding pockets for design of potent and selective kinase inhibitors. *Journal of medicinal chemistry* **2007,** *50* (3), 409-24.
5. Manning, G.; Whyte, D. B.; Martinez, R.; Hunter, T.; Sudarsanam, S., The protein kinase complement of the human genome. *Science* **2002,** *298* (5600), 1912-34.
6. Cohen, P., Protein kinases--the major drug targets of the twenty-first century? *Nature reviews. Drug discovery* **2002,** *1* (4), 309-15.
7. Levinson, N. M.; Kuchment, O.; Shen, K.; Young, M. A.; Koldobskiy, M.; Karplus, M.; Cole, P. A.; Kuriyan, J., A Src-like inactive conformation in the abl tyrosine kinase domain. *PLoS biology* **2006,** *4* (5), e144.
8. Adams, J. A., Kinetic and catalytic mechanisms of protein kinases. *Chemical reviews* **2001,** *101* (8), 2271-90.
9. Liu, Y.; Gray, N. S., Rational design of inhibitors that bind to inactive kinase conformations. *Nature chemical biology* **2006,** *2* (7), 358-64.
10. Johnson, L. N.; Noble, M. E.; Owen, D. J., Active and inactive protein kinases: structural basis for regulation. *Cell* **1996,** *85* (2), 149-58.

11. Roskoski, R., Jr., Src protein-tyrosine kinase structure and regulation. *Biochemical and biophysical research communications* **2004,** *324* (4), 1155-64.

12. Ranjitkar, P.; Brock, A. M.; Maly, D. J., Affinity reagents that target a specific inactive form of protein kinases. *Chemistry & biology 17* (2), 195-206.

13. Seeliger, M. A.; Ranjitkar, P.; Kasap, C.; Shan, Y.; Shaw, D. E.; Shah, N. P.; Kuriyan, J.; Maly, D. J., Equally potent inhibition of c-Src and Abl by compounds that recognize inactive kinase conformations. *Cancer research* **2009,** *69* (6), 2384-92.

14. Boggon, T. J.; Eck, M. J., Structure and regulation of Src family kinases. *Oncogene* **2004,** *23* (48), 7918-27.

15. Hantschel, O.; Nagar, B.; Guettler, S.; Kretzschmar, J.; Dorey, K.; Kuriyan, J.; Superti-Furga, G., A myristoyl/phosphotyrosine switch regulates c-Abl. *Cell* **2003,** *112* (6), 845-57.

16. Okishio, N.; Tanaka, T.; Fukuda, R.; Nagai, M., Differential ligand recognition by the Src and phosphatidylinositol 3-kinase Src homology 3 domains: circular dichroism and ultraviolet resonance Raman studies. *Biochemistry* **2003,** *42* (1), 208-16.

17. Payne, G.; Shoelson, S. E.; Gish, G. D.; Pawson, T.; Walsh, C. T., Kinetics of p56lck and p60src Src homology 2 domain binding to tyrosine-phosphorylated peptides determined by a competition assay or surface plasmon resonance. *Proceedings of the National Academy of Sciences of the United States of America* **1993,** *90* (11), 4902-6.

18. Perera, B. G.; Maly, D. J., Design, synthesis and characterization of "clickable" 4-anilinoquinazoline kinase inhibitors. *Molecular bioSystems* **2008,** *4* (6), 542-50.

19. Hill, Z. B.; Perera, B. G.; Maly, D. J., A chemical genetic method for generating bivalent inhibitors of protein kinases. *Journal of the American Chemical Society* **2009,** *131* (19), 6686-8.

20. Hill, Z. B.; Perera, B. G.; Maly, D. J., Bivalent inhibitors of the tyrosine kinases ABL and SRC: determinants of potency and selectivity. *Molecular bioSystems* **2011,** *7* (2), 447-56.

21. Hill, Z. B.; Perera, B. G.; Andrews, S. S.; Maly, D. J., Targeting diverse signaling interaction sites allows the rapid generation of bivalent kinase inhibitors. *ACS chemical biology* **2012,** *7* (3), 487-95.

22. Han, D.; Lerner, A. G.; Vande Walle, L.; Upton, J. P.; Xu, W.; Hagen, A.; Backes, B. J.; Oakes, S. A.; Papa, F. R., IRE1alpha kinase activation modes control alternate endoribonuclease outputs to determine divergent cell fates. *Cell* **2009,** *138* (3), 562-75.

23. Lin, J. H.; Li, H.; Yasumura, D.; Cohen, H. R.; Zhang, C.; Panning, B.; Shokat, K. M.; Lavail, M. M.; Walter, P., IRE1 signaling affects cell fate during the unfolded protein response. *Science* **2007,** *318* (5852), 944-9.

24. Han, D.; Upton, J. P.; Hagen, A.; Callahan, J.; Oakes, S. A.; Papa, F. R., A kinase inhibitor activates the IRE1alpha RNase to confer cytoprotection against ER stress. *Biochemical and biophysical research communications* **2008,** *365* (4), 777-83.

25. Bjorge, J. D.; Jakymiw, A.; Fujita, D. J., Selected glimpses into the activation and function of Src kinase. *Oncogene* **2000,** *19* (49), 5620-35.

26. Van Etten, R. A., Cycling, stressed-out and nervous: cellular functions of c-Abl. *Trends in cell biology* **1999,** *9* (5), 179-86.

27. Johnson, S. A.; Hunter, T., Kinomics: methods for deciphering the kinome. *Nature methods* **2005,** *2* (1), 17-25.

28. Knight, Z. A.; Shokat, K. M., Chemical genetics: where genetics and pharmacology meet. *Cell* **2007,** *128* (3), 425-30.

29. Lawrence, D. S., Chemical probes of signal-transducing proteins. *Accounts of chemical research* **2003,** *36* (6), 401-9.

30. Shen, K.; Hines, A. C.; Schwarzer, D.; Pickin, K. A.; Cole, P. A., Protein kinase structure and function analysis with chemical tools. *Biochimica et biophysica acta* **2005,** *1754* (1-2), 65-78.

31. Knight, Z. A.; Shokat, K. M., Features of selective kinase inhibitors. *Chemistry & biology* **2005,** *12* (6), 621-37.

32. Fedorov, O.; Marsden, B.; Pogacic, V.; Rellos, P.; Muller, S.; Bullock, A. N.; Schwaller, J.; Sundstrom, M.; Knapp, S., A systematic interaction map of validated kinase inhibitors with Ser/Thr kinases. *Proceedings of the National Academy of Sciences of the United States of America* **2007,** *104* (51), 20523-8.

33. Karaman, M. W.; Herrgard, S.; Treiber, D. K.; Gallant, P.; Atteridge, C. E.; Campbell, B. T.; Chan, K. W.; Ciceri, P.; Davis, M. I.; Edeen, P. T.; Faraoni, R.; Floyd, M.; Hunt, J. P.; Lockhart, D. J.; Milanov, Z. V.; Morrison, M. J.; Pallares, G.; Patel, H. K.; Pritchard, S.; Wodicka, L. M.; Zarrinkar, P. P., A quantitative analysis of kinase inhibitor selectivity. *Nature biotechnology* **2008,** *26* (1), 127-32.

34. Heinis, C.; Schmitt, S.; Kindermann, M.; Godin, G.; Johnsson, K., Evolving the substrate specificity of O6-alkylguanine-DNA alkyltransferase through loop insertion for applications in molecular imaging. *ACS chemical biology* **2006,** *1* (9), 575-84.

35. Keppler, A.; Kindermann, M.; Gendreizig, S.; Pick, H.; Vogel, H.; Johnsson, K., Labeling of fusion proteins of O6-alkylguanine-DNA alkyltransferase with small molecules in vivo and in vitro. *Methods* **2004,** *32* (4), 437-44.

36. Barker, A. J.; Gibson, K. H.; Grundy, W.; Godfrey, A. A.; Barlow, J. J.; Healy, M. P.; Woodburn, J. R.; Ashton, S. E.; Curry, B. J.; Scarlett, L.; Henthorn, L.; Richards, L., Studies leading to the identification of ZD1839 (IRESSA): an orally active, selective epidermal

growth factor receptor tyrosine kinase inhibitor targeted to the treatment of cancer. *Bioorganic & medicinal chemistry letters* **2001,** *11* (14), 1911-4.

37. Brehmer, D.; Greff, Z.; Godl, K.; Blencke, S.; Kurtenbach, A.; Weber, M.; Muller, S.; Klebl, B.; Cotten, M.; Keri, G.; Wissing, J.; Daub, H., Cellular targets of gefitinib. *Cancer research* **2005,** *65* (2), 379-82.

38. Lemercier, G.; Gendreizig, S.; Kindermann, M.; Johnsson, K., Inducing and sensing protein--protein interactions in living cells by selective cross-linking. *Angewandte Chemie* **2007,** *46* (23), 4281-4.

39. Zhang, Y.; So, M. K.; Loening, A. M.; Yao, H.; Gambhir, S. S.; Rao, J., HaloTag protein-mediated site-specific conjugation of bioluminescent proteins to quantum dots. *Angewandte Chemie* **2006,** *45* (30), 4936-40.

40. Tran, T.; Hoffmann, S.; Wiesehan, K.; Jonas, E.; Luge, C.; Aladag, A.; Willbold, D., Insights into human Lck SH3 domain binding specificity: different binding modes of artificial and native ligands. *Biochemistry* **2005,** *44* (45), 15042-52.

41. Blume-Jensen, P.; Hunter, T., Oncogenic kinase signalling. *Nature* **2001,** *411* (6835), 355-65.

42. Thomas, S. M.; Brugge, J. S., Cellular functions regulated by Src family kinases. *Annual review of cell and developmental biology* **1997,** *13*, 513-609.

43. Hantschel, O.; Superti-Furga, G., Regulation of the c-Abl and Bcr-Abl tyrosine kinases. *Nature reviews* **2004,** *5* (1), 33-44.

44. Nagar, B.; Hantschel, O.; Young, M. A.; Scheffzek, K.; Veach, D.; Bornmann, W.; Clarkson, B.; Superti-Furga, G.; Kuriyan, J., Structural basis for the autoinhibition of c-Abl tyrosine kinase. *Cell* **2003,** *112* (6), 859-71.

45. Seeliger, M. A.; Nagar, B.; Frank, F.; Cao, X.; Henderson, M. N.; Kuriyan, J., c-Src binds to the cancer drug imatinib with an inactive Abl/c-Kit conformation and a distributed thermodynamic penalty. *Structure* **2007,** *15* (3), 299-311.

46. Deininger, M.; Buchdunger, E.; Druker, B. J., The development of imatinib as a therapeutic agent for chronic myeloid leukemia. *Blood* **2005,** *105* (7), 2640-53.

47. Lovera, S.; Sutto, L.; Boubeva, R.; Scapozza, L.; Dolker, N.; Gervasio, F. L., The different flexibility of c-Src and c-Abl kinases regulates the accessibility of a druggable inactive conformation. *Journal of the American Chemical Society* **2012,** *134* (5), 2496-9.

48. Schindler, T.; Bornmann, W.; Pellicena, P.; Miller, W. T.; Clarkson, B.; Kuriyan, J., Structural mechanism for STI-571 inhibition of abelson tyrosine kinase. *Science* **2000,** *289* (5486), 1938-42.

49. Huang, W. S.; Zhu, X.; Wang, Y.; Azam, M.; Wen, D.; Sundaramoorthi, R.; Thomas, R. M.; Liu, S.; Banda, G.; Lentini, S. P.; Das, S.; Xu, Q.; Keats, J.; Wang, F.; Wardwell, S.; Ning, Y.; Snodgrass, J. T.; Broudy, M. I.; Russian, K.; Daley, G. Q.; Iuliucci, J.; Dalgarno, D. C.; Clackson, T.; Sawyer, T. K.; Shakespeare, W. C., 9-(Arenethenyl)purines as dual Src/Abl kinase inhibitors targeting the inactive conformation: design, synthesis, and biological evaluation. *Journal of medicinal chemistry* **2009,** *52* (15), 4743-56.

50. Dar, A. C.; Lopez, M. S.; Shokat, K. M., Small molecule recognition of c-Src via the Imatinib-binding conformation. *Chemistry & biology* **2008,** *15* (10), 1015-22.

51. Guimaraes, C. R.; Rai, B. K.; Munchhof, M. J.; Liu, S.; Wang, J.; Bhattacharya, S. K.; Buckbinder, L., Understanding the impact of the P-loop conformation on kinase selectivity. *Journal of chemical information and modeling* **2011,** *51* (6), 1199-204.

52. Wodicka, L. M.; Ciceri, P.; Davis, M. I.; Hunt, J. P.; Floyd, M.; Salerno, S.; Hua, X. H.; Ford, J. M.; Armstrong, R. C.; Zarrinkar, P. P.; Treiber, D. K., Activation state-dependent binding of

small molecule kinase inhibitors: structural insights from biochemistry. *Chemistry & biology* **2010,** *17* (11), 1241-9.

53. Okram, B.; Nagle, A.; Adrian, F. J.; Lee, C.; Ren, P.; Wang, X.; Sim, T.; Xie, Y.; Wang, X.; Xia, G.; Spraggon, G.; Warmuth, M.; Liu, Y.; Gray, N. S., A general strategy for creating "inactive-conformation" abl inhibitors. *Chemistry & biology* **2006,** *13* (7), 779-86.

54. Pargellis, C.; Tong, L.; Churchill, L.; Cirillo, P. F.; Gilmore, T.; Graham, A. G.; Grob, P. M.; Hickey, E. R.; Moss, N.; Pav, S.; Regan, J., Inhibition of p38 MAP kinase by utilizing a novel allosteric binding site. *Nature structural biology* **2002,** *9* (4), 268-72.

55. Angell, R. M.; Angell, T. D.; Bamborough, P.; Bamford, M. J.; Chung, C. W.; Cockerill, S. G.; Flack, S. S.; Jones, K. L.; Laine, D. I.; Longstaff, T.; Ludbrook, S.; Pearson, R.; Smith, K. J.; Smee, P. A.; Somers, D. O.; Walker, A. L., Biphenyl amide p38 kinase inhibitors 4: DFG-in and DFG-out binding modes. *Bioorganic & medicinal chemistry letters* **2008,** *18* (15), 4433-7.

56. DiMauro, E. F.; Newcomb, J.; Nunes, J. J.; Bemis, J. E.; Boucher, C.; Buchanan, J. L.; Buckner, W. H.; Cee, V. J.; Chai, L.; Deak, H. L.; Epstein, L. F.; Faust, T.; Gallant, P.; Geuns-Meyer, S. D.; Gore, A.; Gu, Y.; Henkle, B.; Hodous, B. L.; Hsieh, F.; Huang, X.; Kim, J. L.; Lee, J. H.; Martin, M. W.; Masse, C. E.; McGowan, D. C.; Metz, D.; Mohn, D.; Morgenstern, K. A.; Oliveira-dos-Santos, A.; Patel, V. F.; Powers, D.; Rose, P. E.; Schneider, S.; Tomlinson, S. A.; Tudor, Y. Y.; Turci, S. M.; Welcher, A. A.; White, R. D.; Zhao, H.; Zhu, L.; Zhu, X., Discovery of aminoquinazolines as potent, orally bioavailable inhibitors of Lck: synthesis, SAR, and in vivo anti-inflammatory activity. *Journal of medicinal chemistry* **2006,** *49* (19), 5671-86.

57. O'Hare, T.; Shakespeare, W. C.; Zhu, X.; Eide, C. A.; Rivera, V. M.; Wang, F.; Adrian, L. T.; Zhou, T.; Huang, W. S.; Xu, Q.; Metcalf, C. A., 3rd; Tyner, J. W.; Loriaux, M. M.; Corbin, A.

S.; Wardwell, S.; Ning, Y.; Keats, J. A.; Wang, Y.; Sundaramoorthi, R.; Thomas, M.; Zhou, D.; Snodgrass, J.; Commodore, L.; Sawyer, T. K.; Dalgarno, D. C.; Deininger, M. W.; Druker, B. J.; Clackson, T., AP24534, a pan-BCR-ABL inhibitor for chronic myeloid leukemia, potently inhibits the T315I mutant and overcomes mutation-based resistance. *Cancer cell* **2009,** *16* (5), 401-12.

58. Zhou, T.; Commodore, L.; Huang, W. S.; Wang, Y.; Thomas, M.; Keats, J.; Xu, Q.; Rivera, V. M.; Shakespeare, W. C.; Clackson, T.; Dalgarno, D. C.; Zhu, X., Structural mechanism of the Pan-BCR-ABL inhibitor ponatinib (AP24534): lessons for overcoming kinase inhibitor resistance. *Chemical biology & drug design* **2011,** *77* (1), 1-11.

59. Wen-Chung Shieh, J. M., Joseph A. Sclafani, Song Xue, Michael Girgis, James Vivelo, Branko Radetich, and Kapa Prasad, Syntheses of a Triad of Flt3 Kinase Inhibitors: From Bench to Pilot Plant. *Organic Process Research & Development* **2008,** *12* (6), 1146-1155.

60. Weisberg, E.; Roesel, J.; Bold, G.; Furet, P.; Jiang, J.; Cools, J.; Wright, R. D.; Nelson, E.; Barrett, R.; Ray, A.; Moreno, D.; Hall-Meyers, E.; Stone, R.; Galinsky, I.; Fox, E.; Gilliland, G.; Daley, J. F.; Lazo-Kallanian, S.; Kung, A. L.; Griffin, J. D., Antileukemic effects of the novel, mutant FLT3 inhibitor NVP-AST487: effects on PKC412-sensitive and -resistant FLT3-expressing cells. *Blood* **2008,** *112* (13), 5161-70.

61. Hodous, B. L.; Geuns-Meyer, S. D.; Hughes, P. E.; Albrecht, B. K.; Bellon, S.; Caenepeel, S.; Cee, V. J.; Chaffee, S. C.; Emery, M.; Fretland, J.; Gallant, P.; Gu, Y.; Johnson, R. E.; Kim, J. L.; Long, A. M.; Morrison, M.; Olivieri, P. R.; Patel, V. F.; Polverino, A.; Rose, P.; Wang, L.; Zhao, H., Synthesis, structural analysis, and SAR studies of triazine derivatives as potent, selective Tie-2 inhibitors. *Bioorganic & medicinal chemistry letters* **2007,** *17* (10), 2886-9.

62. Hodous, B. L.; Geuns-Meyer, S. D.; Hughes, P. E.; Albrecht, B. K.; Bellon, S.; Bready, J.; Caenepeel, S.; Cee, V. J.; Chaffee, S. C.; Coxon, A.; Emery, M.; Fretland, J.; Gallant, P.; Gu,

Y.; Hoffman, D.; Johnson, R. E.; Kendall, R.; Kim, J. L.; Long, A. M.; Morrison, M.; Olivieri, P. R.; Patel, V. F.; Polverino, A.; Rose, P.; Tempest, P.; Wang, L.; Whittington, D. A.; Zhao, H., Evolution of a highly selective and potent 2-(pyridin-2-yl)-1,3,5-triazine Tie-2 kinase inhibitor. *Journal of medicinal chemistry* **2007,** *50* (4), 611-26.

63. Espínola, E. E. Analysis of c-Src kinase mutants for understanding conformational plasticity. http://www.mpb.unige.ch/reports/rap_EmilioEspinola.pdf.

64. Soverini, S.; Colarossi, S.; Gnani, A.; Rosti, G.; Castagnetti, F.; Poerio, A.; Iacobucci, I.; Amabile, M.; Abruzzese, E.; Orlandi, E.; Radaelli, F.; Ciccone, F.; Tiribelli, M.; di Lorenzo, R.; Caracciolo, C.; Izzo, B.; Pane, F.; Saglio, G.; Baccarani, M.; Martinelli, G.; Leukemia, G. W. P. o. C. M., Contribution of ABL kinase domain mutations to imatinib resistance in different subsets of Philadelphia-positive patients: by the GIMEMA Working Party on Chronic Myeloid Leukemia. *Clinical cancer research : an official journal of the American Association for Cancer Research* **2006,** *12* (24), 7374-9.

65. Korennykh, A. W., Peter; Li, Han; Dar, Arvin; Shokat, Kevan Methods of inhibiting IRE1. WO 2011047384, 2011.

Curriculum Vitae

B. Gayani K. Perera

University of Washington, Department of Chemistry
Box 351700, Seattle WA 98195-1700
gayani@uw.edu, gayani_sampath@yahoo.com

EDUCATION

Ph. D. in Chemistry 2012
University of Washington
Thesis Advisor: Prof. Dustin J. Maly (*maly@chem.washington.edu)*
Thesis Title: Chemical proteomic tools for studying protein kinase active sites

B.S. in Chemistry (First Class Honors) 2004
University of Colombo
Project Advisor: Prof.Sujatha Hewage (*sujatha@chem.cmb.ac.lk)*
Project Title: Synthesis & Physico Chemical Studies of Helical Metal complexes

RESEARCH EXPERIENCE

University of Washington, Department of Chemistry, U.S.A. 2006-2011
Thesis Advisor: Prof. Dustin J. Maly
Thesis Title: Chemical proteomic tools for studying protein kinase active sites

University of Colombo, Department of Chemistry, Sri Lanka 2003-2004
Project Advisor: Prof. Sujatha Hewage
Project Title: Synthesis & Physico Chemical Studies of Helical Metal complexes

Rubber Research Institute of Sri Lanka
Project Advisor: Dr. W.M.G. Seneviratne
Project Title: Causes and prevention of latex protein allergy in dipped products 2004

PUBLICATIONS

1. Perera, B. G. K.; Ranjitkar, P.; Register, A.; Maly, D. J., Significance of P-loop and activation loop towards type II inhibitor selectivity. **2012**, Manuscript in preparation.

2. Wang, L., Perera, B. G. K.*; Hari, S. B.; Bhhatarai, B.; Backes, B. J.; Seeliger, M. A.; Schürer, S. C.; Oakes, S. A.; Papa, F. R.; Maly, D. J., Divergent allosteric control of the

IRE1α endoribonuclease using kinase inhibitors. *Nature Chemical Biology* **2012**, submitted. *(L.W., B.G.K.P., F.R.P. and D.J.M. contributed equally to this work)

3. Ranjitkar, P., Perera, B. G. K.; Swaney, D.; Larson, E.; Krishnamurty, R.; Hari, S.; Merritt, E.; Villen, J.; Maly, D. J., Conformation-Specific, Photo-Affinity Probes for Profiling Protein Kinase Active Sites. *Journal of the American Chemical Society* **2012,** submitted

4. Hill, Z. B.; Perera, B. G. K.; Andrews, S. S.; Maly, D. J., Targeting diverse signaling interaction sites allows the rapid generation of bivalent kinase inhibitors. *ACS chemical biology* **2012,** *7* (3), 487-95.

5. Larson, E. T.; Ojo, K. K.; Murphy, R. C.; Johnson, S. M.; Zhang, Z.; Kim, J. E.; Leibly, D. J.; Fox, A. M.; Reid, M. C.; Dale, E. J.; Perera, B. G. K.; Kim, J.; Hewitt, S. N.; Hol, W. G.; Verlinde, C. L.; Fan, E.; Van Voorhis, W. C.; Maly, D. J.; Merritt, E. A., Multiple determinants for selective inhibition of apicomplexan calcium-dependent protein kinase CDPK1. *Journal of medicinal chemistry* **2012,** *55* (6), 2803-10.

6. Johnson, S. M.; Murphy, R. C.; Geiger, J. A.; DeRocher, A. E.; Zhang, Z.; Ojo, K. K.; Larson, E. T.; Perera, B. G. K.; Dale, E. J.; He, P.; Reid, M. C.; Fox, A. M.; Mueller, N. R.; Merritt, E. A.; Fan, E.; Parsons, M.; Van Voorhis, W. C.; Maly, D. J., Development of Toxoplasma gondii calcium-dependent protein kinase 1 (TgCDPK1) inhibitors with potent anti-toxoplasma activity. *Journal of medicinal chemistry* **2012,** *55* (5), 2416-26.

7. Hill, Z. B.; Perera, B. G. K.; Maly, D. J., Bivalent inhibitors of the tyrosine kinases ABL and SRC: determinants of potency and selectivity. *Molecular bioSystems* **2011,** *7* (2), 447-56.

8. Murphy, R. C.; Ojo, K. K.; Larson, E. T.; Castellanos-Gonzalez, A.; Perera, B. G. K.; Keyloun, K. R.; Kim, J. E.; Bhandari, J. G.; Muller, N. R.; Verlinde, C. L.; White, A. C., Jr.; Merritt, E. A.; Van Voorhis, W. C.; Maly, D. J., Discovery of Potent and Selective Inhibitors of Calcium-Dependent Protein Kinase 1 (CDPK1) from C. parvum and T. gondii. *ACS medicinal chemistry letters* **2010,** *1* (7), 331-335.

9. Hill, Z. B.; Perera, B. G. K.; Maly, D. J., A chemical genetic method for generating bivalent inhibitors of protein kinases. *Journal of the American Chemical Society* **2009,** *131* (19), 6686-8.

10. Perera, B. G. K.; Maly, D. J., Design, synthesis and characterization of "clickable" 4-anilinoquinazoline kinase inhibitors. *Molecular bioSystems* **2008,** *4* (6), 542-50.

PRESENTATIONS - Poster

1. A Chemical Proteomic Strategy for the Identification of Druggable Kinase Targets in *Trypanosoma brucei*, Seattle Parasitology Conference, Seattle, WA, May 2012

2. A Chemical Proteomic Strategy for the Identification of Druggable Kinase Targets in *Trypanosoma brucei*, Technical and Sci-Mix sessions, 243rd ACS National Meeting, San Diego, CA, March 2012

PRESENTATIONS – Oral

1. "Ligands for studying the conformational dynamics of protein kinase active sites", Department of Chemistry, University of Washington, 2011.

2. "Synthesis & Physico Chemical Studies of Helical Metal complexes", Annual meeting of Royal Society of Chemistry – Sri Lankan section, 2004

3. "Application of Matrix-Assisted Laser Desorption/Ionisation (MALDI) Mass Spectroscopy to Metal Complexes", Joint Academic Sessions of the Faculties of Science and Medicine, University of Colombo, 2004.

TEACHING EXPERIENCE

1. Graduate Teaching Assistant, University of Washington, Department of Chemistry (2006-2012)

2. Assistant Lecturer, University of Colombo, Department of Chemistry (2004-2006)

3. Undergraduate Research Mentor for a student (2011-2012)

DISTINCTIONS

1. Gold Medal for the Best Undergraduate Research Project, All Island Inter University Chemistry Intelligence Test organized by the Royal Society of Chemistry, Sri Lankan section (2004)

2. Bhikaji Framji Khan Gold Medal for Chemistry, Best overall performance in B.S. Chemistry honors Degree (2004)

3. Prof. Pearlyn Pereira Memorial Gold Medal for Physical Chemistry (2004)

4. Dr. C. L. De Silva Memorial Prize in Chemistry for the Best performance in Chemistry (2002)

5. Scholarship for the Best Results in the First Year Examination in Science (Biological Science), University of Colombo (2001)